Aus dem Institut für Anatomie
der Medizinischen Fakultät der Charité – Humboldt-Universität zu Berlin

DISSERTATION

Parakrine Signalwege der Niere – zelluläre Verteilung und Interaktion von NO- und Prostaglandinsynthese

Zur Erlangung des akademischen Grades
Doctor medicinae (Dr. med.)

vorgelegt der Medizinischen Fakultät der Charité – Humboldt-Universität zu Berlin

von

Franziska Theilig

aus Bad Langensalza

Dekane: Prof. Dr. Joachim W. Dudenhausen
Prof. Dr. med. Martin Paul

Gutachter: 1. Prof. Dr. Bachmann
2. Prof. Dr. Gröne
3. Prof. Dr. Galle

Datum der Promotion: 20. 06. 2005

Inhaltsverzeichnis

Abkürzungsverzeichnis

bp	Basenpaare
CCD	kortikales Sammelrohr
cDNA	komplementäre Desoxyribonukleinsäure
cGMP	zyklisches Guanosin Monophosphat
CNT	Verbindungstubulus
COX-1	Zyklooxygenase-1
COX-2	Zyklooxygenase-2
cTAL	kortikale dicke aufsteigende Henle-Schleife
Da	Dalton
DCT	distales Konvolut
EP-1 bis EP-4	Prostaglandin-E Rezeptor 1-4
HRP	Meerrettich-Peroxidase
JGA	Juxtaglomerulärer Apparat
MCD	medulläres Sammelrohr
mRNA	messenger Ribonukleinsäure
mTAL	medulläre dicke aufsteigende Henle-Schleife
Na/Ca	Natrium/Calcium-Austauscher
NADPH	Nikotin-Adenin-Dinukleotid-Phosphat
NCC	Natrium-Chlorid-Kotransporter
NO	Stickstoffmonoxid
NOS1	neuronale Stickstoffmonoxid-Synthase1
PAGE	Polyacrylamid-Gelelektrophorese
PCR	Polymerase-Kettenreaktion
PGES	Prostaglandin E Synthase
PVDF	Polyvenylidin Difluorid
RAAS	Renin-Angiotensin-Aldosteron System
RT	reverse Transkription
sGC	lösliche Guanylatzyklase
THP	Tamm-Horsfall Protein
UE	Untereinheit

Maßeinheiten wurden entsprechend der Nomenklatur des SI (Système international) angegeben.

Abstract

Zu den vielfältigen Aufgaben der Niere gehören die tubuläre Rückresorption körperwichtiger Substanzen sowie die Regulation des renalen und systemischen Blutdrucks. Brennpunkte der vorliegenden Arbeit waren die Kontrollparameter der tubulo-glomerulären Regulation sowie Aspekte des epithelialen Transports im distalen Nephron und Sammelrohr. Das L-Arginin-Stickstoffmonoxyd (NO)-System und die Komponenten renaler Prostaglandinsynthese nehmen hier eine wichtige Stellung ein. Die Schlüssel-Syntheseenzyme NO-Synthase 1 (NOS1) und Zyklooxygenase (COX) Typ 2 sind in der Macula densa lokalisiert. Sie sind im Zusammenhang mit der Filtratbildung reguliert. Weitere Komponenten ihrer Reaktionskaskaden sind jedoch in ihrer zellspezifischen Rolle noch unklar. Wir haben diese daher näher untersucht.

Mit histochemischen und biochemischen Methoden (immunhistochemische Färbungen, RT-PCR, In situ Hybridisierung, Western blot und spezifischen cGMP Nachweisen in Gewebe- und Zellextrakten) wurden NO-Rezeptor (lösliche Guanylatzyklase; sGC), COX-1, COX-2 und die membrangebundene Prostaglandin E_2-Synthase (mPGES) nachgewiesen. Außerdem wurde die Interaktion von NOS1 und COX-2 im 2 Nieren-1 Clip (Goldblatt)-Modell bei der Ratte sowie bei NOS1-defizienten Mäusen untersucht.

Die sGC wurde in den glomerulären Arteriolen, den Renin-produzierenden Zellen, dem Mesangium, den Vasa recta, den interstitiellen Fibroblasten und den Ito-Zellen der Leber detektiert. COX-2 wurde zusammen mit mPGES in der kortikalen aufsteigenden Schleife und der Macula densa gefunden. COX-1 wurde zusammen mit mPGES im terminalen distalen Konvolut, im Verbindungstubulus und im Sammelrohr detektiert. Die medullären interstitiellen Zellen exprimierten gleichzeitig COX-1, COX-2 und mPGES. Im Goldblatt-Modell bestand unilateral (stenotische Seite) eine Stimulation der juxtaglomerulären NOS1 sowie der COX-2 Expression. Entgegen früheren Annahmen konnten wir jedoch keine Hinweise für eine zell-bezogene Interaktion zwischen beiden Produkten finden. Dieses wurde durch die Verwendung der NOS1-defizienten Maus bestätigt, die im Experiment keine Veränderung der COX-2 Expression zeigte.

Die spezifische Lokalisation von NO-Rezeptor und Komponenten der Prostaglandinsynthese unterstreicht ihre Bedeutung für die Regulation von Blutdruck, Salz- und Wasserhomöostase. Die juxtaglomeruläre Synthese von NO und Prostaglandinen folgt ähnlichen Stimuli, ist jedoch voneinander unabhängig.

Abstract

Priciple functions of the kidneys are tubular reabsorption of important solutes and regulation of renal and systemic blood pressure. This work has been focused on parameters to control the tubulo-glomerular feedback and epithelial transport in the distal tubule and collecting duct system. The L-arginine-nitric oxide (NO)-system and components of the renal prostaglandin synthesis are thought to play major roles therein. Key-enzymes are NO-Synthase 1 (NOS1) and cyclooxygenase-2 (COX-2), both are localized in the macula densa and are regulated in dependence of the filtrate formation. The cell-specific role of further components in the signalling cascades remains unclear.

For investigation we used histochemical and biochemical methods (immunohistochemistry, RT-PCR, in situ hybridisation, western blotting and specific cGMP measurements in tissue and cell extracts to localize the NO-receptor (soluble guanylyl cyclase, sGC), COX-1, COX-2 and the membranous prostaglandin E_2-synthase (mPGES). Moreover we analyzed the interaction of NOS1 and COX-2 in the 2 kidney-1 clip (Goldblatt)-model of the rat and in NOS1 deficient mice.

The sGC could be detected in glomerular arterioles, renin-producing cells, mesangium, vasa recta, interstitial fibroblasts and Ito-cells of the liver. COX-2 was co-localized with mPGES in the cortical thick ascending limb and macula densa. COX-1 was co-localized with mPGES in the terminal distal convolutions, connecting tubule and collecting duct. The medullary interstitial cells were positive stained for COX-1, COX-2 and mPGES. In the Goldblatt-model we found an increased expression of juxtaglomerular NOS1 and COX-2 in the stenotic kidney. Against former hypothesises we were unable to find evidences for a cell-specific interaction between both products. This was supported by the evaluation of NOS1 deficient mice which revealed no difference of COX-2 expression under control and variable conditions.

The specific localization of NO-receptor and components of the prostaglandin synthesis emphasizes their relevance for the regulation of blood pressure and salt- and water homeostasis. The juxtaglomerular synthesis of NO and prostaglandins are similarly regulated while COX-2 is NO-independently expressed.

1. Einleitung

Die zentrale Leistung der Niere ist die Ultrafiltration des Plasmas und die resultierende Rückresorption der Menge von ca. 1,5 kg Kochsalz pro Tag. Für diese Leistung stehen eine Reihe von Transportsystemen entlang dem Nephron und Sammelrohrsystem zu Verfügung. Regelsysteme steuern den korrekten Ablauf der Rückresorption. Schwankungen der glomerulären Filtrationsrate bzw. der proximal-tubulären Resorption werden distal im juxtaglomerulären Apparat gemessen. Über ein Feedback-Signal kann kurzfristig eine Korrektur der Filtratbildung eingeleitet werden. Mittel- und längerfristige Beeinflussungen der Filtratbildung und der Resorptionsleistung werden u. a. durch das endokrine Renin-Angiotensin-Aldosteronsystem sowie durch lokale parakrine Faktoren ermöglicht [1-4] .

Zum einen spielt hier der Signalweg der NO-induzierten cGMP-Freisetzung [5-10] eine entscheidende Rolle, indem über Formen der NO-Synthase aus L-Arginin NO freigesetzt wird und – neben anderen Reaktionsmöglichkeiten – an seinen Haupt-Rezeptor, die lösliche Guanlytzyklase bindet und die Bildung von cGMP einleitet. Zum andern sind die Wege der renalen Prostaglandinsynthese imJGA und distalen Tubulus von herausragender Bedeutung. Das dominierende renale Prostaglandin ist PGE2, das aus Arachidonsäure durch Isoformen der Zyklooxygenase (COX-1, COX-2) über den Weg der membrangebundenen Prostaglandin-E Synthase entsteht und an mehrere renal exprimierte Rezeptorformen binden kann [11].

Interessanterweise ist der JGA für beide Systeme ein Brennpunkt, indem die Macula densa selektiv hohe Mengen von „neuronaler“ NOS1 [12] und von „induzierbarer“ COX-2 exprimiert [13]. Beide Komponenten sollen miteinander interagieren. Die Macula densa ist jedoch nicht die einzige Quelle von NOS1 und COX-2. Vielmehr sind spezifische Effekte in den einzelnen Zonen der Niere für Epithelien, Gefäße und das Interstitium beschrieben.

Ein vollständigeres Bild der Verteilung beteiligter Komponenten der beiden Systeme erschien daher anstrebenswert. Die Enzym-Isoformen sollten in Verteilung und Funktion gegeneinander abgegrenzt werden. Die vorliegende Zusammenfassung schildert demgemäß den Inhalt meiner Arbeiten, die ich mit den Mitarbeitern unserer Abteilung zur Detektion der Signalwege von NOS1 und COX-1/2 und zur Charakterisierung ihrer Interaktion durchgeführt habe.

2. Material und Methoden

2.1. Tiere, Gewebe, Zellen

. Unbehandelte männliche Sprague-Dawley Ratten (140-200g), männliche NOS $1^{-/-}$ Mäuse und Wildtyp Kontrollmäuse NOS $1^{+/+}$ (25-30g) wurden von der lokalen Tierabteilung bezogen. Behandelte Ratten, Goldblatt-Modell: Tiere für das 2 Nieren 1 Clip Goldblatt-Modell des renovaskulären Bluthochdruckes und Kontrolltiere wurden über Zeiträume von 3 und 28 Tagen behandelt [14]. Der Blutdruck wurde ab dem 1. Tag nach der Operation schwanzplethysmographisch gemessen und alle Tiere wurden am letzten Tag des Experimentes zur Urinvolumenbestimmung über 24h in metabolischen Käfigen gehalten. Die verwendeten Glomeruli, Mesangialzellen und medulläre Fibroblasten wurden in Zusammenarbeit mit unseren Kooperationspartnern isoliert. Hierzu wurde Nierenkortexgewebe in Zellkulturmedium aufbereitet und durch Stahlsiebe der Porengröße 150 µm gesiebt, zentrifugiert, das entstandene Pellet in einem geringen Volumen aufgenommen und die Glomeruli mikrodisseziert [15]. Zur Isolierung der Mesangialzellen wurden die Glomeruli enzymatisch mit Kollagenase verdaut, in Medium aufgenommen und morphologisch im Phasen-Kontrastmikroskop charakterisiert. [16]. Zur Isolierung der medullären interstitiellen Zellen wurde das innere Nierenmark mit Kollagenase und Hyaluronidase aufgespalten und die Sammelrohrzellen durch Zentrifugation entfernt. Anschließend wurden die Zellen mit *Dolichos biflorus* Agglutinin überzogenen Beads isoliert [17] und durch Dichtegrandientenzentifugation weiter aufgereinigt. Zur Isolierung von Ito-Zellen wurden nichtparenchymale Zellen über Pronase-Kollagenase-Methode [18] isoliert und die Ito-Zellen anschließend durch Dichtegrandientenzentifugation weiter aufgereinigt. Ihre Identifikation erfolgte auf Grund ihrer typischen Strukturmerkmale und ihrer Vitamin-A spezifischen Autofluoreszenz.

Für morphologische und immunhistochemische Untersuchungen wurden die Tiere anästhesiert und retrograd über die abdominale Aorta perfusionsfixiert [14].

2.2. Histochemische und Western blot Analyse.

2.2.1. Antikörper gegen:

Antikörper	**Wirt**	**Herkunft**
β_1 sGC	Kaninchen	D. Koesling
NOS1	Kaninchen	Alexis
Podosynapsin	Maus	P. Mundel
Desmin	Maus	Dako
5´-Ekto-Nukleotidase	Kaninchen	B. Kaissling
NOS1 (Exon2)	Maus	Calbiochem
NOS1 (Exon 12-21)	Kaninchen	Sigma
COX-1	Kaninchen	Caymanchemicals
COX-1	Kaninchen	Santa Cruz
COX-2	Kaninchen	Caymanchemicals

COX-2	Ziege	Santa Cruz
mPGES	Kaninchen	Caymanchemicals
THP	Kaninchen	J. Hoyer
Na-Cl Kotransporter	Kaninchen	D. H. Ellison
Na/Ca Austauscher	Meerschweinchen	R. Reilly
Calbindin	Maus	Sigma

2.2.2. Western blot.

Gewebe (Nieren aufgetrennt in Kortex und Mark; Lunge; Skelettmuskel und Leber) und Zellen (Mesangialzellen; interstitielle Zellen und Ito-Zellen) wurden in Homogenisierungspuffer aufbereitet, zentrifugiert, und das Gewebehomogenat und Zellysat bis zur Verwendung bei –80°C eingefroren. Die Homogenate und Lysate wurden anschließend gelelektrophoretisch in SDS-PAGE aufgetrennt und auf eine PVDF-Membran übertragen, welche anschließend zur Blockierung unspezifischer Proteinbindung in Milch übertragen wurde. Zur Detektion spezifischer Proteine wurde die Membran mit dem jeweiligen Primärantikörper, gefolgt von einem HRP-gebundenen Sekundärantikörper inkubiert. Mit Hilfe eines Chemiluminescenz-Kits wurde das Signal generiert. *Immunhistochemie*. Zur immunhistochemischen Färbung wurden Cryostatschnitte oder Paraffinschnitte verwendet. Nach der Inkubation mit dem Primärantikörper erfolgte die Detektion des Signals durch Fluorochrom oder HRP-konjugierte Antikörper. Durch die Blockierungstests mit dem zur Antikörperproduktion verwendeten antigenen Peptids wurde die Spezifität der anti-β1-sGC und anti-COX-2 Antikörper überprüft.

2.3. Immun-Elektronenmikroskopie.

Für eine ultrastrukturelle Immunperoxidasemarkierung wurden 20µm dicke Vibratomschnitte mit anti-β1-sGC, anti-COX-1 und anti-COX-2 in Mikrotiterplatten inkubiert und anschließend mit 1% Osmiumtetroxid nachfixiert, mit Maleatpuffer gewaschen, *en bloc* mit Uranylacetat markiert und in Epon 812 eingebettet. Die danach hergestellten Semi- und Ultradünnschnitte wurden mit einem Licht bzw. Elektronenmikroskop ausgewertet.

2.4. NADPH-Diaphorase Markierung.

Die katalytische Aktivität der NOS wurde über die enzymatische Reduktion von Nitroblau - Tetrazoliumsalz in Anwesenheit von NADPH (NADPH-Diaphorase Reaktion) demonstriert. Das Gewebe wurde in 0.1 M Phosphatpuffer bei 37°C inkubiert und bei Sichtbarwerden des Signals abgestoppt.

2.5. In situ Hybridisierung.

Die Lokalisation der mRNA Expressionen, α_1 sGC, β_1 sGC, COX-1, COX-2 und mPGES, wurden durch die In situ Hybridisierung untersucht. Digoxigenin-markierte RNA-Sonden (sense und antisense) wurden über *in vitro* Transkription der entsprechenden cDNA hergestellt und auf Nierengewebe aufgetragen [14]. Nach der Inkubation mit einem alkalische Phosphatase-konjugierten anti-Digoxigenin Antikörper wurde das Signal durch eine Farbreaktion generiert.

2.6. RT-PCR.

Die RNA aus dem Nierenkortex, dem Nierenmark, den isolierten Glomeruli und aus der Leber wurden nach der Guanidinium Thiocyanat-Methode extrahiert, spektrophotometrisch bei 260 nm quantifiziert und anschließend revers transkribiert. Passende Oligonukleotidprimer für α_1 sGC, β_1 sGC, COX-1, COX-2, PGES und GAPDH wurden zur Amplifizierung der cDNA mit einer *Taq* Polymerase benutzt. Nach der Auftrennung im Agarosegel und Ethidiumbromidfärbung wurden die spezifischen cDNA Fragmente im Ultraviolettlicht überprüft.

2.7. Messungen intrazellulärer zytosolischer cGMP Fraktionen in Geweben und isolierten Zellen.

Zytosolische Proteine aus Nieren-, Leber- und Lungengewebe sowie isolierte Podozyten, Mesangial-, interstielle- und Ito-Zellen wurden in Anwesenheit von 3-isobutyl-1-methylxanthine mit einem NO-Donor inkubiert und anschließend die Konzentration des gebildeten cGMP über Radioimmunoassay oder enzymatisch gebundenen Immunabsorptionsassay gemessen.

3. Ergebnisse.

3.1. Identifikation immunhistochemisch markierter Strukturen in Niere und Leber.

Zur Identifikation wurden immunhistochemisch markierte Strukturen morphologisch und in Doppelmarkierungsexperimenten ausgewertet. Es wurden Desmin für die Markierung des intra- und extraglomerulären Mesangiums, Podosynapsin für die Podozyten, 5´-Ekto-Nukleotidase für die kortikalen Fibroblasten, NADPH-diaphorase-Reaktion und NOS1 Färbung für die Macula densa, THP für die TAL, NCC für den DCT und Na/Ca und Calbindin für den CNT verwendet.

3.2. Lokalisation der Komponenten des L-Arginin-NO-Systems.

NO-Synthese in der Niere findet sich im Endothel von nahezu allen Gefäßen einschließlich der Kapillaren und der Glomerulumgefäße. Hier konnte die endotheliale Isoform NOS3 identifiziert werden. Das kortikale Interstitium war weitgehend frei von NO-Synthasen, während im inner-medullären Interstitium gelegentlich NOS1-positive Fibroblasten detektiert wurden. In den Nephronepithelien wurde ausschließlich NOS1 gefunden. NOS1 Expression beschränkte sich auf die Macula densa und benachbarte Zellen der aufsteigenden Schleife als Teil des juxtaglomerulären Apparats. Dies wurde über eine Kolokalisation von NOS1 mit der NADPH-Diaphorase Reaktion und über In situ Hybridisierung für NOS1 mRNA gezeigt [12]. Die Lokalisation des wichtigsten NO-„Rezeptors“, der löslichen Guanylatzyklase (sGC) war Schwerpunkt der vorliegenden Studie. Immunhistochemie mit einem Antikörper gegen die β_1 Untereinheit der sGC zeigte eine positive Reaktion im Glomerulus, in Gefäßmuskelzellen sowie in interstitiellen Zellen. Im Glomerulus fand sich die sGC im Mesangium des Kapillarknäuels. Weiterhin waren die Strukturen des JGAs markiert. So fand sich die sGC in der Wand der kleinen Widerstandsgefäße, wie der afferenten Arteriole mit ihren granulierten, renin-enthaltenden Zellen, der efferenten Arteriole sowie des extraglomerulären Mesangiums zwischen den Arteriolen. Das Signal zeigte zellulär eine

zytosolische Lokalisation. Diese Befunde wurden über In situ Hybridisierung der α_1 und β_1 sGC bestätigt. Zusätzlich wurde mit Hilfe von RT-PCR in isolierten Glomeruli die mRNA beider sGC Untereinheiten lokalisiert. In isolierten Mesangialzellen wurde per Western blot die $ß_1$ Untereinheit (UE) des Enzyms identifiziert. Die NO-abhängige cGMP-Produktion wurde ebenfalls in Mesangialzellen über Gabe eines NO-Donors bestätigt. Neben dem JGA zeigten die aus der efferenten Arteriole der juxtamedullären Nephrone entspringenden absteigenden Vasa recta in ihren kontraktilen Abschnitten eine starke sGC-Immunreaktivität. Die Perizyten, welche die Aufgabe der Kontraktion wahrnehmen und sie fassreifenförmig umgeben, waren hierbei stark markiert. Die Fibroblasten des kortikalen Labyrinths sowie die entlang der Gefäßbündel waren positiv gefärbt. Die In situ Hybridisierung für beide UE, welche mRNA Signale in peritubulärer und perivaskulärer Lokalisation mit einem Verteilungsmuster analog der typischen interstitiellen Fibroblasten zeigte, sowie Western blot Analyse und Messung der Enzymreaktivität nach NO-Donor Gabe von medullär isolierten Fibroblasten konnten diese Resultate unterstützen. Die Lokalisation der sGC in der Leber zeigte ein kräftiges immunhistochemisches Signal im Interstitium. Hier waren generell die Ito-Zellen positiv mit schwächer werdender Intensität von periportal zur Zentralvene hin. Positive Wandstrukturen größerer Lebergefäße wie portale Venulen und größere Venen wurden ebenfalls beobachtet. Unterstützend hierfür waren die Western blot Analyse von Leberhomogenat und isolierten Ito-Zellen, die In situ Hybridisierung und RT-PCR beider UE in der Leber sowie die Messung der Enzymreaktivität nach NO-Donor Gabe.

3.3. *Lokalisation der Enzyme der Prostaglandinsynthese in der Niere.*

Die Aktionen der Prostaglandine betreffen die Modulation der lokalen Hämodynamik, die Reninfreisetzung und die tubuläre Salz- und Wasserresorption. Die Hauptenzyme der Prostaglandinsynthese sind COX-1, COX-2 und für die Umwandlung in das renale Prostaglandin, PGE_2, die mPGES. Die Wirkung der Prostaglandine ist zum einen abhängig von deren Produktionsort und zum anderen von der Lokalisation und Dichte der spezifischen Rezeptoren. Am JGA ist die COX-2 abhängige Prostaglandinfreisetzung im Zusammenhang mit einer EP-4-vermittelten Signaltransduktion zur Synthese und Freisetzung von Renin beschrieben worden [19]. Wir fanden hier in der Ratte die COX-2 sowie auch die mPGES in Zellen der Macula densa und des umgebenden TAL lokalisiert. Die Maus besaß dagegen COX-2 Immunoreaktivität ausschließlich in der Macula densa. Die COX-1 konnten wir im extraglomerulären Mesangium und schwach im intraglomerulären Mesangium vorfinden. Neben der Beeinflussung der Reninsynthese sind zahlreiche über den EP-1- und EP-3-vermittelte tubuläre Effekte im Rahmen des Salz und -Wassertransports beschrieben worden [11]. Entlang des Tubulus war COX-1 in der Ratte im terminalen DCT, im CNT und in den Hauptzellen des CCD und MCD mit einer milden zytoplasmatischen und einer stärkeren Kernmembranfärbung nachweisbar. Es bestand kein Unterschied zwischen der Ratte und der Maus. COX-2 war auf einzeln verteilte, oder in Gruppen auftretende Zellen des TAL mit einer prominenten zytosolischen und einer schwächeren

Kernmembranfärbung nachweisbar. mPGES war in beiden Spezies sowohl mit COX-1 als auch mit COX-2 gemeinsam lokalisiert. Diese tubulären Befunde wurden durch In situ Hybridisierung bestätigt. Enzyme der Prostaglandinsynthese waren weiterhin in vaskulären und interstitiellen Strukturen vorhanden. Vaskulär konnten COX-1 deutlich und COX-2 nur gelegentlich im Endothel lokalisiert werden. Die kortikalen Fibroblasten waren in der Maus positiv für COX-1 wie auch für mPGES, während hier in der Ratte kein Signal für diese Enzyme gefunden wurde. Die medullären Lipid-beladenen interstitiellen Zellen sind ein schon früher definierter Produktionsort für Prostaglandine. COX-1, COX-2 und mPGES wurden in starkem Ausmaß sowohl in der Ratte als auch in der Maus in diesen Zellen exprimiert. Hier wurde ebenfalls eine Kolokalisation von PGES mit COX-1 bzw. COX-2 durch Doppelmarkierungen bestätigt.

3.4. Analyse der NOS1 Interaktion mit COX-2.

Sowohl die NOS1 vermittelte NO-Synthese wie auch die COX-2 abhängige Prostaglandinsynthese findet in der Macula densa und dem unmittelbar benachbarten TAL Segment statt. Beide Enzyme werden konstitutiv und teilweise kolokalisiert exprimiert. Diese zeigten analoge Expressionsänderungen unter verschiedenen Stimuli, wie unter renovaskulärer Hypertonie (2K1C Goldblatt-Modell), unter Inhibition des Na-K-2Cl-Kotransporters durch Furosemid oder Salzbeladung und Salzrestriktion [20-23]. Da NO COX-2 aktivieren kann [24] und eine Inhibition der NOS1 zu einem Absinken der juxtaglomerulären COX-2 Expresssion [5, 25, 26] führte, nahmen wir an, dass NO ein positiver Regulator der COX-2 ist. So untersuchten wir die Koexpression beider Enzyme durch Auszählung einzelner, für das jeweilige Antigen immunpositiver Zellen des JGA von Ratte und Maus unter veränderten Bedingungen.

COX-2 immunreaktive Zellen wurden nach 3 typischen Lokalisationen unterteilt: die Macula densa selbst, die Macula densa Region und die kortikale dicke aufsteigende Henle-Schleife (cTAL). Doppelmarkierungen von COX-2 und NOS1 ergaben, dass in der NOS1 positiven Macula densa nur eine oder zwei doppelt markierte Zellen, in der Macula densa Region jedoch mehrere solcher Zellen vorkamen. Im benachbarten cTAL wurden COX-2 positive Zellen grundsätzlich allein vorgefunden. Die Anzahl der Zellen, welche COX-2 allein oder zusammen mit NOS1 exprimieren, wurde in den experimentellen Modellen erhoben und mit dem Durchschnitt der entsprechenden Kontrollen verglichen.

Folgende Resultate wurden im Goldblatt-Modell erhalten:

Gruppe	COX-2 in der Macula densa selbst	COX-2 in der Macula densa Region	COX-2 in der cTAL	NOS1 gesamt
stenotische Niere (Kurzzeit)	+ 81 %	+ 71%	+ 73%	+ 35%
nichtstenotische Niere (Kurzzeit)	- 53%	- 41%	-14 %	- 14%
stenotische Niere (Langzeit)	+ 90%	+ 90%	+ 75%	+ 50%
nichtstenotische Niere (Langzeit)	- 70%	- 31%	-16%	- 16%

Die numerischen Veränderungen COX-2 positiver Zellen im Experiment zeigen demnach keinen Bezug zur Koexpression mit NOS1, woraus wir schließen, dass NO – zuminderst in der Zell-autonomen Betrachtungsebene - nicht für die Veränderungen der COX-2 erforderlich ist. Zur Überprüfung unserer Resultate wurden NOS1 defiziente, experimentell gleichfalls stimulierte Mäuse benutzt; diese bestätigten die Beobachtung, dass eine Stimulation von COX-2 auch bei Fehlen von NOS1 erfolgte.

4. Diskussion

Die hier in Kurzform dargelegten Resultate zeigen die Lokalisation von Schlüsselprodukten des L-Arginin-NO-Systems und des Prostaglandinsynthese-Systems sowie funktionelle Implikationen und Aspekte ihrer Interaktion.

4.1. Juxtaglomerulärer Apparat.

Der JGA besteht grundsätzlich aus den Glomerulumgefäßen, dem extraglomerulärem Mesangium und der Macula densa. NOS1 und NOS3 fanden wir in der Macula densa bzw. im Endothel [27-29], COX-2 jedoch nur im Epithel der Macula densa und benachbarter aufsteigender Schleife; wir bestätigten z. T. hiermit bestehende Vorarbeiten [22]. Für bedeutsam halten wir die Lokalisation der sGC in den glattmuskulären Elementen des JGA (Extraglomeruläres Mesangium und arterioläre Wandzellen) und die mPGES in der Macula densa, da diese Befunde Hypothesen stützen, die im Rahmen der tubulo-vaskulären Signaltransduktion aufgestellt worden sind [2]. Hierbei stand im Vordergrund, dass eine Hemmung des NKCC2-abhängigen Salztransports der aufsteigenden Schleife NOS1 und COX-2 stimuliert, und dass parallel sich Antworten in der gesteigerten Reninfreisetzung und in einer Dämpfung der konstriktiven TGF-Antwort der afferenten Arteriole messen ließen [2]. In vitro-Messungen ergaben einen Hinweis auf die permissive Rolle von cGMP bei der Reninfreisetzung [30]. Unsere Resultate bestätigen diesen Befund in situ, indem die cGMP-

freisetzende sGC in den Zielzellen, den granulierten Zellen des JGA nachweisbar war. Der Nachweis von sGC in den benachbarten Gefäßwandzellen und dem extraglomeurlären Mesangium weist ferner auf die Rolle von cGMP beim TGF hin und bestätigt damit Befunde an isolierten Präparationen [25, 26]. Unsere Befunde liefern somit das zellbezogene Substrat zur Bestätigung funktioneller vorausgegangener physiologischer Experimente. Dass hiermit die funktionelle Bedeutung der lokalen NO Freisetzung erschöpfend geklärt wäre, kann aufgrund neuester Befunde allerdings nicht ohne Einschränkung behauptet werden [31]. In ähnlicher Weise stützt unser Nachweis von mPGES in der Macula densa funktionelle Beobachtung der Rolle von Prostaglandin E_2 und $-I_2$ bei der Stimulation der Reninfreisetzung [32-35]. In einer vorausgegangenen Arbeit war hingegen das Fehlen dieses Enzyms auf mRNA-Ebene in Diskrepanz zu unseren Befunden [36]. Neuere Ergebnisse konnten unsere Arbeit zur Lokalisation der mPGES in der Macula densa bestätigen [37]. Unsere Befunde sind im Einklang mit der heraushebenden Rolle Macula densa-lokalisierter COX-2 bei verringertem Transport und bei Hemmung des RAS durch Angiotensin II-Rezeptorblocker [22, 23, 38] über das Effektorsystem von PGE_2 und deren spezifische Rezeptoren [19].Für die andere COX-Isoform, COX-1, welche wir ebenfalls innerhalb des JGA im EGM lokalisierten, konnte durch spezifische Hemmversuche keine Wirkung auf das RAAS nachwiesen werden [35].

4.2. Glomerulus.

Hier konnten wir sGC in den intraglomerulären Mesangialzellen vorfinden. Diese verankern die glomerulären Kapillarschlingen an ihrem Befestigungsapparat und sind an der mechanischen Integrität des glomerulären Hilus beteiligt. Rezeptoren für konstriktiv wirkende Hormone konnten durch andere Gruppen an den Mesangialzellen nachgewiesen werden [39]. Von den konstitutiven NOS parakrin freigesetztes NO könnte zum Ort seines Rezeptors diffundieren und über die zelluläre cGMP Produktion in den Mesangialzellen antagonistisch wirken. Auch die lokale Prostaglandinsynthese ist im Glomerulum von Bedeutung [40]. Hier konnten wir die COX-1 gleichfalls im intraglomerulären Mesangium lokalisieren und damit Interpretationen von Soler at.al [41], welche PGH_2 als Prostaglandinvorstufe in Mesangialzellen vorfanden, unterstützen. Obwohl wir mittels RT-PCR COX-2 mRNA in Glomerulumextrakt amplifizierten, konnten wir COX-2 Immunreaktivität nicht verlässlich detektieren. Dies wurde von einer anderen Arbeitsgruppe auf Proteinebene immunchemisch bestätigt [42, 43].

4.3. Vaskuläre Aspekte.

Für die Regulation der renalen Durchblutung sind die Widerstandsarteriolen des Kortex sowie die aus den Vasa efferentia der juxtamedullären Glomeruli entspringenden absteigenden Vasa recta relevant. Größere kortikale Widerstandsgefäße, mit Ausnahme der Glomerulumarteriolen, waren im Gegensatz zu den medullären absteigenden Vasa recta weniger stark für sGC-positiv. Die sGC-Immunreaktivität der Vasa recta lässt auf eine NO Abhängikeit in Zusammenhang mit der medullären Durchblutung schließen und ist somit das morphologische Korrelat zu den etablierten Effekten von NO auf die medulläre Durchblutung [12, 44]. Die Enzyme der Prostaglandinsynthese

ließen sich in der Ratte und Maus unter Kontrollbedingungen nicht sicher nachweisen. Hier konnte lediglich im Endothel größerer Gefäße die COX-1 gefunden werden. Dies steht im Widersrpuch zur Expression der Enzyme der Prostaglandinsythese in der menschlichen Niere [45]. Beide COX Isoformen sind human im renalen Gefäßbett weit verbreitet und spielen in der Pathophysiologie des Bluthochdrucks eine entscheidende Rolle.

4.4. Renales Interstitium.

Kortikale interstitielle Fibroblasten sind perikapillär angeordnet und nehmen Aufgaben der mechanischen Festigung sowie der funktionellen Integration tubulärer und vaskulärer Parameter wahr. Es bestehen Hinweise auf ihre Funktion, indem sie die Produktionsorte für Adenosin als Mediator des TGF [1] sowie für Erythropoetin [46] und NADPH Oxidase [47] in der Niere sind. Die sGC war in diesen kortikalen Zellen stark exprimiert. Dies kann den hohen cGMP Gehalt interstitieller Flüssikeit [48] in der Niere erklären und Hinweise auf die Signalvermittlung geben. Mit einer Diffusionslänge von 220µm und einer Lebenszeit von 60 Sekunden könnte man sich vorstellen, dass interstitiell gebildetes cGMP basolateral vom proximalen Tubulus aufgenommen wird, wie gezeigt in [48], und dort die Natriumresorption beeinflusst [49]. Dies könnte ein Teilaspekt der NO Wirkung auf den tubulären Transport sein. Im Gegensatz zur Ratte konnten wir in der Maus COX-1 und mPGES in den kortikalen interstitiellen Fibroblasten lokalisieren, während in beiden Spezies COX-1 und -2 und mPGES im Nierenmark in den medullären Fibroblasten vorkamen. Das Nierenmark wird oft auch als Prostaglandindrüse bezeichnet, welches die hohe Konzentration dieser widerspiegelt. Funktionell bieten sie ein Apoptoseschutz und verhindern eine Schädigung, wenn das Nierenmark osmotischen Veränderungen, wie zum Beispiel der Wasserrestriktion, ausgesetzt ist [50].

4.5. Epitheliale Aspekte.

Entgegen den früher publizierten PCR und immunhistochemischen Daten, welche sGC mRNA in den verschiedenen tubulären Epithelien und α_2 sGC Immunreaktivität im Sammelrohr detektierten [51-53], gelang es uns nicht die sGC im Epithel zu markieren. Die Diskrepanz zwischen diesen Resultaten mag an einem Sensitivitäts- oder Spezifitätsproblem liegen. Wir konnten sGC mRNA und Protein in einer Reihe verschiedener Zelltypen nachweisen, so dass es tubulär zumindest in einer niedrigeren Konzentration vorkommen müsste.

4.5.1. Dicke aufsteigende Henle'sche Schleife.

Entlang des Nephrons war der cTAL der erste positive Lokalisationsort für die Prostaglandinsynthese. Hier konnten wir COX-2, in einzeln verteilten Zellen, und mPGES in der Nähe der Macula densa vorfinden. Die Anzahl COX-2 positiver TAL Zellen beläuft sich auf 2% [54], welche den physiologischen Status reflektiert und die Möglichkeit einer Expressionssteigerung der COX-2 unter experimentellen Bedingungen zulässt. Dies reflektiert die induzierbare Natur des COX-2 im TAL wie auch in anderen Lokalisationen. Erwähnenswert beim Menschen ist, dass das COX-2 Protein in der MD nur im Alter und während pathologischer Veränderungen sichtbar

gemacht werden kann [55-57]. Über COX-2 gebildete Prostaglandine sind relevant für die epitheliale Funktion. So erlauben sie die Wirkung der Schleifendiuretika [21] und üben damit einen inhibitorischen Effekt auf den Na-K-2Cl-Kotransport in mTAL Zellen aus [58]. Auch in *in vitro* perfundierten mTAL konnte für PGE_2 eine inhibitorische Wirkung auf die Salzresorption nachgewiesen werden [11]. Die lokale Verteilung der PGE_2 Rezeptoren wird derzeit noch kontrovers diskutiert [11, 19]. Hervorzuheben ist die besondere Bedeutung des COX-2 während der perinatalen Entwicklung der Niere. Die deutlich stärkere neonatale Expression [59] konnte durch die Beobachtung unterstützt werden, dass COX-2 defiziente Mäuse einen Nephronschaden während der Entwicklung erleiden [60]. Die intrazelluläre Signalkaskade, hervorgerufen durch die über COX-2 und mPGES gebildeten Prostaglandine, ist zum Teil erfasst und beinhaltet eine schnelle Phosphorylierung von p38 und ERK1/2 Kinasen sowie die Stimulation von MAP Kinasen [61].

4.5.2. Distales Konvolut und Sammelrohr

. Die Lokalisation von COX-1 und mPGES begann mit der 2. Hälfte des DCT und erstreckte sich weiter über den CNT, CCD und das gesamt medulläre Sammelrohr, ausgenommen die Schaltzellen dieser Segmente. Dies traf sowohl für die Ratte wie für die Maus zu. Diese Beobachtungen sind teilweise in Einklang mit einer früheren Beschreibung der COX-1 im Sammelrohr [56, 62]., jedoch entgegengesetzt zu Befunden von Ferguson et.al [63] welcher sowohl COX-1 und wie auch COX-2 nur in den Schaltzellen des CCD vorfand. Probleme der Antikörper-Spezifität könnten hierfür die Grundlage sein. Die Wirkung der Prostaglandine ist in diesem Segment über die Prostaglandin E-Rezeptoren EP-1 und EP-3 vermittelt, welche durch pharmakologische Hemmstudien hier lokalisiert worden sind [11]. Die Funktionen der hier gebildeten Prostaglandine betreffen die Feinregulation der Salz- und Wasserhomöostase. So konnte gezeigt werden, dass endogen gebildetes ebenso wie exogen zugeführtes PGE_2 die bekannten Effekte von Vasopressin auf die Wasserausscheidung des Sammelrohres inhibieren [64]. PGE_2 kann weiterhin die Salzresorption im CCD über einen Kalzium-gekoppelten Mechanismus vermindern [65]. Eine streng basolateral gerichtete Gabe von PGE2 führte zu einer vermehrten Wasserausscheidung, so dass hier vermutlich die Lokalisation des Rezeptors im Epithel von Bedeutung ist [65]. Unsere Untersuchungen zeigten ebenfalls sehr starke Signale für COX-1 und mPGES im DCT und CNT. Hier könnten lokale Wirkungen über den EP-4 Rezeptor vermittelt werden [19] oder mit dem lokalen Kallikrein-Bradykininsystem [66], der Aldosteronwirkung oder dem Amilorid-sensitiven epithelialen Natriumkanal interagieren [67].

4.6. <u>Ito-Zellen der Leber.</u>

Die Lokalisation der sGC und lokale cGMP Freisetzung steht mit funktionellen Daten über diesen Zelltyp im Einklang. Ito-Zellen wurden als leberspezifische Perizyten beschrieben, welche sich im Disse-Raum befinden und hier lange Ausläufer zwischen Sinusendothel und Parenchymzellen besitzen [68]. Sie sind mit den renalen kortikalen interstitiellen Zellen verwandt, indem sie Eigenschaften wie die Erythropoetinproduktion [69] und die Expression der neutrophilen NADPH

Oxidase und 5´Ektonukleotidase [47] mit diesen teilen. Die Lokalisation der sGC in Ito-Zellen weist auf die Funktion des NO und CO in Hinblick auf die Einstellung des kontraktilen Tonus der Ito-Zellen hin. So kommt der sGC hier auch eine Bedeutung bei der Regulation der sinusoidalen Mikrozirkulation und damit auch des portalen Blutdrucks. In Übereinstimmung mit unseren Resultaten sind die Beobachtungen von Kawada et al, die cGMP Freisetzung aus Ito-Zellen nach NO-Gabe berichten[70].

4.7. Zusammenhang zwischen NOS1 und COX-2.

Die räumliche Nähe der Expression von COX-2 und NOS1 im Bereich der MD und ihre bei einigen Versuchsbedingungen gleichsinnige Expressionsänderung führten im Verein mit funktionellen Studien zu der Interpretation, dass zwischen beiden Enzymen ein funktioneller Zusammenhang besteht. Die Einflussnahme von in der Macula densa gebildetem NO auf die COX-2 der Macula densa und ihrer Nachbarzellen ist dadurch gegeben, dass NO mit Häm-Proteinen interagieren kann [71] und COX-2 ein Enzym mit einer Häm-Domäne ist [72]. In kultivierten Zellen verschiedener Herkunft konnte nachgewiesen werden, dass NO in der Lage ist die Prostaglandinproduktion zu stimulieren [73-75]. Dies wurde auch in cTAL Zellen gezeigt, in denen sich die Expression von COX-2 unter Zugabe von NO-Donor oder cGMP signifikant erhöhte bzw. sich durch Gabe eines selektiven NOS1 Inhibitors erniedrigen ließ [76], während in anderen Modellen gegensätzliche Reaktionen beobachtet wurden [77]. Unsere Untersuchungen an verschieden stimulierten Rattenmodellen ergaben für die COX-2 der Macula densa und Nachbarzellen, die auch NOS1 exprimieren, gleiche Expressionsänderungen wie in entfernter liegenden, NOS1-negativen Zellen des TAL. Summarisch zeigte die Auswertung dieser Zellen ähnliche Änderungen für NOS1 und COX-2 wie in früher beschriebenen Studien [14, 20-23, 63]. Auch NOS1 defiziente Mäuse zeigten unter normalen und stimulierten Konditionen keinen Unterschied der Expressionsänderungen von COX-2 im Vergleich zu den entsprechenden Wildtyptieren. Wir schließen hieraus, dass intrazelluläres NO für die COX-2 Synthese nicht notwendig ist. Damit spiegeln unsere *in vivo* Daten nicht die in Zellkultur erhobenen Ergebnisse wider. Es ist denkbar, dass NO in denjenigen Zellen, die beide Enzyme exprimieren, die Expression von COX-2 dennoch bestimmt, dass jedoch in den lediglich COX-2 exprimierenden Zellen auch andere Signalwege wirksam sind. So ist ein generell gültiger Mechanismus der COX-2 Stimulation über eine Chlorid-bezogene Verringerung der Na-K-2Cl-Tranportleistung durch die Freisetzung von PGE2 gut belegt [78].

4.8. Zusammenfassend

haben wir mit der Lokalisation der sGC in der Niere vaskuläre und interstitielle Strukturen gekennzeichnet, die sich mit zuvor aufgestellten Konzepten NO-stimulierbarer Signalwege für Nierenkortex und Mark in Übereinstimmung bringen lassen und diese im Detail verdeutlichen. Dies gilt auch für die hepatischen Ito-Zellen. Die Analyse der Verteilung der Enzyme der Prostaglandinsynthese in der Niere konnte ebenso die funktionellen Interpretationen von ortsspezifischer PGE2 Wirkung auf die Regulation des Blutflusses und der Salz- und

Wasserhomöostase präzisieren. Eine zuvor postulierte Abhängigkeit der COX-2 von lokaler NO-Freisetzung durch ko-exprimierte NOS1 ließ sich nicht erhärten.

7. Referenzliste

1. Schnermann J: Juxtaglomerular cell complex in the regulation of renal salt excretion. Am.J.Physiol 274:R263-R279, 1998

2. Schnermann J: Homer W. Smith Award lecture. The juxtaglomerular apparatus: from anatomical peculiarity to physiological relevance. J.Am.Soc.Nephrol. 14:1681-1694, 2003

3. Osswald H, Hermes HH, Nabakowski G: Role of adenosine in signal transmission of tubuloglomerular feedback. Kidney Int.Suppl 12:S136-S142, 1982

4. Sun D, Samuelson LC, Yang T, Huang Y, Paliege A, Saunders T, Briggs J, Schnermann J: Mediation of tubuloglomerular feedback by adenosine: evidence from mice lacking adenosine 1 receptors. Proc.Natl.Acad.Sci.U.S.A 98:9983-9988, 2001

5. Persson PB, Baumann JE, Ehmke H, Hackenthal E, Kirchheim HR, Nafz B: Endothelium-derived NO stimulates pressure-dependent renin release in conscious dogs. Am.J.Physiol 264:F943-F947, 1993

6. Beierwaltes WH: Macula densa stimulation of renin is reversed by selective inhibition of neuronal nitric oxide synthase. Am.J.Physiol 272:R1359-R1364, 1997

7. Schricker K, Kurtz A: Liberators of NO exert a dual effect on renin secretion from isolated mouse renal juxtaglomerular cells. Am.J.Physiol 265:F180-F186, 1993

8. Wagner C, Godecke A, Ford M, Schnermann J, Schrader J, Kurtz A: Regulation of renin gene expression in kidneys of eNOS- and nNOS-deficient mice. Pflugers Arch. 439:567-572, 2000

9. Kurtz A, Gotz KH, Hamann M, Kieninger M, Wagner C: Stimulation of renin secretion by NO donors is related to the cAMP pathway. Am.J.Physiol 274:F709-F717, 1998

10. Beavo JA: Cyclic nucleotide phosphodiesterases: functional implications of multiple isoforms. Physiol Rev. 75:725-748, 1995

11. Breyer MD, Breyer RM: Prostaglandin E receptors and the kidney. Am.J.Physiol Renal Physiol 279:F12-F23, 2000

12. Bachmann S, Bosse HM, Mundel P: Topography of nitric oxide synthesis by localizing constitutive NO synthases in mammalian kidney. Am.J.Physiol 268:F885-F898, 1995

13. Harris RC, McKanna JA, Akai Y, Jacobson HR, Dubois RN, Breyer MD: Cyclooxygenase-2 is associated with the macula densa of rat kidney and increases with salt restriction. J.Clin.Invest 94:2504-2510, 1994

14. Bosse HM, Bohm R, Resch S, Bachmann S: Parallel regulation of constitutive NO synthase and renin at JGA of rat kidney under various stimuli. Am.J.Physiol 269:F793-F805, 1995

15. Kreisberg JI, Hoover RL, Karnovsky MJ: Isolation and characterization of rat glomerular epithelial cells in vitro. Kidney Int. 14:21-30, 1978

16. Pavenstadt H, Bengen F, Spath M, Schollmeyer P, Greger R: Effect of bradykinin and histamine on the membrane voltage, ion conductances and ion channels of human glomerular epithelial cells (hGEC) in culture. Pflugers Arch. 424:137-144, 1993

17. Grupp IL, Lorenz JN, Walsh RA, Boivin GP, Rindt H: Overexpression of alpha1B-adrenergic receptor induces left ventricular dysfunction in the absence of hypertrophy. Am.J.Physiol 275:H1338-H1350, 1998

18. Knook DL, Seffelaar AM, de Leeuw AM: Fat-storing cells of the rat liver. Their isolation and purification. Exp.Cell Res. 139:468-471, 1982

19. Jensen BL, Stubbe J, Hansen PB, Andreasen D, Skott O: Localization of prostaglandin E(2) EP2 and EP4 receptors in the rat kidney. Am.J.Physiol Renal Physiol 280:F1001-F1009, 2001

20. Mann B, Hartner A, Jensen BL, Hilgers KF, Hocherl K, Kramer BK, Kurtz A: Acute upregulation of COX-2 by renal artery stenosis. Am.J.Physiol Renal Physiol 280:F119-F125, 2001

21. Mann B, Hartner A, Jensen BL, Kammerl M, Kramer BK, Kurtz A: Furosemide stimulates macula densa cyclooxygenase-2 expression in rats. Kidney Int. 59:62-68, 2001

22. Harris RC, McKanna JA, Akai Y, Jacobson HR, Dubois RN, Breyer MD: Cyclooxygenase-2 is associated with the macula densa of rat kidney and increases with salt restriction. J.Clin.Invest 94:2504-2510, 1994

23. Jensen BL, Kurtz A: Differential regulation of renal cyclooxygenase mRNA by dietary salt intake. Kidney Int. 52:1242-1249, 1997

24. Salvemini D, Currie MG, Mollace V: Nitric oxide-mediated cyclooxygenase activation. A key event in the antiplatelet effects of nitrovasodilators. J.Clin.Invest 97:2562-2568, 1996

25. Ito S, Ren Y: Evidence for the role of nitric oxide in macula densa control of glomerular hemodynamics. J.Clin.Invest 92:1093-1098, 1993

26. Welch WJ, Wilcox CS: Role of nitric oxide in tubuloglomerular feedback: effects of dietary salt. Clin.Exp.Pharmacol.Physiol 24:582-586, 1997

27. Mundel P, Bachmann S, Bader M, Fischer A, Kummer W, Mayer B, Kriz W: Expression of nitric oxide synthase in kidney macula densa cells. Kidney Int. 42:1017-1019, 1992

28. Bachmann S, Mundel P: Nitric oxide in the kidney: synthesis, localization, and function. Am.J.Kidney Dis. 24:112-129, 1994

29. Wilcox CS, Welch WJ: Macula densa nitric oxide synthase: expression, regulation, and function. Kidney Int.Suppl 67:S53-S57, 1998

30. Kurtz A, Della BR, Pfeilschifter J, Taugner R, Bauer C: Atrial natriuretic peptide inhibits renin release from juxtaglomerular cells by a cGMP-mediated process. Proc.Natl.Acad.Sci.U.S.A 83:4769-4773, 1986

31. Castrop H, Schweda F, Mizel D, Huang Y, Briggs J, Kurtz A, Schnermann J: Permissive role of nitric oxide in macula densa control of renin secretion. Am.J.Physiol Renal Physiol 286:F848-F857, 2004

32. Larsson C, Weber P, Anggard E: Arachidonic acid increases and indomethacin decreases plasma renin activity in the rabbit. Eur.J.Pharmacol. 28:391-394, 1974

33. Gerber JG, Nies AS, Olsen RD: Control of canine renin release: macula densa requires prostaglandin synthesis. J.Physiol 319:419-429, 1981

34. Jensen BL, Schmid C, Kurtz A: Prostaglandins stimulate renin secretion and renin mRNA in mouse renal juxtaglomerular cells. Am.J.Physiol 271:F659-F669, 1996

35. Traynor TR, Smart A, Briggs JP, Schnermann J: Inhibition of macula densa-stimulated renin secretion by pharmacological blockade of cyclooxygenase-2. Am.J.Physiol 277:F706-F710

36. Vitzthum H, Abt I, Einhellig S, Kurtz A: Gene expression of prostanoid forming enzymes along the rat nephron. Kidney Int. 62:1570-1581, 2002

37. Guan Y, Zhang Y, Schneider A, Riendeau D, Mancini JA, Davis L, Komhoff M, Breyer RM, Breyer MD: Urogenital distribution of a mouse membrane-associated prostaglandin E(2) synthase. Am.J.Physiol Renal Physiol 281:F1173-F1177, 2001

38. Cheng HF, Wang JL, Zhang MZ, Miyazaki Y, Ichikawa I, McKanna JA, Harris RC: Angiotensin II attenuates renal cortical cyclooxygenase-2 expression. J.Clin.Invest 103:953-961, 1999

39. Schlondorff D: The glomerular mesangial cell: an expanding role for a specialized pericyte. FASEB J. 1:272-281, 1987

40. Hartner A, Pahl A, Brune K, Goppelt-Struebe M: Upregulation of cyclooxygenase-1 and the PGE2 receptor EP2 in rat and human mesangioproliferative glomerulonephritis. Inflamm.Res. 49:345-354, 2000

41. Soler M, Camacho M, Sola R, Vila L: Mesangial cells release untransformed prostaglandin H2 as a major prostanoid. Kidney Int. 59:1283-1289, 2001

42. Dunlop ME, Muggli EE: Hyaluronan increases glomerular cyclooxygenase-2 protein expression in a p38 MAP-kinase-dependent process. Kidney Int. 61:1729-1738, 2002

43. Fujihara CK, Antunes GR, Mattar AL, Andreoli N, Malheiros DM, Noronha IL, Zatz R: Cyclooxygenase-2 (COX-2) inhibition limits abnormal COX-2 expression and progressive injury in the remnant kidney. Kidney Int. 64:2172-2181, 2003

44. Rhinehart KL, Pallone TL: Nitric oxide generation by isolated descending vasa recta. Am.J.Physiol Heart Circ.Physiol 281:H316-H324, 2001

45. Therland KL, Stubbe J, Thiesson HC, Ottosen PD, Walter S, Sorensen GL, Skott O, Jensen BL: Cycloxygenase-2 is expressed in vasculature of normal and ischemic adult human kidney and is colocalized with vascular prostaglandin E2 EP4 receptors. J.Am.Soc.Nephrol. 15:1189-1198, 2004

46. Bachmann S, Le Hir M, Eckardt KU: Co-localization of erythropoietin mRNA and ecto-5'-nucleotidase immunoreactivity in peritubular cells of rat renal cortex indicates that fibroblasts produce erythropoietin. J.Histochem.Cytochem. 41:335-341, 1993

47. Bachmann S, Ramasubbu K: Immunohistochemical colocalization of the alpha-subunit of neutrophil NADPH oxidase and ecto-5'-nucleotidase in kidney and liver. Kidney Int. 51:479-482, 1997

48. Jin XH, Siragy HM, Carey RM: Renal interstitial cGMP mediates natriuresis by direct tubule mechanism. Hypertension 38:309-316, 2001

49. Jin XH, McGrath HE, Gildea JJ, Siragy HM, Felder RA, Carey RM: Renal interstitial guanosine cyclic 3', 5'-monophosphate mediates pressure-natriuresis via protein kinase G. Hypertension 43:1133-1139, 2004

50. Castrop H, Vitzthum H, Schumacher K, Schweda F, Kurtz A: Low tonicity mediates a downregulation of cyclooxygenase-1 expression by furosemide in the rat renal papilla. J.Am.Soc.Nephrol. 13:1136-1144, 2002

51. Terada Y, Tomita K, Nonoguchi H, Marumo F: Polymerase chain reaction localization of constitutive nitric oxide synthase and soluble guanylate cyclase messenger RNAs in microdissected rat nephron segments. J.Clin.Invest 90:659-665, 1992

52. Ujiie K, Drewett JG, Yuen PS, Star RA: Differential expression of mRNA for guanylyl cyclase-linked endothelium-derived relaxing factor receptor subunits in rat kidney. J.Clin.Invest 91:730-734, 1993

53. Mundel P, Gambaryan S, Bachmann S, Koesling D, Kriz W: Immunolocalization of soluble guanylyl cyclase subunits in rat kidney. Histochem.Cell Biol. 103:75-79, 1995

54. Vio CP, Cespedes C, Gallardo P, Masferrer JL: Renal identification of cyclooxygenase-2 in a subset of thick ascending limb cells. Hypertension 30:687-692, 1997

55. Khan KN, Venturini CM, Bunch RT, Brassard JA, Koki AT, Morris DL, Trump BF, Maziasz TJ, Alden CL: Interspecies differences in renal localization of cyclooxygenase isoforms: implications in nonsteroidal antiinflammatory drug-related nephrotoxicity. Toxicol.Pathol. 26:612-620, 1998

56. Komhoff M, Grone HJ, Klein T, Seyberth HW, Nusing RM: Localization of cyclooxygenase-1 and -2 in adult and fetal human kidney: implication for renal function. Am.J.Physiol 272:F460-F468, 1997

57. Nantel F, Meadows E, Denis D, Connolly B, Metters KM, Giaid A: Immunolocalization of cyclooxygenase-2 in the macula densa of human elderly. FEBS Lett. 457:475-477, 1999

58. Kaji DM, Chase HS, Jr., Eng JP, Diaz J: Prostaglandin E2 inhibits Na-K-2Cl cotransport in medullary thick ascending limb cells. Am.J.Physiol 271:C354-C361, 1996

59. Zhang MZ, Wang JL, Cheng HF, Harris RC, McKanna JA: Cyclooxygenase-2 in rat nephron development. Am.J.Physiol 273:F994-1002, 1997

60. Morham SG, Langenbach R, Loftin CD, Tiano HF, Vouloumanos N, Jennette JC, Mahler JF, Kluckman KD, Ledford A, Lee CA, .: Prostaglandin synthase 2 gene disruption causes severe renal pathology in the mouse. Cell 83:473-482, 1995

61. Cheng HF, Wang JL, Zhang MZ, McKanna JA, Harris RC: Role of p38 in the regulation of renal cortical cyclooxygenase-2 expression by extracellular chloride. J.Clin.Invest 106:681-688, 2000

62. Smith WL, DeWitt DL, Garavito RM: Cyclooxygenases: structural, cellular, and molecular biology. Annu.Rev.Biochem. 69:145-182, 2000

63. Ferguson S, Hebert RL, Laneuville O: NS-398 upregulates constitutive cyclooxygenase-2 expression in the M-1 cortical collecting duct cell line. J.Am.Soc.Nephrol. 10:2261-2271, 1999

64. Hebert RL, Jacobson HR, Fredin D, Breyer MD: Evidence that separate PGE2 receptors modulate water and sodium transport in rabbit cortical collecting duct. Am.J.Physiol 265:F643-F650, 1993

65. Guan Y, Zhang Y, Breyer RM, Fowler B, Davis L, Hebert RL, Breyer MD: Prostaglandin E2 inhibits renal collecting duct Na+ absorption by activating the EP1 receptor. J.Clin.Invest 102:194-201, 1998

66. Rodriguez F, Llinas MT, Moreno C, Salazar FJ: Role of Cyclooxygenase-2-Derived Metabolites and NO in Renal Response to Bradykinin. Hypertension 37:129-134, 2001

67. Bachmann S, Bostanjoglo M, Schmitt R, Ellison DH: Sodium transport-related proteins in the mammalian distal nephron - distribution, ontogeny and functional aspects. Anat.Embryol.(Berl) 200:447-468, 1999

68. Ekataksin W, Kaneda K: Liver microvascular architecture: an insight into the pathophysiology of portal hypertension. Semin.Liver Dis. 19:359-382, 1999

69. Schuster SJ, Koury ST, Bohrer M, Salceda S, Caro J: Cellular sites of extrarenal and renal erythropoietin production in anaemic rats. Br.J.Haematol. 81:153-159, 1992

70. Kawada N, Tran-Thi TA, Klein H, Decker K: The contraction of hepatic stellate (Ito) cells stimulated with vasoactive substances. Possible involvement of endothelin 1 and nitric oxide in the regulation of the sinusoidal tonus. Eur.J.Biochem. 213:815-823, 1993

71. Ignarro LJ: Haem-dependent activation of guanylate cyclase and cyclic GMP formation by endogenous nitric oxide: a unique transduction mechanism for transcellular signaling. Pharmacol.Toxicol. 67:1-7, 1990

72. Smith WL, Marnett LJ: Prostaglandin endoperoxide synthase: structure and catalysis. Biochim.Biophys.Acta 1083:1-17, 1991

73. Salvemini D, Seibert K, Masferrer JL, Misko TP, Currie MG, Needleman P: Endogenous nitric oxide enhances prostaglandin production in a model of renal inflammation. J.Clin.Invest 93:1940-1947, 1994

74. Salvemini D, Seibert K, Masferrer JL, Settle SL, Misko TP, Currie MG, Needleman P: Nitric oxide and the cyclooxygenase pathway. Adv.Prostaglandin Thromboxane Leukot.Res. 23:491-493, 1995

75. Tetsuka T, Daphna-Iken D, Miller BW, Guan Z, Baier LD, Morrison AR: Nitric oxide amplifies interleukin 1-induced cyclooxygenase-2 expression in rat mesangial cells. J.Clin.Invest 97:2051-2056, 1996

76. Cheng HF, Wang JL, Zhang MZ, McKanna JA, Harris RC: Nitric oxide regulates renal cortical cyclooxygenase-2 expression. Am.J.Physiol Renal Physiol 279:F122-F129, 2000

77. Habib A, Bernard C, Lebret M, Creminon C, Esposito B, Tedgui A, Maclouf J: Regulation of the expression of cyclooxygenase-2 by nitric oxide in rat peritoneal macrophages. J.Immunol. 158:3845-3851, 1997

78. Peti-Peterdi J, Komlosi P, Fuson AL, Guan Y, Schneider A, Qi Z, Redha R, Rosivall L, Breyer MD, Bell PD: Luminal NaCl delivery regulates basolateral PGE2 release from macula densa cells. J.Clin.Invest 112:76-82, 2003

8. Publikationen

8.1. Theilig F, Bostanjoglo M, Pavenstädt H, Grupp C, Holland G, Slosarek I, Gressner AM, Russwurm M, Koesling D, Bachmann S: Cellular distribution and function of soluble guanylyl cyclase in rat kidney and liver. J Am Soc Nephrol 12: 2209-2220, 2001

8.2. Theilig F, Câmpean V, Paliege A, Breyer M, Briggs JP, Schnermann J, Bachmann S: Epithelial COX-2 expression is not regulated by NO: Colocalization studies in rat and mouse renal cortex. Hypertension 39: 848-853, 2002

8.3. Câmpean V, Theilig F, Paliege A, Breyer M, Bachmann S: Key enzymes for renal prostaglandin synthesis: site-specific expression in rodent kidney (rat, mouse). Am J Physiol 285: F19-F32, 2003

J Am Soc Nephrol 12: 2209–2220, 2001

Cellular Distribution and Function of Soluble Guanylyl Cyclase in Rat Kidney and Liver

FRANZISKA THEILIG,* MAGDALENA BOSTANJOGLO,* HERMANN PAVENSTÄDT,† CLEMENS GRUPP,‡ GUDRUN HOLLAND,* ILKA SLOSAREK,* AXEL M. GRESSNER,§ MICHAEL RUSSWURM,‖ DORIS KOESLING,‖ and SEBASTIAN BACHMANN*

**Department of Anatomy, Charité, Humboldt University, Berlin, Germany; †Department of Nephrology, University of Freiburg, Freiburg, Germany; ‡Department of Nephrology, University of Göttingen, Göttingen, Germany; §Department of Clinical Chemistry, Rheinisch-Westfälische Technische Hochschule Aachen, Aachen, Germany; and ‖Department of Pharmacology, Ruhr University, Bochum, Germany.*

Abstract. Soluble guanylyl cyclase (sGC) catalyzes the biosynthesis of cGMP in response to binding of L-arginine-derived nitric oxide (NO). Functionally, the NO-sGC-cGMP signaling pathway in kidney and liver has been associated with regional hemodynamics and the regulation of glomerular parameters. The distribution of the ubiquitous sGC isoform $\alpha1\beta1$ sGC was studied with a novel, highly specific antibody against the $\beta1$ subunit. In parallel, the presence of mRNA encoding both subunits was investigated by using *in situ* hybridization and reverse transcription-PCR assays. The NO-induced, sGC-dependent accumulation of cGMP in cytosolic extracts of tissues and cells was measured *in vitro*. Renal glomerular arterioles, including the renin-producing granular cells, mesangium, and descending vasa recta, as well as cortical and medullary interstitial fibroblasts, expressed sGC. Stimulation of isolated mesangial cells, renal fibroblasts, and hepatic Ito cells with a NO donor resulted in markedly increased cytosolic cGMP levels. This assessment of sGC expression and activity in vascular and interstitial cells of kidney and liver may have implications for understanding the role of local cGMP signaling cascades.

Guanylyl cyclase [GTP pyrophosphate-lyase (cyclizing), EC 4.6.1.2] exists in two isoenzyme forms and catalyzes the biosynthesis of cGMP from GTP. The membrane-bound forms are monomers that are stimulated by different peptide hormones. Soluble guanylyl cyclase (sGC) is a heme-containing heterodimer consisting of one α subunit (73 to 88 kD) and one β subunit (70 kD) (for review, see reference 1). The $\alpha1\beta1$ isoenzyme is thought to be the major form. In addition, two other subunits, $\alpha2$ and $\beta2$, have been cloned, and an $\alpha2\beta1$ isoform has been functionally characterized (2,3). sGC is the most well characterized receptor for nitric oxide (NO); binding of L-arginine-derived NO to the heme group of sGC results in marked stimulation of the enzyme, thus increasing the intracellular cGMP concentration (4). Increases in cGMP levels are responsible for cellular events that ultimately lead to decreases in intracellular calcium concentrations and smooth muscle relaxation (5) or to regulation of multiple genes through interactions with their respective promoters (6).

Received November 14, 2000. Accepted April 16, 2001.

Correspondence to Dr. Sebastian Bachmann, AG Anatomie/Elektronenmikroskopie, Charité CVK, BMFZ, Augustenburger Platz 1, D-13353 Berlin, Germany. Phone: +49-30-450-528-411; Fax: +49-30-450-528-922; E-mail: sbachm@charite.de

1046-6673/1211-2209
Journal of the American Society of Nephrology

In the kidney, both vascular and tubular effects of NO have been observed (for review, see references 7, 8, and 9), and the cellular sources for constitutive NO synthase (NOS), which catalyzes the formation of NO, have been identified (10,11). Because of the wide diversity of cell types in this organ, a detailed knowledge of sGC distribution is required for an understanding of local, cGMP-mediated effects of NO. A number of earlier studies demonstrated the organ- and cell-specific presence of sGC mRNA, by PCR and Northern blot analyses (12–15), and of the immunoreactive protein, by immunohistochemical and Western blot analyses (16,17). To date, however, there is still disagreement with respect to the reported immunohistochemical distribution of sGC and functional data. This study was performed in kidneys, to test the hypothesis that more structures than previously established are involved in NO-sGC-cGMP signaling as a major regulatory pathway in end-organ perfusion and specific cell function. We used a newly generated, affinity-purified antibody against a carboxy-terminal domain of $\beta1$ sGC, which, because of its monospecificity in Western blotting analyses and its cellular localization spectrum, was clearly superior to previously used antisera. Immunohistochemical data obtained with this antibody were corroborated by Western blot analyses of extracts from tissues and isolated cell preparations, by *in situ* hybridization, by reverse transcription (RT)-PCR assays of tissues and isolated cell extracts (using probes for both $\alpha1$ and $\beta1$ sGC), and by *in vitro* assessment of NO-dependent accumulation of cGMP in

tissues and cultured cells. The liver was studied to compare cell type specificity of sGC localization and function with another end-organ with a well established role of the NO-sGC-cGMP pathway. Mechanisms involved in NO-dependent regulation of local hepatic microcirculation were previously identified (18–20). Common aspects of cGMP-dependent signaling in kidney and liver are discussed.

Materials and Methods

Animals and Tissue Preparation

Male Sprague-Dawley rats weighing between 200 and 450 g were obtained from the local animal facilities of the Departments of Anatomy, Charité, and Nephrology, University of Freiburg, and of the Department of Clinical Chemistry, University of Aachen. Male Wistar rats (Harlan-Winkelmann, Borchen, Germany) were used for the experiments on isolated renal fibroblasts. All animals had been maintained with standard chow and tap water. For morphologic and immunohistochemical evaluations, a total of six rats (approximate body weight, 200 g) were used. For perfusion-fixation, animals were anesthetized by intraperitoneal injection of Nembutal (40 mg/kg body wt; Sanofi, Hannover, Germany). Animals underwent cannulation of the abdominal aorta and perfusion with sucrose-phosphate-buffered saline (PBS) solution (330 mosmol, pH 7.3) for 15 to 20 s at a pressure of 220 mmHg, directly followed by perfusion with paraformaldehyde (3% in PBS, pH 7.3) for 90 s at 220 mmHg and then for 200 s at 100 mmHg. Fixative was removed from the animal by subsequent perfusion with sucrose-PBS solution for 60 s at 100 mmHg. Tissues were then removed and dissected for further preparations. For *in situ* hybridization and conventional immunohistochemical analyses, tissues were immersed in 800-mosmol sucrose-PBS solution (pH 7.3) for 12 h, shock-frozen in liquid nitrogen-cooled isopentane, and stored at −70°C. For pre-embedding immunohistochemical analyses, tissue blocks were postfixed for 12 h in paraformaldehyde (3% in PBS containing 0.5% glutaraldehyde) and stored in sucrose-PBS solution (330 mosmol) at 4°C until embedding in agarose and sectioning (30 μm) with a Vibratome (1000S; Leica, Weiterstadt, Germany) tissue slicer.

Isolation of Glomeruli

Glomeruli were isolated as described previously (21). As for all other tissue isolation procedures described in this section, rats were anesthetized with sodium pentobarbital (50 mg/kg body wt). Kidneys were removed and prepared, under sterile conditions, in ice-cold RPMI 1640 medium (Seromed, Berlin, Germany). Cortices were sieved by using steel sieves with pore sizes of 150 μm and then 100 μm. The sieved structures were captured with a smaller sieve (pore size, 50 μm), transferred to 50-ml tubes, and centrifuged (4000 rpm, 4°C, 10 min). The pellet was then transferred into a small volume (2 to 3 ml) and divided into aliquots (100 μl). The aliquots were transferred to a microdissection chamber, 200 glomeruli/aliquot were microdissected, and aliquots were pooled and centrifuged (15,000 rpm, 1 min, 4°C). The resulting pellet was then prepared for mRNA extraction.

Isolation of Renal Mesangial Cells and Podocytes

Mesangial cells were isolated and cultured as described previously (22). In brief, glomeruli were obtained as described above, incubated with collagenase (1 g/L; Sigma, Deisenhofen, Germany) for 15 min, and suspended in RPMI 1640 medium supplemented with 170 g/L fetal calf serum, 2.5 mM L-glutamine, 0.1 mM sodium pyruvate, 100 U/ml penicillin, 100 mg/L streptomycin, 0.2 g/L nonessential amino acids (all from Seromed, Berlin, Germany), and 5 mg/L insulin-transferrin-sodium selenite supplement (Roche, Mannheim, Germany). Approximately 50 glomeruli/cm^2 were plated onto collagen-coated glass coverslips (Greiner, Nürtingen, Germany) and incubated at 37°C in an incubator with a water-saturated atmosphere of 5% CO_2/95% air. Mesangial cells were morphologically characterized by phase-contrast microscopy. They stained positively for smooth muscle actin, desmin, and vimentin but not for cytokeratin and factor VIII, which demonstrates the absence of glomerular epithelial and endothelial cells. Cells responded to 10^{-4} mM angiotensin II with increases in free cytosolic calcium concentrations.

Podocytes were isolated and cultured as described (23). Briefly, immortalized mouse podocytes carrying the thermosensitive variant of the SV40 T antigen inserted into the mouse genome were used. These podocytes proliferate at 33°C in the presence of interferon γ, whereas cells are transformed into the quiescent differentiated phenotype at 37°C in the absence of interferon γ. Podocytes then stain positively for the podocyte differentiation markers WT-1 and synaptopodin. Cells between passage 14 and passage 20 were seeded at 37°C onto collagen-coated plates and cultured for at least 7 d, until cells were differentiated, in standard RPMI 1640 medium containing 10% fetal calf serum, 100 U/ml penicillin, and 100 mg/L streptomycin.

Isolation and Culture of Renal Medullary Fibroblasts

Detailed procedures for the isolation and culture of rat inner medullary fibroblasts were published previously (24). In brief, rats were euthanized by cervical dislocation. Kidneys were immediately removed, and the inner medulla was excised. Tissue was placed in 290-mosmol, ice-cold, Hepes-Ringer's buffer (118 mM NaCl, 16 mM H-Hepes, 16 mM Na-Hepes, 14 mM glucose, 3.2 mM KCl, 2.5 mM $CaCl_2$, 1.8 mM $MgSO_4$, 1.8 mM KH_2PO_4, pH 7.4), minced with a razor blade, and subsequently incubated for 75 min at 37°C in Hepes-Ringer's buffer containing 0.2% (wt/vol) collagenase (CLS II; Cooper, Frankfurt, Germany) and 0.2% (wt/vol) hyaluronidase (Roche Diagnostics, Mannheim, Germany). After completion of the incubation procedure, the majority of the collecting duct cells in suspension were removed by low-speed centrifugation. The supernatants from the first two low-speed centrifugations, containing the majority of interstitial cells, were further separated from collecting duct cells with the use of beads coated with *Dolichos biflorus* agglutinin, as described (24). The resulting cell suspension was then subjected to single-step density gradient centrifugation with Nycodenz (Nyegaard Co., Oslo, Norway). After centrifugation, interstitial cells were maximally enriched, with a density of 1.081 to 1.093 g/cm^3. After removal of the Nycodenz, cells were plated in culture wells and maintained in Dulbecco's modified Eagle's medium/nutrient mixture Ham's F-12 medium (1:1) supplemented with 2 mM glutamine, 1 mM sodium pyruvate, 1% (vol/vol) nonessential amino acids, 50 U/ml penicillin, 50 U/ml streptomycin, and 10% fetal calf serum (all from Life Technologies, Eggenstein, Germany). Passage 1 cultures were examined.

Isolation and Culture of Hepatic Ito Cells

The isolation and culture of liver Ito cells from male Sprague-Dawley rats (body weight, 500 to 600 g) were performed as described previously (25). In brief, nonparenchymal liver cells were isolated by using the pronase-collagenase method (26). Ito cells were purified by single-step density gradient centrifugation in Nycodenz (see above) and were identified on the basis of their typical light-microscopic appearance and vitamin A-specific autofluorescence. The mean purity

of freshly isolated cells was 90 ± 5%, cell viability was >95%, and the yield ranged from 30 to 50 × 10^6 cells/liver. Ito cells were seeded at a density of 0.2 × 10^6 cells/cm^2, in 2 ml of Dulbecco's modified Eagle's medium containing 4 mM L-glutamine, 10% fetal calf serum, 1000 U/ml penicillin, and 100 mg/ml streptomycin. Cells were maintained in a humidified atmosphere of 5% CO_2/95% air at 37°C. The medium was changed approximately 20 h after seeding, after which the purity of Ito cells was >97%. The second medium change was approximately 28 h after seeding, at which time fetal calf serum supplementation was reduced to 0.2%.

Histochemical and Western Blotting Protocols

Primary Antibodies. A polyclonal antibody against the carboxy-terminus of the β1 subunit (SRKNTGTEETEQDEN) of bovine lung sGC (27) was raised in rabbits and immunopurified using the antigenic peptide coupled to SulfoLink coupling gel (Pierce, Boston, MA). A rabbit polyclonal antibody against NOS1 purified from porcine cerebellum (28) was a gift from Bernd Mayer (Graz, Austria). A mouse monoclonal antibody against the podocyte-specific antigen podosynapsin was kindly provided by Peter Mundel (New York, NY). A mouse monoclonal antibody against human α-smooth muscle actin was acquired from Dako (Glostrup, Denmark). A mouse monoclonal antibody against human desmin was also acquired from Dako. A rabbit polyclonal antibody against ecto-5'-nucleotidase was a gift from Brigitte Kaissling (Zurich, Switzerland).

Western Blot Analyses. Freshly isolated kidneys, lungs, skeletal muscle, and liver from rats were rapidly dissected and cut into small pieces. The cortex and medulla from kidneys were separated. Isolated Ito cells, mesangial cells, and interstitial cells were also assayed. These samples were homogenized on ice in homogenization buffer [175 mM NaCl, 1 mM ethylenediaminetetraacetate, 50 mM triethanolamine-HCl, pH 7.4, 2 mM dithiothreitol (DTT), 1 μM pepstatin, 0.2 mM benzamidine, 0.5 mM phenylmethylsulfonyl fluoride], using a glass/glass homogenizer. The homogenate was then centrifuged for 30 min at 4°C at 200,000 × *g*. The supernatant (cytosol) was supplemented with 50% (vol/vol) glycerol and stored at −20°C. Cytosolic proteins (16 to 20 μg) were separated by sodium dodecyl sulfate-polyacrylamide gel electrophoresis (7.5%) and blotted onto nitrocellulose membranes. Blots were blocked for 30 min with Roti-Block (Roth, Karlsruhe, Germany) and incubated overnight at 4°C with antibody against β1 sGC. After extensive washing, blots were incubated with a horseradish peroxidase-linked anti-rabbit IgG (Sigma). Immunoreactive bands at 70 kD were detected on the basis of chemiluminescence, using an enhanced chemiluminescence kit (Amersham Pharmacia, Freiburg, Germany). In blots generated from extracts of the renal cortex, a degradation band of approximately 55 kD was detected.

Immunohistochemical Analyses. Immunolabeling was performed with cryostat sections of 3- to 5-μm thickness. After being blocked with 5% skim milk in PBS (pH 7.4), sections were incubated with primary antibody for 2 h at room temperature and then overnight at 4°C. The different primary antibodies were administered simultaneously in double-labeling experiments. Thorough rinsing in PBS was followed by signal detection with Cy3-conjugated goat anti-rabbit IgG serum (diluted 1:250 in skim milk-PBS) and Cy2-conjugated donkey anti-mouse IgG (diluted 1:100), for 1 h at room temperature (all secondary antisera from Dianova, Hamburg, Germany). In double-labeling experiments, secondary antibodies coupled to different fluorochromes were applied. Control experiments to confirm the specificity of the antibody against β1 sGC were performed with omission of specific antibody, as well as competition with the antigenic peptide.

Ultrastructural Pre-Embedding Histochemical Analyses. For fine structural immunolabeling and immunoperoxidase labeling, an established protocol was used (10); for incubation of 20-μm-thick slices generated with a Vibratome, anti-β1 sGC antibody was used at dilutions between 1:25 and 1:50. Sections were incubated overnight in microtiter plates, postfixed with 1% osmium tetroxide, rinsed in maleate buffer, stained *en bloc* with uranyl acetate, and flat-embedded in Epon 812. Semithin sections were produced and photographed by using a light microscope. Ultrathin sections were then cut and viewed by using an electron microscope. Control experiments were performed by replacing primary antibodies with skim milk-PBS controls.

NADPH-Diaphorase Staining. The catalytic activity of NOS was demonstrated by enzymatic reduction of nitro blue tetrazolium in the presence of NADPH (NADPH-diaphorase reaction) (28). Slides were washed in PBS and incubated for 15 to 20 min in 0.1 M phosphate buffer containing 0.3% Triton X-100, 0.01% nitro blue tetrazolium, and 0.1% NADPH. No reaction product was observed when NADPH was replaced by NADH.

***In Situ* Hybridization.** The mRNA expression of the α1 and β1 subunits of sGC was investigated by *in situ* hybridization using digoxigenin-labeled riboprobes made from the bovine cDNA coding for the respective subunits. According to the protocol provided by the manufacturer (Roche), sense and antisense riboprobes were generated by *in vitro* transcription of the 647-bp α1 or 2000-bp β1 sGC cDNA fragment, using T3 and T7 polymerases and digoxigenin-labeled UTP, followed by time-controlled alkaline hydrolysis. For *in situ* hybridization, 7-μm cryostat sections were treated according to an established protocol (10). Briefly, 10 ng sGC antisense mRNA/μl hybridization mixture was incubated for 18 h at 48°C. The slides were washed sequentially with decreasing concentrations of SSC at 40°C and then with buffer 1 (0.1 M Tris-HCl, 0.15 M NaCl, pH 7.5) at room temperature and were then incubated for 30 min with buffer 1 containing 1% blocking reagent and 0.5% bovine serum albumin. Sheep anti-digoxigenin-alkaline phosphatase conjugate (diluted 1:500 in blocking medium) was applied for 60 min at room temperature and then overnight at 4°C. The slides were washed twice with buffer 1 and rinsed in buffer 3 (0.1 M Tris-HCl, 0.1 M NaCl, 0.05 M $MgCl_2$, pH 9.5). A solution of 4-nitro blue tetrazolium chloride, 5-bromo-4-chloro-3-indolylphosphate, and levamisole dissolved in buffer 3 was then used for the color reaction. The reaction was stopped by two washes with buffer 4 (0.1 M Tris-HCl, 1 mM ethylenediaminetetraacetate, pH 8.0). As a control, sense probes were applied in parallel with antisense probes. Slides were rinsed with PBS and coverslipped with PBS-glycerol.

RT-PCR

Total RNA was isolated from kidney cortex, medulla, and liver by using a commercially available kit (InViTek, Berlin, Germany). RNA was extracted with phenol/chloroform, precipitated with isopropanol, and resuspended in diethylpyrocarbonate-treated water. RNA from isolated glomeruli was extracted by using the guanidinium thiocyanate method (29). All samples were quantified by spectrophotometric analyses at 260 nm. Five micrograms of total RNA from each sample were reverse-transcribed with 60 U of murine Moloney leukemia virus reverse transcriptase for 25 min at 37°C, in a total volume of 15 μl, according to the protocol provided by the manufacturer (Roche). The samples were then heated at 70°C for 5 min, to inactivate the enzyme. These cDNA were used to compare the amounts of α1 sGC mRNA or β1 sGC mRNA *versus* glyceraldehyde-3-phosphate dehydrogenase (GAPDH) mRNA in different tissues. PCR were performed with specific primers for α1 sGC (5'-CCACATCAACACCG-

GCTAAT-3' and 5'-GAAGTGCAAGDTTCAGTCTC-3'), for β1 sGC (5'-CGGATGCCACGGTATTGTCT-3' and 5'-CTCCTGGCTT-GACGCACATT-3'), and for GADPH (5'-TATCCGTTGTGGATCT-GAC-3' and 5'-TGGTCCAGGGGTTTCTTAC-3' or 5'-ACCA-CAGTCCATGCCATCAC-3' and 5'-TCCACCACCCTGTTGCTGTA-3'). cDNA fragments of the expected sizes of 331 bp (α1 sGC), 329 bp (β1 sGC), and 304 and 446 bp (GAPDH with the two different primer pairs used) were amplified in 35 cycles (20 s at 94°C, 20 s at 59°C/63°C, and 30 s at 72°C) with 0.06 U/ml *Taq* polymerase and 50 mM $MgCl_2$. The PCR products were separated on 3% agarose gels, stained with ethidium bromide, and observed with ultraviolet illumination.

Quantitative RT-PCR

Quantitative RT-PCR is based on the assumptions that the cDNA template and a competitive internal template compete equally for the primers and that amplification is colinear. The PCR fragment obtained with the β1 sGC primers (see above) contains two sites for the restriction enzyme *Nla*III. Digestion of the β1 sGC PCR product with *Nla*III yielded three fragments, which were separated on agarose gels and then purified. The outer two fragments were ligated and served as a competitive template. A 0.3-μg sample of total RNA was reverse-transcribed in the presence of decreasing amounts of the internal standard (20 ng, 2 ng, 200 pg, 20 pg, and 2 pg), in 25 μl. Each assay included 0.06 U/ml *Taq* polymerase (InViTek), 50 mM $MgCl_2$, 25 mM dNTP, 0.1 mM DTT, and 10 mM concentrations of the aforementioned β1 sGC primers. The cDNA were amplified in 30 cycles (20 s at 94°C, 20 s at 59°C, and 30 s at 72°C), size-fractionated in 3% agarose gels, stained with ethidium bromide, and observed with ultraviolet illumination.

Determination of sGC Activity in Cytosolic Fractions by RIA

Cytosolic proteins (10 μg each) from the indicated tissues were incubated in the presence of 300 μM GTP, 3 mM $MgCl_2$, 3 mM DTT, 0.5 mg/ml bovine serum albumin, 0.25 g/L creatine phosphokinase, 5 mM creatine phosphate, 1 mM 3-isobutyl-1-methylxanthine (RBI, Köln, Germany), and 50 mM triethanolamine hydrochloride (pH 7.4), in a total volume of 0.1 ml. Stimulation of sGC was performed by addition of 300 μM *S*-nitrosoglutathione (Alexis, Grünberg, Germany). The incubation was stopped by the addition of ice-cold ethanol (final concentration, 70%). Formed cGMP was measured by RIA, as described (30).

Measurements of Intracellular cGMP Levels in Isolated Cells

Cells were cultured in six-well plates, maintained at 37°C, and rinsed with physiologic Ringer's solution. After preincubation with 0.5 M 3-isobutyl-1-methylxantine for 5 min, cells were exposed to *S*-nitroso-*N*-acetylpenicillamine (SNAP) (100 μM and, in the case of podocytes, 1000 μM; Biomol, Hamburg, Germany) for 30 or 60 min. In control experiments, 1*H*-(1,2,4)oxadiazole[4,3-a]quinoxalin-1-one (10 μM; Alexis) was added simultaneously with SNAP for 30 min. For termination of the assay, the supernatants were rapidly removed and cells were rinsed with ice-cold 70% ethanol. After ethanol extraction, cGMP concentrations were measured with an enzyme-linked immunosorbent assay (Amersham Buchler, Braunschweig, Germany). To confirm the specificity of the cGMP pathway, we tested atrial natriuretic peptide (ANP) (1 μM; Sigma), which stimulates the membrane-bound guanylyl cyclase, for 30 min.

Results

Localization of sGC in Kidney

Histochemical staining revealed significant amounts of β1 sGC in the renal vasculature and in interstitial cells. Intra- and juxtaglomerular structures demonstrated marked selective staining with a polyclonal antibody against β1 sGC. In double-staining analyses with either anti-desmin, as a marker of the intra- and extraglomerular mesangium (Figure 1, a and b), or anti-synaptopodin, as a podocyte marker (Figure 1, c and d), sGC immunoreactivity was clearly recognizable in the mesangial axes of the intraglomerular mesangium. sGC was also detected in the extraglomerular mesangium, including the contact areas with the macula densa, which was identified on the basis of NADPH-diaphorase and NOS1 immunostaining (Figure 2, a to d). Ultrastructural immunoperoxidase labeling demonstrated uniform cytosolic distribution of sGC label exclusively in the mesangial cells (Figures 1e and 2e). Prominent signal was also detected in the mesangial angles, where extensions of the mesangial cells are connected to the glomerular basement membrane via fine microfibrils (Figure 1e). Podocytes remained unstained (Figure 1e). In both the afferent and efferent arterioles, significant sGC immunoreactivity was observed in the muscular media. The afferent arteriolar wall was immunostained up to the intraglomerular site where it branches into the glomerular capillaries (Figure 3a). The preglomerular portion, containing the granular renin-producing cells, was also strongly labeled; in the granular cells, cytosolic labeling was obvious in the vicinity of the renin-containing granules (which were unreactive) (Figure 3c). Staining of the efferent arteriole wall was generally strong (Figure 3d) but was particularly intense in juxtamedullary nephrons, from which the descending vasa recta originate. *In situ* hybridization also demonstrated prominent labeling in the glomerular arteriolar walls, using probes for α1 and β1 subunits (Figure 3b). Intraglomerular structures did not reliably exhibit an *in situ* hybridization signal, which may be attributable to insufficient sensitivity of the method used. A weak signal was observed in the extraglomerular mesangium, sometimes in continuity with reactive portions of the glomerular arterioles.

In the cortical interstitium, fibroblasts were labeled throughout the cortical labyrinth, the medullary rays, and the perivascular areas. The immunoreactive cells were identified by double-labeling with an antibody directed against ecto-5'-nucleotidase, an enzyme that is typically located along the cell membranes of cortical fibroblasts (Figure 4, a and b). sGC-immunoreactive fibroblasts were further identified throughout the outer medulla and along the vascular bundles extending to the inner medulla. Ultrastructural immunoperoxidase staining revealed intense, evenly distributed, cytosolic β1 sGC staining in these cells, sparing all major organelles (Figure 4c). *In situ* hybridization also produced strong α1 and β1 sGC mRNA signals in peritubular and perivascular locations, with a distribution pattern analogous to that typical of interstitial fibroblasts (Figure 4d).

In the renal medulla, the descending vasa recta demonstrated continuous strong β1 sGC immunoreactivity within the con-

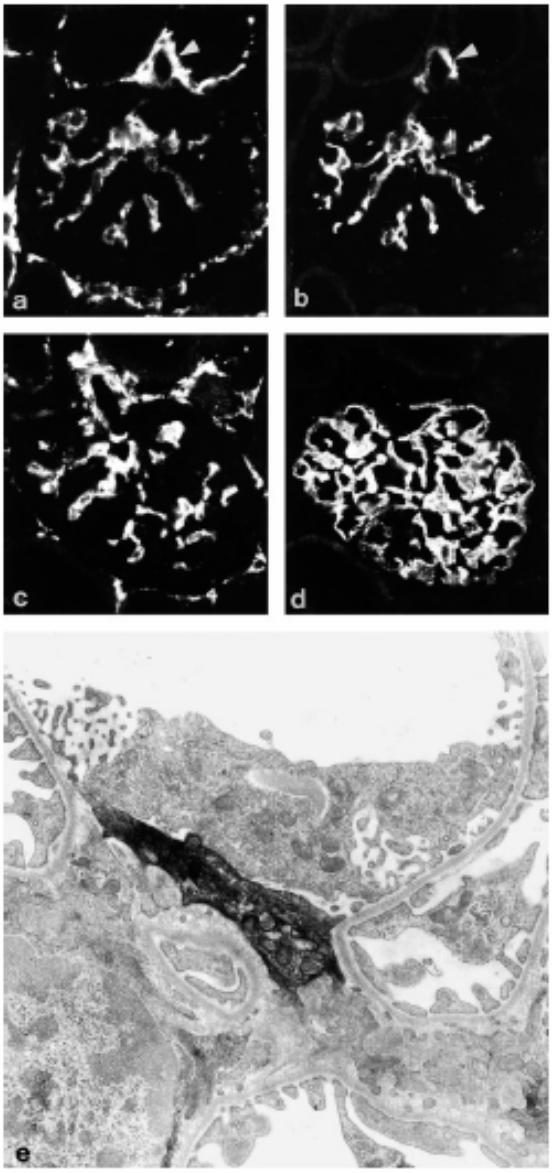

Figure 1. Identification of renal intraglomerular β1 soluble guanylyl cyclase (sGC) immunoreactivity. (a and c) Anti-β1 sGC (Cy3-labeled) (a) and anti-desmin (Cy2-labeled) (c) immunostaining. Prominent glomerular structures stained with anti-β1 sGC are the mesangial axes of the glomerular tuft and the afferent arteriolar wall (arrowhead); these structures are double-stained with anti-desmin. (c and d) Anti-β1 sGC (c) and anti-synaptopodin (Cy2-labeled) (d) immunostaining. Synaptopodin is a selective podocyte marker. It should be noted that the two staining patterns are complementary. (e) Ultrastructural anti-β1 sGC immunoperoxidase labeling of a glomerular capillary loop, focusing on a mesangial angle. Selective β1 sGC signal is present in a mesangial cell process at the site where it anchors the glomerular basement membrane. Magnifications: ×250 in a to d; ×11,000 in e.

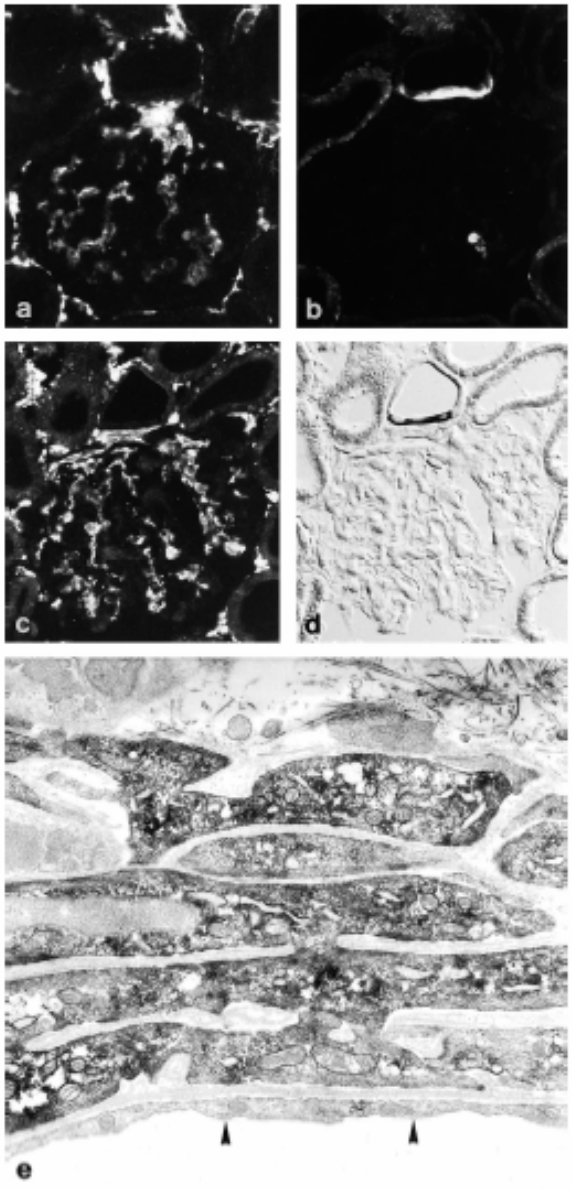

Figure 2. Renal β1 sGC immunoreactivity in the intra- and extraglomerular mesangium. (a to d) Two different views of the mesangium, using double-staining with anti-β1 sGC antibody (Cy3-labeled) (a and c), anti-nitric oxide (NO) synthase 1 (NOS1) antibody (Cy2-labeled) (b), and NADPH-diaphorase staining (d). The strong β1 sGC signal of the extraglomerular mesangium is located next to the β1 sGC-unreactive, NOS1-positive macula densa. The intraglomerular mesangium is also β1 sGC-positive; the continuity between extra- and intraglomerular immunostaining is evident (c), next to the diaphorase-positive macula densa (d). (e) Ultrastructural anti-β1 sGC immunoperoxidase labeling of the extraglomerular mesangium, demonstrating strong cytosolic labeling. An adjacent portion of the endothelium (arrowheads) is unreactive. Magnifications: ×250 in a to d; ×12,000 in e.

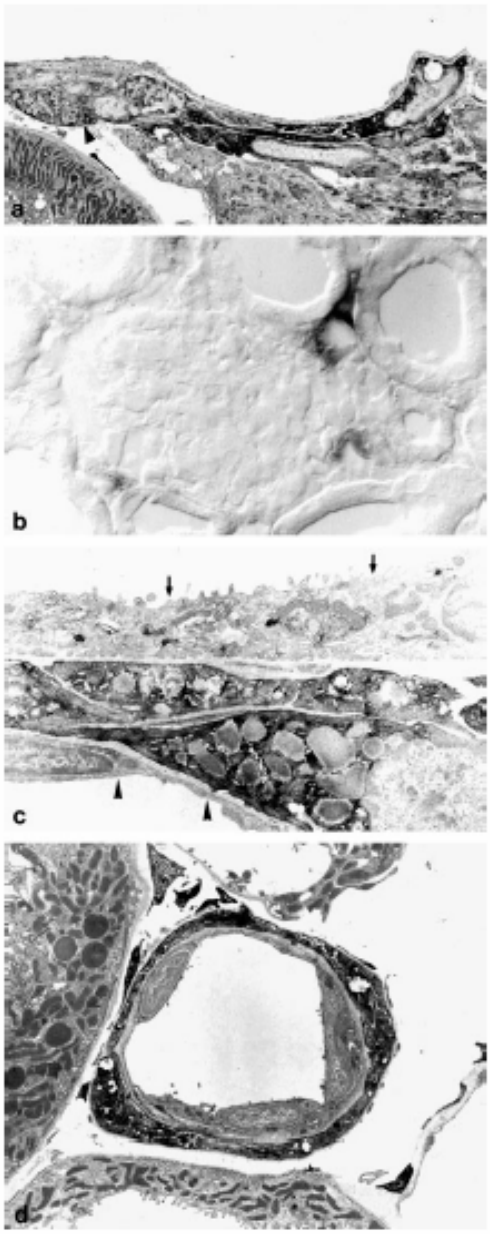

Figure 3. Cortical renal vasculature expressing β1 sGC. (a) Ultrastructural anti-β1 sGC immunoperoxidase labeling shows prominent staining of the glomerular afferent arteriolar wall, including the renin-containing granular cells (arrowhead). On the right, extraglomerular mesangium is also stained. (b) *In situ* hybridization shows prominent expression of β1 sGC mRNA in the wall of the glomerular arterioles. Intraglomerular expression is not detectable. (c) Renin-containing granular cells are shown at high resolution; labeling is restricted to the cytosol. Adjacent endothelium (arrowheads) and thick ascending limb epithelium (arrows) are unstained. (d) Muscular media cells of an afferent arteriole demonstrate strong β1 sGC signal. The endothelium is unstained. Magnifications: ×2000 in a; ×350 in b; ×4100 in c; ×3300 in d.

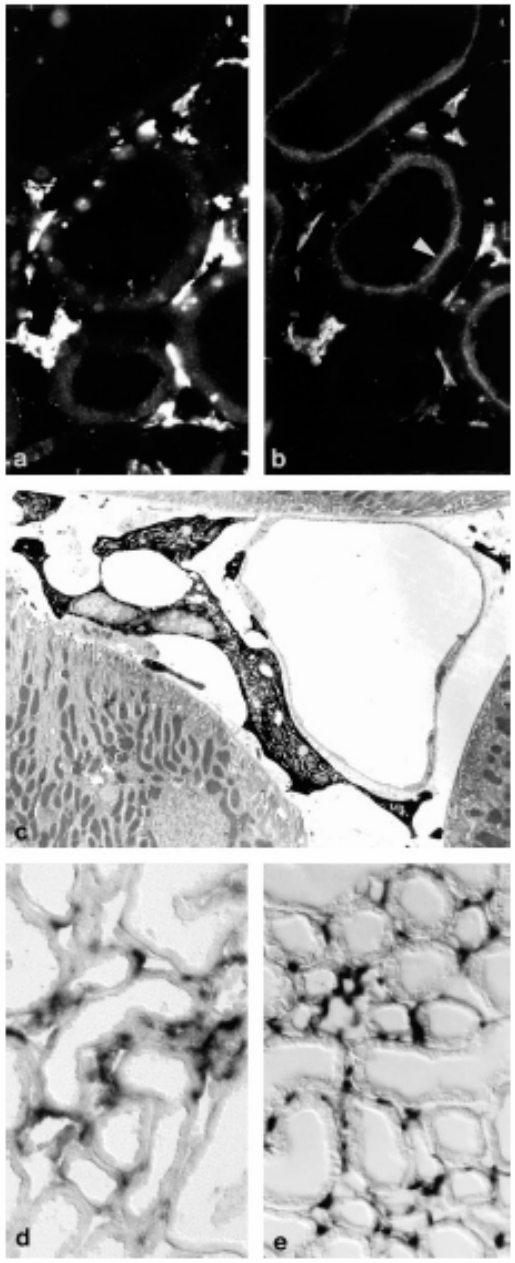

Figure 4. Renal β1 sGC expression in the cortical interstitium. (a and b) Double-immunostaining with anti-β1 sGC (Cy3-labeled) (a) and anti-ecto-5′-nucleotidase (Cy2-labeled) (b), showing that peritubular cells are double-stained, whereas the proximal tubule brush border is only anti-ecto-5′-nucleotidase-positive (arrowhead in b). (c) Ultrastructural anti-β1 sGC immunoperoxidase labeling, showing dense reactivity in a typical interstitial fibroblast. (d) *In situ* hybridization for sGC mRNA expression (α1 subunit), showing that sites of interstitial peritubular fibroblasts are prominently labeled. (e) *In situ* hybridization, demonstrating that, as in d, fibroblasts are labeled with a probe specific for sGC (β1 subunit). Magnifications: ×650 in a and b; ×3200 in c; ×220 in d and e.

tractile media along their initial portions; in the terminal portions, the remaining pericytes, which were typically arranged around the circumference of these vessels, were positively stained (Figure 5). Strong labeling in pericytes was particularly evident in the vascular bundles of the outer and inner stripes of the outer medulla. In the inner medulla, the number of immunoreactive cells progressively decreased toward the papillary tip. Immunoreactive perivascular fibroblasts in the vascular bundles were identified on the basis of their characteristic branched morphologic features, which are distinct from those of vascular pericytes (Figure 5a). Ascending vasa recta were not regularly accompanied by β1 sGC-immunoreactive cells. The locations of signals produced by *in situ* hybridization with probes for the α and β subunits of sGC corresponded to the immunoreactivity distribution. We detected mRNA signal primarily in perivascular pericytes and fibroblasts of the vascular bundles (outer medulla), whereas interstitial fibroblasts in the inter-bundle regions were rarely labeled. In the inner medulla, only a few interstitial cells were positively stained.

Localization of sGC in Liver

In the liver, hepatic stellate (Ito) cells expressed significant levels of β1 sGC immunoreactivity and α1/β1 sGC mRNA, as revealed by *in situ* hybridization (Figure 6, a and b). In the periphery of a hepatic lobule, nearly all Ito cells were intensively immunostained for sGC; the intensity decreased toward the central vein, however, and no signal was detectable in the innermost region around the central vein. High-resolution immunoperoxidase labeling permitted identification of these cells on the basis of their typical perisinusoidal location in the space of Disse and their regular content of large lipid vacuoles, which were surrounded by an intense signal for the cyclase (Figure 6c). The walls of portal venules and larger veins were also observed to be sGC-immunopositive.

The specificity of the immunohistochemical labeling was verified by preabsorption of the β1 sGC-specific antibody with the peptide used for immunization. No signal was observed in kidney or liver after incubation with this mixture. For *in situ* hybridization analyses, sense and antisense probes transcribed from α1 and β1 cDNA, respectively, were routinely used on sections. No signals were obtained with the sense probes.

Measurements of NO-Stimulated cGMP Formation in Extracts from Tissues and Isolated Cells

Determination of NO-stimulated sGC activity revealed significant increases in cGMP formation in the cytosolic fractions from different tissues. The kidney cortex demonstrated an 87-fold increase in cGMP formation (56 ± 53 to 4899 ± 686 pmol cGMP/min per mg) (Figure 7A) after stimulation with *S*-nitrosoglutathione, and the renal medulla demonstrated a 65-fold increase (33 ± 18 to 2133 ± 445 pmol cGMP/min per mg). We observed a 232-fold increase in the liver (8 ± 6 to 1856 ± 866 pmol cGMP/min per mg) and a 59-fold increase in the lung (112 ± 101 to 6659 ± 650 pmol cGMP/min per mg). The stimulation factors thus ranged between 56- and 232-fold, demonstrating that the observed rates of cGMP formation were substantially and significantly enhanced by NO-dependent ac-

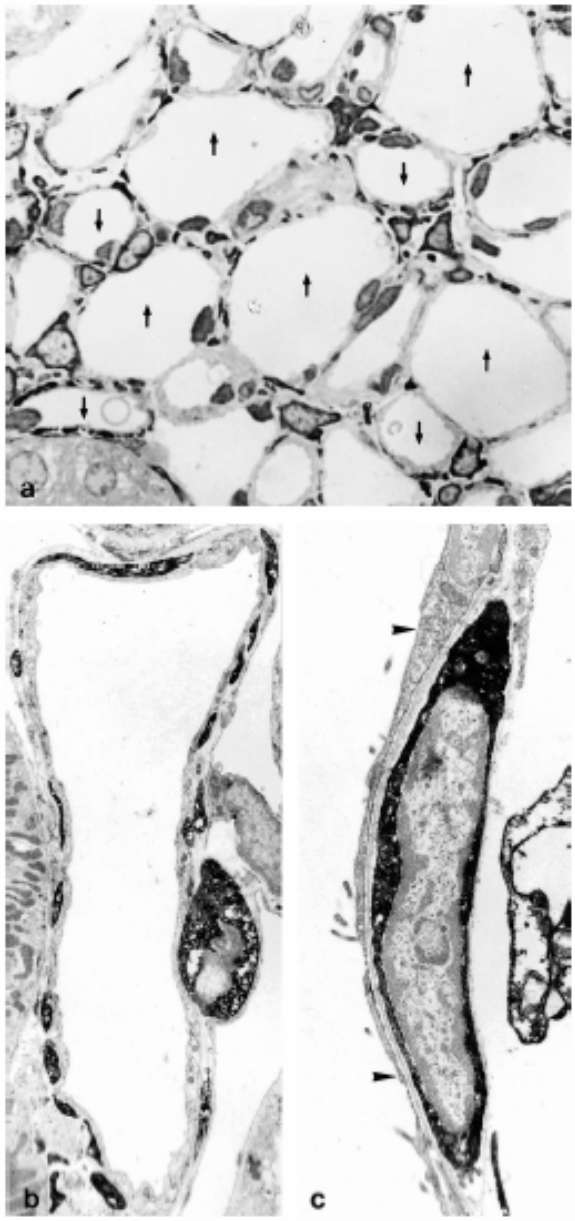

Figure 5. Renal β1 sGC immunoperoxidase labeling in the medulla. (a) Vascular bundle at the transition between the outer and inner stripes of the outer medulla. Media cells and pericytes of the descending vasa recta (arrows pointing down) and interstitial fibroblasts show marked immunostaining; no particular staining is observed in the ascending vasa recta (arrows pointing up). (b) Ultrastructural β1 sGC immunoperoxidase labeling in a descending vas rectum (inner stripe). Significant staining of the cross-sectional profiles of circumferentially arranged pericytes forming the muscle wall should be noted. (c) β1 sGC immunoperoxidase labeling of a single pericyte from a descending vas rectum (outer medulla). The adjacent endothelium (arrowheads) is negative. Magnifications: ×980 in a; ×3200 in b; ×7400 in c.

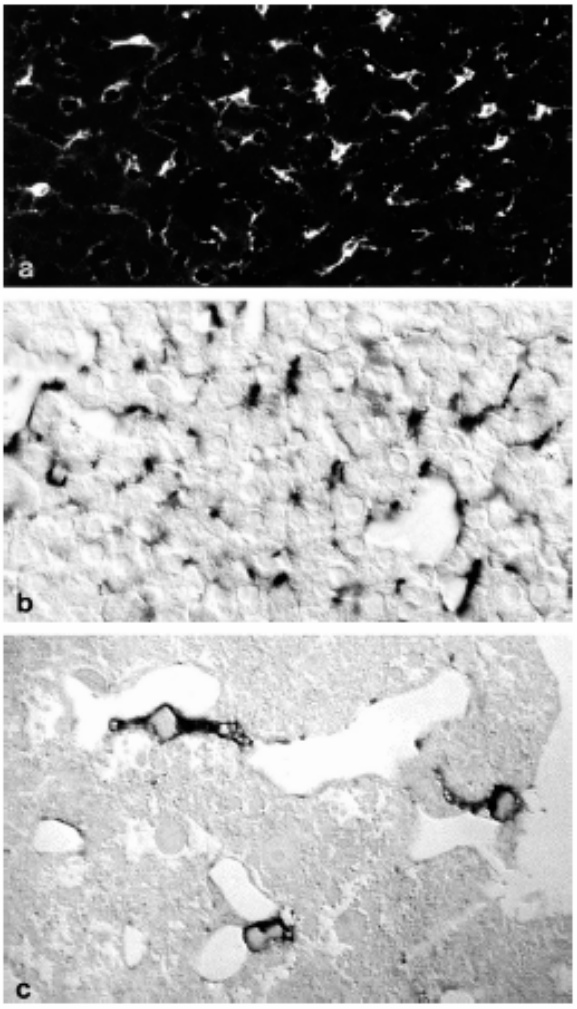

Figure 6. Expression of β1 sGC in the liver. (a) Immunohistochemical staining shows marked signal in the Ito cells and their extended processes; cells were otherwise identified by autoluminescence of their lipoid granular contents (data not shown). (b) In corresponding locations, *in situ* hybridization with β1 sGC riboprobe demonstrates signal in nonparenchymal cells likely to be Ito cells. (c) A semithin section shows anti-β1 sGC staining (immunoperoxidase labeling). Signal is present exclusively in Ito cells, which can be identified on the basis of their liposome contents and perisinusoidal locations. Magnifications: ×320 in a and b; ×650 in c.

tivation of sGC and that, in absolute terms, the lung exhibited the highest levels of cGMP generation, as expected.

Incubation of extracts from freshly prepared mesangial cells with the NO donor SNAP led to a 39-fold increase in cGMP levels (153 ± 46 to 5922 ± 1168 pmol/well) (Figure 7B), incubation of extracts from renal medullary interstitial cells with SNAP led to a 52-fold increase (27 ± 4 to 1396 ± 366 pmol/well), and incubation of extracts from isolated hepatic Ito cells with SNAP led to a 47-fold increase (26 ± 7 to 1218 ± 177 pmol/well). The cGMP accumulation induced by the NO donor was almost completely inhibited when cells were stimulated in the presence of the specific sGC inhibitor 1*H*-(1,2,4)oxadiazole[4,3-a]quinoxalin-1-one. Incubation of extracts from cultured podocytes with various concentrations of the NO donor SNAP, however, never produced an increase in cGMP levels, compared with control values; in contrast, ANP produced a significant 39-fold increase (21 ± 17 to 819 ± 112 pmol/well) (Figure 7C).

Western Blot Analyses

Qualitative immunoblotting was performed with anti-β1 sGC antibody, using tissue extracts from kidney cortex, kidney medulla, liver, lung, and muscle and extracts of isolated Ito cells, mesangial cells, and interstitial cells that had been tested in the cGMP assays described above. A principal band was identified, with an apparent molecular mass of approximately 70 kD (Figure 8). Lower-molecular mass bands were attributable to degradation. The weak signal in extracts from interstitial cells may be attributable to the origin of these cells from the renal medulla, where the number of sGC-immunoreactive fibroblasts is smaller than in the cortex. The immunohistochemical signal obtained with antibody against β1 sGC was also weaker.

RT-PCR Analysis

We performed a quantitative analysis of β1 sGC mRNA in extracts from renal cortex, to verify the histochemical results regarding sGC mRNA expression. Approximately equal amounts of sGC cDNA and internal standard were amplified at a concentration of 0.02 pg of standard DNA (Figure 9A). As a result, a value of 66 pg sGC mRNA/μg total renal cortical mRNA was calculated. The presence of mRNA for both α1 and β1 subunits was further assessed in tissue extracts by using RT-PCR, with GAPDH as a reference standard. Significant bands for both subunits were observed for RNA extracts obtained from kidney cortex, isolated glomeruli, and liver (Figure 9, B to E).

Discussion

The results of our histochemical investigations assign sGC expression precisely to vascular and interstitial cell types in kidney and liver. A newly generated, highly specific antibody to the β1 subunit of sGC allowed us to substantially extend previous data on sGC localization (17,31). sGC requires the coexpression of one α and one β subunit for catalytic action (3,27). Because we were limited to detection of only the β1 subunit with reliable immunohistochemical specificity, we supplemented our data with results from *in situ* hybridization and RT-PCR assays with specific probes for both of the "universal" subunits (α1 and β1) and with findings from functional assays on cultivated cells that were selected according to their histochemical identification *in situ*.

The renal distribution of sGC revealed vascular and interstitial components. This study demonstrates, for the first time, the presence of sGC in all contractile cells of the kidney, with different expression levels. In glomeruli, the smooth muscle-

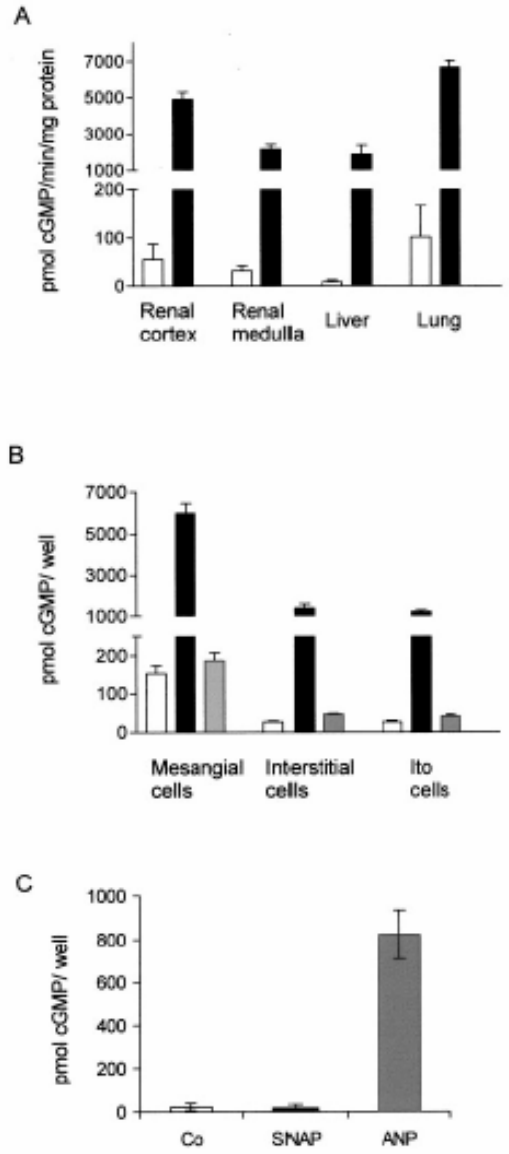

Figure 7. Stimulation of sGC in cytosolic fractions from various tissues (A) and isolated cells (B and C), using *S*-nitrosoglutathione (A) or *S*-nitroso-*N*-acetylpenicillamine (SNAP) (B and C) as a NO donor. (A) Enzyme activity in the cytosolic fractions from various tissues was determined in the absence (□) or presence (■) of 300 μM *S*-nitrosoglutathione. Data are the means ± SD of three representative experiments. (B) Enzyme activity in the cytosolic fractions from various isolated cells was determined in the absence (□) or presence of 100 μM SNAP (■) or 100 μM SNAP added with the inhibitor 1*H*-(1,2,4)oxadiazole[4,3-a]quinoxalin-1-one (10 μM) (▨). (C) Enzyme activity in the cytosolic fractions from immortalized cultured mouse podocytes was determined in the absence (Co) or presence of 100 μM SNAP or 100 nM atrial natriuretic peptide (ANP). In B and C, each column represents the mean ± SD of six experiments, performed in triplicate.

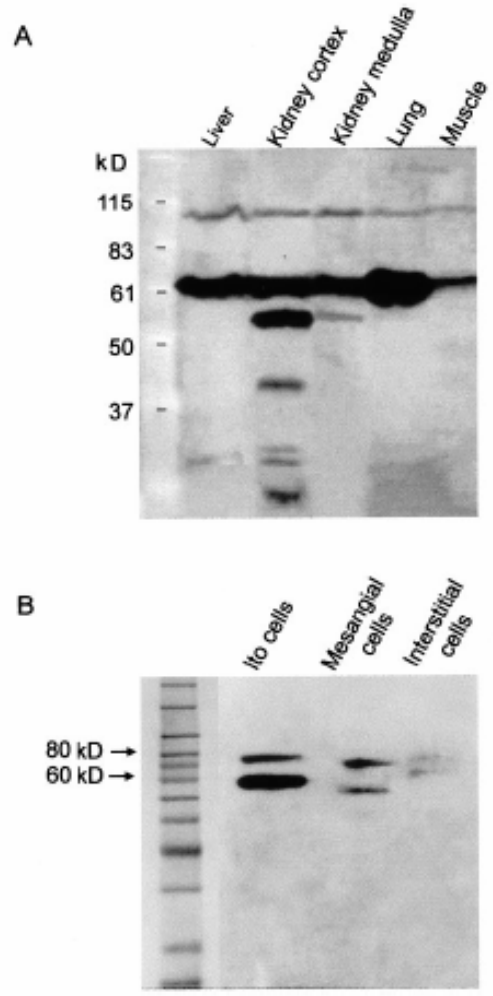

Figure 8. Detection of β1 sGC in various tissue (A) and isolated cell (B) lysates by Western blot analysis. The smaller bands observed in addition to the dominant 70-kD protein are degradation products. Signal generation was performed by using a chemiluminescence kit.

derived cells of the intra- and extraglomerular mesangium were sGC-immunoreactive. RT-PCR data for isolated glomeruli support the presence of mRNA coding for α1 and β1 sGC. The intraglomerular mesangial cells are thought to maintain mechanical strength by anchoring the capillary loops in the glomerular tuft (32); receptors for vasoactive hormones related to the contractility of these cells have been identified (for review, see reference 33). Local effects of the NO-sGC-cGMP pathway may counteract these effects. *In vivo*, NO may be derived from constitutive NOS activity of the adjacent glomerular capillary endothelium or may diffuse from the nearby macula densa (8,10). Significant sGC staining, as detected, in the mesangial angles anchoring the glomerular basement membrane (32) suggests a particular role for cGMP in maintaining

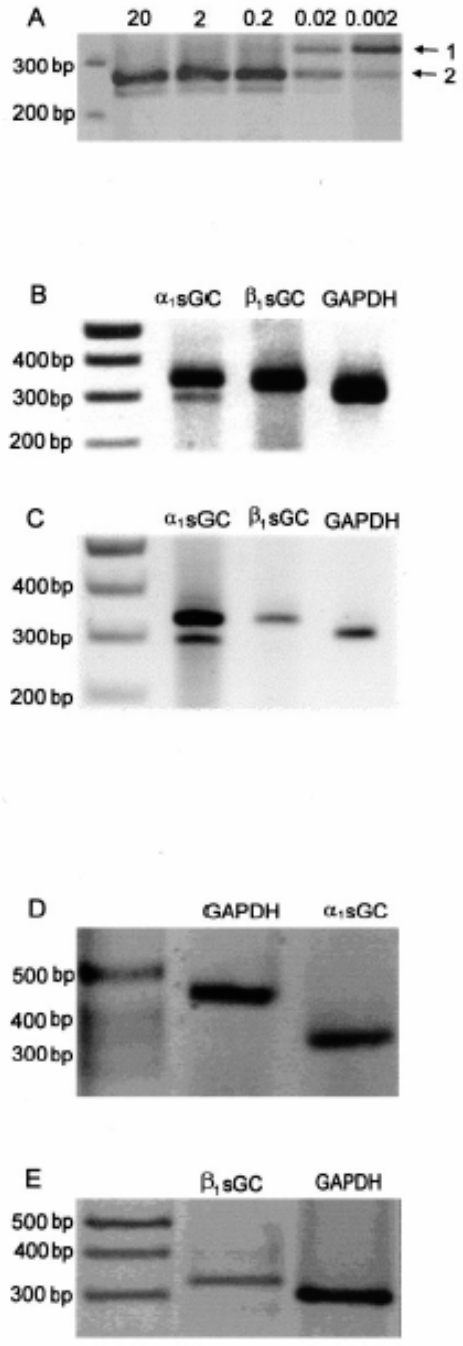

Figure 9. (A) Quantification of β1 sGC mRNA in kidney cortex by reverse transcription (RT)-PCR with an internal standard. (B and C) Representative RT-PCR assays for sGC subunits, using glyceraldehyde-3-phosphate dehydrogenase (GAPDH) as a reference probe, in kidney cortex (B) and isolated glomeruli (C). (D and E) Representative RT-PCR assays for sGC subunits (D, α1; E, β1), using GAPDH as a reference probe, in liver.

adequate contractile tone at these sites. Stimulation with a NO agonist was highly effective in increasing cGMP accumulation in mesangial cells *in vitro*, which confirms earlier data (34) and supports the hypothesis that cGMP may play an important role in these cells.

The histochemical presence of β1 sGC in mesangial cells and not in podocytes, as observed in this study, is in contrast to previous findings reporting α1 sGC immunoreactivity exclusively in podocytes (31). However, because those earlier attempts to localize sGC did not reveal a plausible overall distribution pattern for the enzyme and failed to demonstrate colocalization of its subunits, the significance of those experiments must be reconsidered in light of the findings presented here. Our *in vitro* data demonstrated, in fact, that addition of a NO donor to cultured immortalized mouse podocytes failed to stimulate sGC, whereas the same cells demonstrated a response after stimulation with ANP; these results highlight the absence of sGC but confirm earlier findings on the presence of the particulate form of the enzyme in these cells in rats. Of course, discrepancies between the two species with respect to sGC expression cannot be entirely ruled out by the reported assay results.

Marked expression of β1 sGC in cells of the extraglomerular mesangium may have functional implications. Because the mechanical integrity of the glomerular hilus is thought to be supported by these cells forming a "closure device" for the entrance into the glomerulus (35), NO-dependent regulation of their contractility, mediated by the nearby constitutive NOS in the macula densa, seems plausible (36). Extraglomerular mesangial cells are thought to transmit stimuli from the macula densa to the glomerular vasculature and the renin-containing granular cells, and the NO-sGC-cGMP pathway may represent one of the principal components in this information transfer, possibly in conjunction with structurally established intercellular communication via gap junctional coupling (9,36,37).

The findings of significant sGC immunoreactivity and transcript levels in the glomerular arteriolar walls, including the granular cells, confirm functional observations regarding the local effects of NO on these vascular cells (7–9,38). Adjustment of tubuloglomerular feedback action in response to changes in tubular NaCl load and macula densa constitutive NOS activity (8,38) may thus be related to the local abundance of sGC. The presence of sGC in the cytosol directly surrounding the renin-containing granules of the renin-producing cells supports a stimulatory role for cGMP (7,9). Prominent sGC immunoreactivity in the muscular wall of the efferent arterioles further suggests that local release of NO in this vascular portion may have important vasodilatory effects. The particularly high sGC signal in juxtamedullary efferent arterioles suggests a NO-dependent dilatory mechanism, which may determine renal medullary perfusion. Such an effect would be supported by the continuous strong sGC immunostaining in the myocytes constituting the wall of the descending vasa recta and in the pericytes of the terminal portions of these vessels within the vascular bundles. These data may represent the morphologic equivalent of the otherwise well established effects of NO on renal medullary circulation (10,11). The overall weaker β1

sGC immunostaining of larger renal cortical arteries and arterioles, compared with small resistance vessels, suggests preferential responsiveness to NO in the latter.

Significant expression of sGC was also observed in interstitial fibroblasts in the renal cortex and, to a lesser extent, in the medulla; *in situ* hybridization results and the *in vitro* data on NO-dependent cGMP formation, using freshly isolated medullary interstitial cells, confirmed the immunohistochemical findings, demonstrating that this cell type has a particular role in the NO-sGC-cGMP signaling pathway in renal parenchyma. These data agree with an earlier report on mRNA expression of α1 and β1 sGC subunits in long-term cultivated rat medullary interstitial cells and on their NO-specific responsiveness (39). *In situ*, a proportion of the cortical interstitial fibroblasts were previously identified as the main source of erythropoietin (40). These cells also express high levels of NADPH oxidase (41), and they are involved in the synthesis of extracellular adenosine; however, it remains to be established whether these products functionally interact and what role local cGMP release could play.

The complete absence of tubular histochemical labeling in this study is in contrast to previous PCR and immunohistochemical data that reported sGC mRNA in a variety of tubular epithelia and β2 sGC immunoreactivity in collecting ducts (12,13,31). The discrepancy between these results may be attributable to sensitivity or specificity problems; however, anti-β1 sGC immunoreactivity was reliably detected in a variety of renal and hepatic cell types, so that tubular expression, at least of β1 sGC, must be at a low level. Also, we never observed coincident histochemical localization of NOS and sGC, which suggests that NO, as a signal molecule for cGMP generation, acts through paracrine diffusion to its target, rather than by intracellular signaling.

Our results on sGC in the Ito cells of the liver agree with functional concepts of these cells. Ito cells have been described as liver-specific pericytes that are located in the space of Disse and possess long cell processes extending between the sinusoid endothelia and the parenchymal cells (42). They are related to renal cortical interstitial cells, inasmuch as the two cell types share a number of properties. In addition to the common expression of sGC, they are the principal sources of erythropoietin production by the body (43) and both express neutrophil NADPH oxidase and ecto-5'nucleotidase (41) and play a central role in organ fibrosis (25). In response to vasoactive substances such as NO, carbon monoxide, and endothelin, the contractile tone of Ito cells may be adjusted to regulate sinusoidal microcirculation and portal BP. Both locally formed NO and carbon monoxide are thought to target a common biologic effector limb via binding to sGC and generation of cGMP (18–20). The identification of Ito cells as a source of abundant sGC expression thus corroborates the evidence of this signaling cascade, which is also confirmed by the effective stimulation of cGMP release by Ito cells, as assayed *in vitro*. Kawada *et al.* (19) reported much weaker release of cGMP in response to Ito cell stimulation by a NO donor than we detected; this difference was probably attributable to differences in cultivation times. Total cGMP-forming activity after stimulation with NO was much lower in liver than in lung and kidney cortex. This difference is likely to be related to the fact that the parenchymal hepatocytes were sGC-negative and the Ito cells, which represent only a small proportion of the entire tissue mass, were the sGC-reactive cell type, in conjunction with venous wall cells.

In conclusion, this study presents an entirely new range of cell types expressing sGC in kidney and liver. Compared with previous data, we thus provide a more solid, extended pattern of sGC distribution, with the use of improved histochemical and *in vitro* methods. Significant expression was localized to vascular wall cells in both organs, with particularly high intensity in the glomerular arterioles and descending vasa recta of the kidney and in perisinusoidal Ito cells. These sites are crucial for the local adjustment of vascular tone and thus of regional end-organ perfusion. Common properties of Ito cells and renal cortical fibroblasts have been emphasized by the results presented here, which may facilitate an understanding of the functional mechanisms that are active in these cell types. The localization of sGC in renin-producing granular cells corroborates functional concepts of the role of cGMP in renin release. Significant mesangial expression of sGC and effective stimulation of cultured mesangial cells by NO suggest a prominent role for cGMP in adjustment of the contractile tone of the glomerular tuft, with possible implications for diseases of the glomeruli.

Acknowledgments

This work was supported by funds from the Deutsche Forschungsgemeinschaft (Grant Ba700/14-1).

References

1. Koesling D, Friebe A: Soluble guanylyl cyclase: Structure and regulation. *Rev Physiol Biochem Pharmacol* 135: 41–65, 1999
2. Nakane M, Arai K, Saheki S, Kuno T, Buechler W, Murad F: Molecular cloning and expression of cDNAs coding for soluble guanylate cyclase from rat lung. *J Biol Chem* 265: 16841–16845, 1990
3. Russwurm M, Behrends S, Harteneck C, Koesling D: Functional properties of a naturally occurring isoform of soluble guanylyl cyclase. *Biochem J* 335: 125–130, 1998
4. Arnold WP, Mittal CK, Katsuki S, Murad F: Nitric oxide activates guanylate cyclase and increases guanosine 3':5'-cyclic monophosphate levels in various tissue preparations. *Proc Natl Acad Sci USA* 74: 3203–3207, 1977
5. McDonald LJ, Murad F: Nitric oxide and cyclic GMP signaling. *Proc Soc Exp Biol Med* 211: 1–6, 1996
6. Idriss SD, Gudi T, Casteel DE, Kharitonov VG, Pilz RB, Boss GR: Nitric oxide regulation of gene transcription via soluble guanylate cyclase and type I cGMP-dependent protein kinase. *J Biol Chem* 274: 9489–9493, 1999
7. Kurtz A, Wagner C: Role of nitric oxide in the control of renin secretion. *Am J Physiol* 275: F849–F862, 1998
8. Persson AEG, Bachmann S: Constitutive nitric oxide synthesis in the kidney: Functions at the juxtaglomerular apparatus. *Acta Physiol Scand* 169: 317–324, 2000
9. Schnermann JB: Juxtaglomerular cell complex in the regulation of renal salt excretion. *Am J Physiol* 274: R263–R279, 1998

10. Bachmann S, Bosse HM, Mundel P: Topography of nitric oxide synthesis by localizing constitutive NO synthases in mammalian kidney. *Am J Physiol* 268: F885–F898, 1995
11. Bachmann S: Distribution of NOSs in the kidney. In: *Nitric Oxide and the Kidney: Physiology and Pathophysiology*, edited by Goligorsky MS, Gross SS, New York, Chapman & Hall, 1997, pp 133–157
12. Terada Y, Tomita K, Nonoguchi H, Marumo F: Polymerase chain reaction localization of constitutive nitric oxide synthase and soluble guanylate cyclase messenger RNAs in microdissected rat nephron segments. *J Clin Invest* 90: 659–665, 1992
13. Ujiie K, Drewett JG, Yuen PS, Star A: Differential expression of mRNA for guanylyl cyclase-linked endothelium-derived relaxing factor receptor subunits in rat kidney. *J Clin Invest* 91: 730–734, 1993
14. Yuen ST, Pottier LR, Garbers DL: A new form of guanylyl cyclase is preferentially expressed in rat kidney. *Biochemistry* 29: 10872–10878, 1990
15. Kummer W, Behrends S, Schwarzmüller T, Fischer A, Koesling D: Subunits of soluble guanylyl cyclase in rat and guinea-pig sensory ganglia. *Brain Res* 721: 191–195, 1996
16. Brandes RP, Kim DY, Schmitz-Winnenthal FH, Amidi M, Gödecke EA, Mülsch A, Busse R: Increased nitrovasodilator sensitivity in endothelial nitric oxide synthase knockout mice: Role of soluble guanylyl cyclase. *Hypertension* 35: 231–236, 2000
17. Dean AD, Vehaskari VM, Ritter D, Greenwald JE: Distribution and regulation of guanylyl cyclase type B in the rat nephron. *Am J Physiol* 270: F311–F318, 1996
18. Suematsu M, Wakabayashi Y, Ishimura Y: Gaseous monoxides: A new class of microvascular regulator in the liver. *Cardiovasc Res* 32: 679–686, 1996
19. Kawada N, Tran-Thi TA, Klein H, Decker K: The contraction of hepatic stellate (Ito) cells stimulated with vasoactive substances: Possible involvement of endothelin 1 and nitric oxide in the regulation of the sinusoidal tonus. *Eur J Biochem* 213: 815–823, 1993
20. Rockey DC, Chung JJ: Inducible nitric oxide synthase in rat hepatic lipocytes and the effect of nitric oxide on lipocyte contractility. *J Clin Invest* 95: 1199–1206, 1995
21. Kreisberg JI, Hoover RL, Karnovsky MJ: Isolation and characterization of glomerular epithelial cells *in vitro*. *Kidney Int* 14: 21–30, 1978
22. Pavenstädt H, Gloy J, Leipziger J, Klar B, Pfeilschifter J, Schollmeyer P, Greger R: Effect of extracellular ATP on contraction, cytosolic calcium activity, membrane voltage and ion currents of rat mesangial cells in primary culture. *Br J Pharmacol* 109: 953–959, 1993
23. Mundel P, Reiser J, Zuniga A, Pavenstädt H, Kriz W, Davidson GR, Zeller R: Rearrangements of the cytoskeleton and cell contacts induce process formation during differentiation of conditionally immortalized mouse podocyte cell lines. *Exp Cell Res* 36: 248–258, 1997
24. Grupp C, Troche I, Steffgen J, Langhans S, Cohen DI, Brandl L, Müller GA: Highly specific separation of heterogeneous cell populations by lectin coated beads: Application for the isolation of inner medullary collecting duct cells. *Exp Nephrol* 6: 542–550, 1998
25. Schäfer S, Zerbe O, Gressner AM: The synthesis of proteoglycans in fat storing cells of rat liver. *Hepatology* 7: 680–687, 1987
26. Knook DL, Deleeuw AM: Isolation and characterization of fat storing cells from the rat liver. In: *Sinusoidal Liver Cells*, edited by Knook DL, Wisse E, Rijswijk, Elsevier Biomedical Press, 1982, p 45–52
27. Koesling D, Herz J, Gausepohl H, Niroomand F, Hinsch KD, Mülsch H, Böhme E, Schultz G, Frank R: The primary structure of the 70 kDa subunit of bovine soluble guanylyl cyclase. *FEBS Lett* 239: 29–34, 1988
28. Mundel P, Bachmann S, Bader M, Fischer A, Kummer W, Mayer B, Kriz W: Expression of nitric oxide synthase in kidney macula densa cells. *Kidney Int* 42: 1017–1019, 1992
29. Chomczynski P, Sacchi N: Single-step method of RNA isolation by acid guanidinium thiocyanate-phenol-chloroform extraction. *Anal Biochem* 162: 156–159, 1987
30. Friebe A, Mullershausen F, Smolenski A, Walter U, Schultz G, Koesling D: YC-1 potentiates nitric oxide- and carbon monoxide-induced cyclic GMP effects in human platelets. *Mol Pharmacol* 54: 962–967, 1998
31. Mundel P, Gambaryan S, Bachmann S, Koesling D, Kriz W: Immunolocalization of soluble guanylyl cyclase subunits in rat kidney. *Histochemistry* 103: 75–79, 1995
32. Kriz W, Elger M, Lemley KV, Sakai T: Mesangial cell-glomerular basement membrane connections counteract glomerular capillary and mesangium expansion. *Am J Nephrol* 10: 4–13, 1990
33. Schlöndorff D: The glomerular mesangial cell: An expanding role for a specialized pericyte. *FASEB J* 1: 272–280, 1987
34. Chevalier RL, Fern RJ, Garmey M, El-Dahr SS, Gomez RA, Devente JA: Localization of cGMP after infusion of ANP or nitroprusside in the maturing rat. *Am J Physiol* 262: F417–F424, 1992
35. Kriz W, Sakai T, Hosser H: Morphological aspects of glomerular function. In: *Nephrology*, edited by Davison AM, London, Baillière Tindall, 1988, p 23–38
36. Bosse HM, Bachmann S: Immunohistochemically detected protein nitration indicates sites of renal nitric oxide release in Goldblatt hypertension. *Hypertension* 30: 948–952, 1997
37. Taugner R, Schiller A, Kaissling B, Kriz W: Gap junctional coupling between the JGA and the glomerular tuft. *Cell Tissue Res* 186: 279–285, 1978
38. Wilcox CS, Welch J: Interaction between nitric oxide and oxygen radicals in regulation of tubuloglomerular feedback. *Acta Physiol Scand* 168: 119–124, 2000
39. Ujiie K, Hogath L, Danziger R, Drewett JG, Yuen PST, Pang IH, Star RA: Homologous and heterologous desensitization of a guanylyl cyclase-linked nitric oxide receptor in cultured rat medullary interstitial cells. *J Pharmacol Exp Ther* 270: 761–767, 1994
40. Bachmann S, Le Hir M, Eckardt KU: Co-localization of erythropoietin mRNA and ecto-5'-nucleotidase immunoreactivity in peritubular cells of rat renal cortex indicates that fibroblasts produce erythropoietin. *J Histochem Cytochem* 41: 335–341, 1993
41. Bachmann S, Ramasubbu K: Immunohistochemical colocalization of the α-subunit of neutrophil NADPH oxidase and ecto-5'-nucleotidase in kidney and liver. *Kidney Int* 51: 479–482, 1997
42. Ekataksin W, Kaneda K: Liver microvascular architecture: An insight into the pathophysiology of portal hypertension. *Semin Liver Dis* 19: 359–382, 1999
43. Schuster SJ, Koury ST, Bohrer M, Salceda S, Caro J: Cellular sites of extrarenal and renal erythropoietin production in anaemic rats. *Br J Haematol* 81: 153–159, 1992

Epithelial COX-2 Expression Is Not Regulated By Nitric Oxide in Rodent Renal Cortex

Franziska Theilig, Valentina Cânpean, Alexander Paliege, Matthew Breyer, Josie P. Briggs, Jürgen Schnermann, Sebastian Bachmann

Abstract—In the adult rodent kidney cortex, cyclooxygenase-2 (COX-2), NO synthase (NOS1), and renin synthesis change in parallel on alterations in distal tubular NaCl concentration, and their products in part may mutually determine synthesis and activity of these enzymes. Epithelial NO synthesis has been postulated to exert a stimulatory role on COX-2 expression. Changes in COX-2 and NOS1 may be assessed histochemically by determining changes in the number of positive cells. In rat, macula densa and adjacent cells may co-express COX-2 and NOS1, whereas cell groups of the upstream thick ascending limb (cTAL) express COX-2 alone. We have tested whether the stimulation of COX-2 expression by short- and long-term unilateral renal artery stenosis, low salt, and furosemide treatment depends on co-expression of NOS1. These conditions produced significant respective increases (40% to 351%, $P<0.05$) in the number of COX-2 immunoreactive cells, regardless of whether NOS1 was present or not, suggesting that co-expression of NOS1 is not necessary to produce these changes. Under high-salt conditions, analogous though inverse changes were recorded (−62% to −73%, $P<0.05$). In mice with genetic deletion of NOS1, low- and high-salt diets caused similar changes of COX-2 immunoreactivity (106% and −52%, $P<0.05$) than those seen in wild-type mice (43% and −78%, $P<0.05$). We conclude that alterations of distal tubular NaCl concentration and presumably NaCl transport induce changes in epithelial COX-2 expression that does not depend on presence of co-expressed NOS1. It therefore seems unlikely that NO is part of a signal transduction chain between tubular chloride sensing and the modulating effects of prostaglandins in tubulo-vascular information transfer. (*Hypertension*. 2002;39:848-853.)

Key Words: nitric oxide synthase ■ macula densa ■ renin ■ juxtaglomerular apparatus ■ prostaglandins

The mammalian kidney is an important site for the synthesis and action of products derived from cyclooxygenase (COX) isoforms (prostaglandin synthase, G2/H2), which catalyze the metabolism of arachidonic acid into biologically active prostanoids.[1] Functional roles for eicosanoid products of COX include the orthograde formation of the nephron during ontogenesis[2] and the modulation of renal salt and water excretion.[3] Recent evidence has highlighted the roles of COX-2 in the tubulo-vascular signaling mechanism of the juxtaglomerular apparatus.[4–8] The macula densa mechanism for control of renin secretion depends on COX-2–mediated prostaglandin synthesis, because the stimulation of renin activity, secretion, and mRNA expression in response to a decrease in luminal NaCl concentration could be reduced by the administration of COX-2 inhibitors or nonsteroidal anti-inflammatory drugs.[8–10] Additional evidence came from COX-2–deficient mice that failed to increase renal renin content under low-salt conditions.[11] In the rodent renal cortex, the principal site of COX-2 expression is the cortical thick ascending limb (cTAL), including the macula densa region.[12,13] COX-2 expression is increased in high-renin states whether induced by blockade of the renin angiotensin system,[14,15] salt restriction,[9,12,16] unilateral renal artery stenosis,[10,17] or Na,K,2Cl-cotransport inhibition.[18]

Neuronal NO synthase (NOS1) is partly co-localized with COX-2–expressing cells of the macula densa and neighboring cTAL cells,[13] and conditions that alter COX-2 expression have earlier been shown to induce analogous changes of NOS1.[13,19–21] It has therefore been proposed that NO may also be involved in the modulation of the tubulo-vascular responses.[3] Because NO can activate COX[22] and because inhibition of NOS can decrease juxtaglomerular COX-2 levels,[5,14] it was suggested that NO may be a positive regulator of COX-2. To further investigate whether local NO synthesis is required for a stimulation of COX-2 expression, we studied the co-expression of COX-2 and NOS1 at the level of the single cell in rat models in which global upregulation of these 2 enzymes has previously been established. NOS1-deficient mice were used to corroborate our results.

Received September 27, 2001; first decision December 11, 2001; revision accepted January 3, 2002.

From the Anatomisches Institut, Charité, Humboldt Universität (F.T., V.C., A.P., S.B.), Berlin, Germany; Department of Nephrology (M.B.), Nashville, Tenn; and National Institutes of Health (J.P.B., J.S.), Bethesda, Md.

Correspondence to Prof Dr Sebastian Bachmann, AG Anatomie der Charité, Elektronenmikroskopie, Campus Virchow Klinikum, Augustenburger Platz 1, 13353 Berlin, Germany. E-mail sbachm@charite.de

Hypertension is available at http://www.hypertensionaha.org

DOI: 10.1161/01.HYP.0000013082.99285.35

Methods

Animals

Adult male Sprague Dawley rats, male NOS1-null mutant mice ($NOS1^{-/-}$), and wild-type control mice ($NOS1^{+/+}$) were from the local animal facilities.

Treatments

All treatments and the settings of the control groups were as detailed earlier[19,21]: (1) 2-kidney, 1-clip Goldblatt model of renovascular hypertension during a 3-day early phase and a 28-day maintenance phase (total, n=16) and (2) continuous infusion of furosemide by subcutaneously implanted minipumps for 5 days (total, n=8). The treated rats received 0.3% NaCl and 0.1% KCl as drinking fluid to compensate for the loss of electrolytes.[19] (3) Low- (LSD), normal- (NSD), and high-salt (HSD) diets for 8 days in rats (total, n=12), and (4) LSD and HSD for 11 days in mice (total, n=8). Body weight and urine osmolality (24-hour values from metabolic cages) were controlled throughout all experiments. Kidneys of all animals were perfusion-fixed at the end of the experiments.

Histochemistry

For histochemical demonstration of NOS tissue activity, the enzymatic reduction of nitroblue tetrazolium in the presence of NADPH (NADPH diaphorase reaction) was used on cryostat sections as described.[13,19] For immunohistochemistry, the following primary antibodies were used: (1) rabbit monoclonal antibody against an exon 2–encoded NOS1 domain (amino acids 1 to 181 from rat brain; Sigma), (2) rabbit polyclonal antibody against an exon 12 to 21–encoded NOS1 domain (Calbiochem), (3) goat polyclonal antibody against a C-terminal COX-2 peptide (Santa Cruz Biotechnology), and (4) rabbit polyclonal antibody against rat Tamm Horsfall protein (THP; against the whole protein; gift from J. Hoyer, Philadelphia). For detection, Cy3-coupled goat anti-rabbit or donkey anti-goat, and Cy2-coupled mouse anti-rabbit antisera were used (Dianova). Cell nuclei were stained with 4′,6-diamino-2-phenylindole (Sigma). Standard incubation procedures were used as described.[13,19] In double-labeling experiments, suitable secondary antibodies coupled to different fluorochromes were applied.

In Situ Hybridization

For visualization of mRNA expression, in situ hybridization was performed using digoxigenin-UTP labeled riboprobes made from 1300-bp COX-2 cDNA fragments and using an alkaline-phosphatase–generated signal detection as given in a previously established protocol.[13]

Histochemical Quantification of COX-2 and NOS1 Signals

For histochemical quantification of COX-2– and NOS1-positive cells, an earlier described methodology was adapted.[13,19] Renal cortical immunoreactive signals were determined by counting COX-2– and NOS1-positive cells in 3 distinct microanatomical locations: (1) within the macula densa proper, as defined by the absence of Tamm Horsfall protein[23]; (2) in the macula densa region identified by double staining for both antigens; and (3) in the cTAL, counting only those cells that were NOS1-negative in COX-2/NOS1 double-stained sections. In mice, COX-2 staining was restricted to the macula densa, so only these cells were counted.

To verify changes in NOS1 activity, NADPH diaphorase staining was evaluated as described.[19] Results indicated the same tendency and extent of changes in all experimental groups, as reported in the previous paper, and are not shown.

COX-2 mRNA expression was quantified in sections treated with in situ hybridization. All positively labeled sites were counted throughout the renal cortex. Whenever >1 signal was located in the same tubular profiles, the signals were counted as a single signal.

Results from numerical evaluation were expressed as the number of labeled cells or sites per 100 glomeruli. For all quantifications, which were blinded to the evaluator, a total volume of 400 to 600 glomeruli was considered. For statistical analysis, the Lord test (1-way test), which is used for small sample numbers,[24] or ANOVA were applied where appropriate. Differences of a level of $P<0.05$ were considered significant.

Results

Microanatomical Distribution of COX-2

COX-2 immunoreactive cells were encountered in 3 typical locations: in the macula densa proper, as defined by the THP-negative portions of the cTAL; in the macula densa region of the cTAL adjacent or opposite to the macula densa; and in upstream portions of the cTAL, located at varying distances to the glomerular attachment site (Figure 1). In macula densa cells, COX-2 was detected as a faint nuclear membrane–associated signal compared with that in cTAL cells, where the intracellular signal was generally more widespread and stronger. Double staining of COX-2 and NOS1 revealed that in the NOS1 immunopositive macula densa proper, no more than 1 or 2 COX-2–expressing cells were encountered per positive site, whereas cells co-expressing NOS1 and COX-2 were more frequent in the macula region (Figure 1a through 1m). In sites of the cTAL distant to the glomerulus, single cells or groups of cells showing COX-2 immunoreactivity alone were found (Figure 1n through 1r), whereas NOS1 co-expressing cells were principally absent from these portions, independent of the physiological status of the animal. In situ hybridization for COX-2 in rats showed a lower number of labeled cells compared with that obtained with the corresponding antibody (Figure 2i and 2k). With both techniques, however, signals were located in analogous positions of the distal nephron. In contrast to rats, COX-2 immunoreactivity in control mice was located mostly in macula densa cells proper, whereas cTAL cells were rarely stained (Figure 2g and 2h); as in rats, the COX-2 signal was confined to a perinuclear zone. COX-2 mRNA expression was restricted to single scattered cells in the juxtaglomerular region (data not shown). $NOS1^{-/-}$ mice were used to test whether COX-2 expression is regulated in the absence of epithelial NOS1 activity. Because residual NOS1 activity in these mice may potentially be derived from splice variants lacking exon 2 (NOS1β variant), we evaluated NOS1 activity by the NADPH diaphorase reaction, and NOS1 expression by in situ hybridization with a NOS1 3′-specific riboprobe and by immunocytochemistry with an antibody against an N-terminal domain of the protein. These approaches did not identify NOS1 in macula densa or any other tubular epithelial sites in the $NOS1^{-/-}$ mice (Figure 2a through 2f).

Regulation of COX-2 Expression in Rats

The number of cells expressing COX-2 and/or NOS1 was determined in rats with short-term or long-term unilateral renal artery stenosis, and in rats treated with LSD, NSD, HSD, or with furosemide, and compared with the mean of the respective control group.

The number of COX-2 immunoreactive cells in the macula densa proper, as defined by the lack of concomitant THP immunoreactivity and the obligatory expression of NOS1, was increased by 81% after short constriction and 90% after

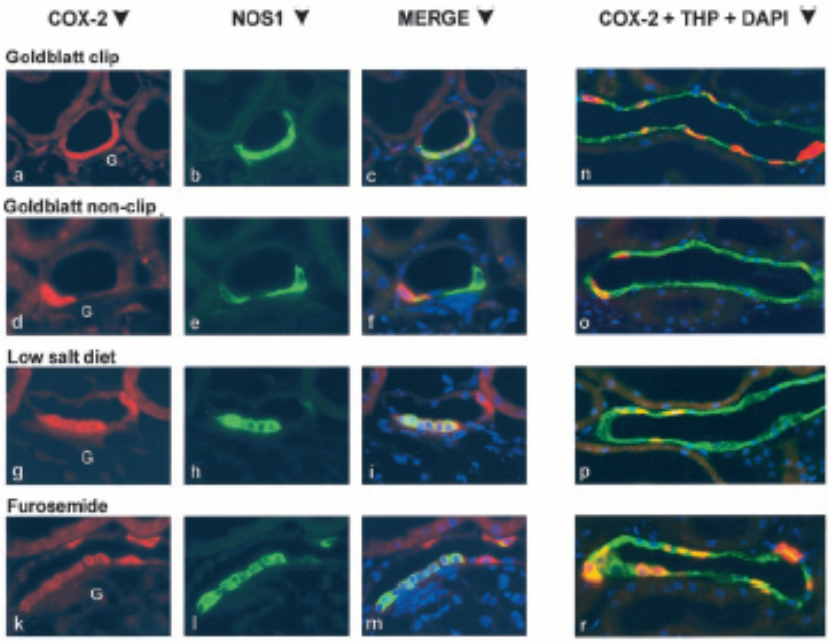

Figure 1. Representative views of differences in specific immunoreactivity of the macula densa region (a through m) and TAL (n through r) from rat kidneys subjected to various experimental conditions as indicated on the left. a through m, Single fluorescent signals of COX-2 (red) and NOS1 (green), and overlay images of signals indicated by merge are documented. n through r, Only overlay images of COX-2 (red) and THP (green) are presented; NOS1 was absent from these segments. In the left block, signals for COX-2 and NOS1 are high in the clipped Goldblatt kidneys (a through c), low in the nonclipped kidneys (d through f), and high after LSD (g through i) and furosemide treatment (k through m). In the right block, analogous quantitative changes are shown for scattered COX-2 immunoreactive cells. Nuclei are 4',6-diamino-2-phenylindole–stained for better identification. G indicates glomerulus.

long constriction ($P<0.01$) in the clipped kidney, by 40% in the LSD group ($P<0.05$), and by 195% in the furosemide group ($P<0.01$). By contrast, COX-2–positive cells were decreased by 53% in the nonclipped kidney after short constriction, by 70% after long constriction ($P<0.01$), and by 60% in the HSD group ($P<0.01$; Figures 1 and 3a).

The number of COX-2 immunoreactive cells of the macula densa region, where cells express both NOS1 and COX-2, increased by 71% after short constriction and 90% after long constriction ($P<0.01$) in the clipped kidney, by 45% in the LSD group ($P<0.05$), and by 70% in the furosemide group ($P<0.01$). The number of these cells had decreased by 41% in the nonclipped kidney after short constriction, by 31% after long constriction ($P<0.05$), and by 68% in the HSD group ($P<0.01$; Figures 1 and 3b).

Finally, the number of COX-2 immunoreactive cells of the upstream cTAL portions, which throughout all experiments did not express NOS1, had increased by 73% after short constriction and 75% after long constriction ($P<0.01$) in the clipped kidney, by 59% in the LSD group ($P<0.05$), and by 351% in the furosemide group ($P<0.01$). By contrast, the cell number had decreased by 14% after short constriction and 13% after long constriction (P=NS) in the nonclipped kidney and by 73% in the HSD group ($P<0.01$; Figures 1 and 3c).

The number of NOS1 immunoreactive cells of the macula densa and macula densa region together had increased by 35% ($P<0.05$) in the short-term and 50% ($P<0.01$) in the long-term clipped kidney, by 41% ($P<0.01$) in the LSD group, and by 44% ($P<0.01$) in the furosemide group and decreased by 14% in the short-term clipped kidney ($P<0.05$), by 16% ($P<0.01$) in the long-term clipped kidney, and by 30% in the HSD group ($P<0.01$; Figures 1 and 3d).

The number of cortical COX-2 mRNA-expressing sites was increased by 66% in the clipped kidneys and decreased by 36% in the nonclipped kidneys in the maintenance phase of renal artery stenosis ($P<0.05$). In the furosemide group, a 491% increase was measured ($P<0.01$; Figures 2i, 2k, and 3e). Results in rats are summarized in Figure 4.

Regulation of COX-2 Expression in Mice

In these experiments, the number of COX-2–expressing cells was compared between wild-type control mice and NOS1$^{-/-}$ mice. Because COX-2 immunoreactivity is restricted to the macula densa in mice, only macula densa cells were evaluated. The numbers of COX-2–positive cells were not different between NOS1$^{-/-}$ and wild-type under control conditions. After LSD treatment, COX-2 immunoreactive cells were increased by 43% in weight and by 106% in NOS1$^{-/-}$ compared with the respective genotype on a control diet ($P<0.05$), and decreased after HSD by 78% in wild-type and 52% in NOS1$^{-/-}$ ($P<0.05$; Figure 2g and 2h. Absolute values are given in Figure 3f).

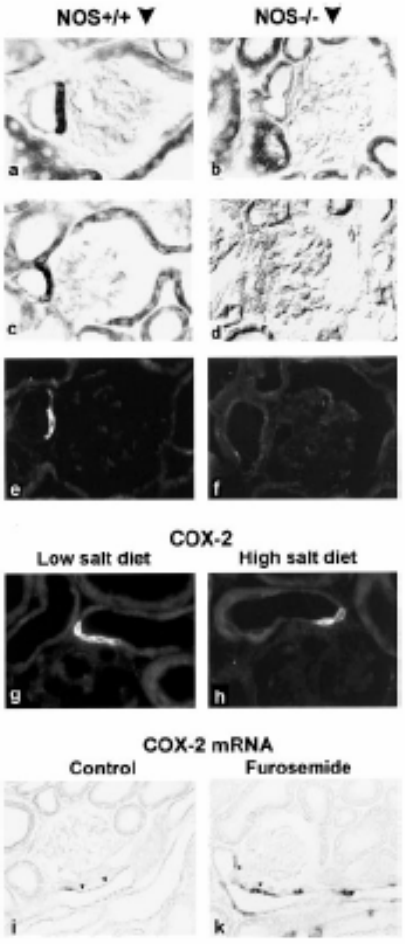

Figure 2. Representative views of NOS1 activity/mRNA expression/immunoreactivity in control and NOS1$^{-/-}$ mice (a through f), of the effects of LSD and HSD on COX-2 immunostaining in NOS1$^{-/-}$ mice (g and h), and of COX-2 mRNA expression in furosemide-treated rats (i and k). NADPH diaphorase staining (a and b), NOS1 in situ hybridization using NOS1 3′-specific riboprobe (c and d), and NOS1 immunostaining using an antibody directed against an exon 12 to 21–encoded NOS1 domain of the protein (e and f) show clear signals in macula densa of the wild-type mice, but no signal in the knockout mice. COX-2 signal is markedly stronger after LSD and stains more macula densa cells (g) than after HSD (h). COX-2 mRNA expression is much stronger in furosemide-treated rats (k) than in untreated controls (i); macula densa between arrowheads. The mRNA signals in panels i and k are mostly in cTAL.

Discussion

Partial co-expression and the co-regulation of COX-2 and NOS1 have been the basis of the hypothesis that local NO synthesis may be a determinant of COX-2 activity or COX-2 expression. In the present studies, we have used a quantitative histochemical approach to examine whether known COX-2–inducing stimuli can be differentiated in their stimulatory potency depending on the exact location of the COX-2 expressing tubular cells. In particular, we aimed at disclosing whether co-expression of NOS1 is required for COX-2 regulation. Thus, we have distinguished levels of COX-2 expression between cells characterized by presence (macula densa region) or absence (upstream cTAL) of co-expression with NOS1. In view of the well-established similarities in the expression of transport-related gene products between these sites,[3,25] a comparison between these cells is a useful test of a role of NOS1 on the regulation of COX-2 expression.

The experimental conditions used in rats in this study resulted in changes of COX-2 and NOS1 expression that were comparable to those reported earlier under similar circum-

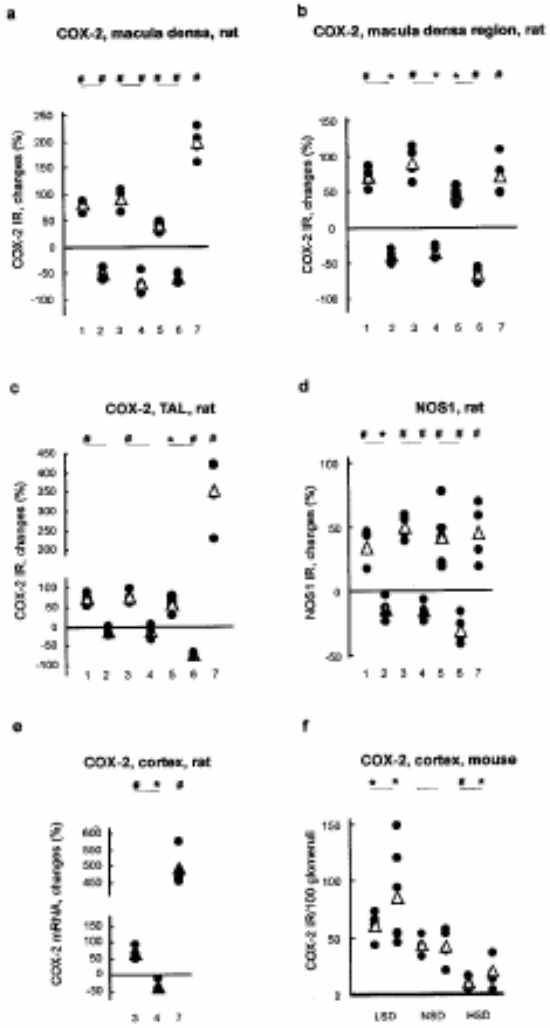

Figure 3. Calculated changes in numbers of COX-2– and NOS1-positive cells in kidney cortex. Experimental conditions in a through e (1, short-term clip; 2, short-term nonclip; 3, long-term clip; 4, long-term nonclip; 5, LSD; 6, HSD; and 7, furosemide treatment) are compared with the respective control levels within the distinct epithelial locations. f, Values show absolute cell numbers in wild-type (left) and NOS1$^{-/-}$ mice (right) under LSD, NSD, and HSD, respectively; statistical analysis compares LSD and HSD groups to their respective NSD controls. ● indicates individual values; △, mean values. *P<0.05, #P<0.01.

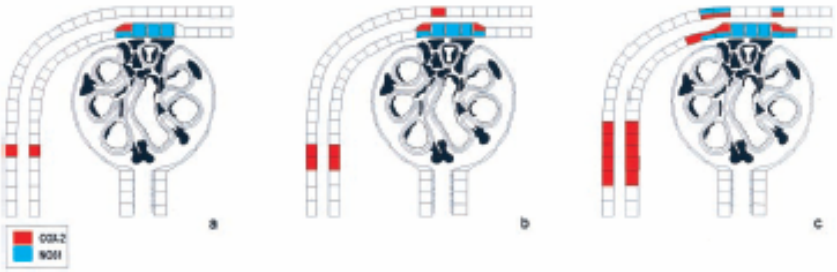

Figure 4. Schematic topographical representation of COX-2 immunoreactive cells in control rats (b), and in rats subjected to inhibitory (a) or stimulatory interventions (c). NOS1 immunoreactive cells may express NOS1 alone, or concomitantly with COX-2 (red and blue). Three cell populations—ie, macula densa cells proper (3 columnar cells adjacent to glomerulus), cells of the macula densa region (flatter cells near macula), and cells of the cortical thick ascending limb (upstream populations distant to glomerulus)—are involved in the changes.

stances.[7,8,10,12,17,26] These whole animal studies, and studies in isolated preparations of the juxtaglomerular apparatus[8] and in cultured lines of macula densa–derived[7] and cTAL cells,[14,18] have contributed to a general concept of the local regulation of COX-2 synthesis and function. One of the conclusions has been that either NKCC2 inhibition with loop diuretics or a lowering of ambient Cl^- levels may act as a trigger to stimulate COX-2 activation and PGE2 release.[7] Our present results are consonant with this notion, in that experimental conditions associated with NKCC2 inhibition (furosemide treatment) or with a reduced luminal NaCl concentration and presumably reduced NKCC2 activity along the cTAL (clipped Goldblatt kidney, salt deprivation) are associated with increased COX-2 expression.

The transduction mechanism coupling NKCC2 activity and COX-2 enzyme activity is unclear. Published evidence has indicated a functional dependence of COX-2 on constitutive NOS activity in whole-animal studies and isolated juxtaglomerular preparations.[5,8,9,14] These studies indicated that in salt depletion or during NKCC2 inhibition, NO plays a significant stimulatory role in COX-2 activation. A preliminary study of our laboratory, however, had produced contradictory results. Using several ways for a chronic application of the NOS1 specific inhibitor 7-nitroindazole in rats, we were unsuccessful to confirm the stimulatory role of NOS1 activity in a whole-animal setting.

In our present results, stenosis of the renal artery, salt deprivation, and NKCC2 blockade all produced a significant numerical recruitment of COX-2– and NOS1-positive cells independent of a co-expression of these parameters. The numerical reduction of these cells below control levels in a condition suppressing both parameters (volume expansion by high salt intake) produced analogous inversely directed changes. From these observations, we conclude that the intracellular availability of NO or its regulation is not a necessary requirement for the augmentation of COX-2–positive cells.

It is conceivable that NO contributes to the regulation of COX-2 in cells that express NOS1, but that COX-2 regulation uses other pathways in cells without concomitant NOS1 expression. In fact, in the work of Cheng et al,[14] it appears that the suppression of COX-2 by 7-nitroindazole is most pronounced in the macula densa and less dramatic in the surrounding cTAL cells. A direct, cGMP-dependent activation of COX-2 in cultured rabbit cTAL cells has also been reported.[14] We had previously found that at least in rat, however, neither cTAL nor macula densa cells contained detectable amounts of soluble guanylyl cyclase, the cGMP-catalyzing enzyme.[27] Thus, it is unclear whether an NO-dependent cGMP pathway can affect prostaglandin synthesis within the same cell in situ.

Recently an alternative, cGMP-independent intracellular mechanism of COX-2 induction initiated by phosphorylation of extracellular signal-regulated kinase (ERK)1/2 as well as p38 kinase[7,18] has been described that may be active in the present conditions; ERK and p38 activation may in fact stimulate COX-2 gene expression by transcriptional and posttranscriptional regulation.[28]

Our complementary studies in mice show that macula densa COX-2 immunoreactivity was not different between wild-type controls and NOS1 knockout mice, suggesting that presence of local NOS1 is not a prerequisite for macula densa–specific expression of COX-2. Furthermore, stimulation of COX-2 expression in macula densa cells by a LSD was comparable in $NOS1^{-/-}$ and wild-type mice. Because we documented total absence of tubular NOS1 expression in the $NOS1^{-/-}$ mice, these results confirm our conclusions from the rat studies that an intracellular co-expression of COX-2 and NOS1 and the direct availability of NO is not required.

In summary, our results indicate that an activation of epithelial COX-2 expression by a reduction in NaCl uptake in rats is comparable in macula densa cells and in cTAL cells near or distant from the macula densa, and that coexpression of NOS1 does not modify the degree of COX-2 stimulation. Furthermore, NOS1-deficient mice express COX-2 at similar levels as those of wild-type mice, and a low salt intake stimulates COX-2 expression to a similar degree in both strains of mice. We therefore conclude that intracellular or ambient NO levels are not required for the activation of COX-2.

Acknowledgments

This work was supported by funds from the Deutsche Forschungsgemeinschaft (Ba 700/14-1 and -2).

References

1. Kam PC, See AU. Cyclo-oxygenase isoenzymes: physiological and pharmacological role. *Anaesthesia*. 2000;55:442–449.

2. Morham SG, Langenbach R, Loftin CD, Tiano HF, Vouloumanos N, Jennette JC, Mahler JF, Kluckman KD, Ledford A, Lee CA, et al. Prostaglandin synthase 2 gene disruption causes severe renal pathology in the mouse. *Cell*. 1995;83:473–482.
3. Schnermann J. Juxtaglomerular cell complex in the regulation of renal salt excretion. *Am J Physiol*. 1998;274:R263–R279.
4. Jensen BL, Schmid C, Kurtz A. Prostaglandins stimulate renin secretion and renin mRNA in mouse renal juxtaglomerular cells. *Am J Physiol*. 1996;271:F659–F669.
5. Ichihara A, Imig JD, Inscho EW, Navar LG. Cyclooxygenase-2 participates in tubular flow-dependent afferent arteriolar tone: interaction with neuronal NOS. *Am J Physiol*. 1998;275:F605–F612.
6. Ito S, Carretero OA, Abe K, Beierwaltes WH, Yoshinaga K. Effect of prostanoids on renin release from rabbit afferent arterioles with and without macula densa. *Kidney Int*. 1989;35:1138–1144.
7. Yang T, Park JM, Arend L, Huang Y, Topaloglu R, Pasumarthy A, Praetorius H, Spring K, Briggs JP, Schnermann J. Low chloride stimulation of prostaglandin E2 release and cyclooxygenase-2 expression in a mouse macula densa cell line. *J Biol Chem*. 2000;275:37922–37929.
8. Traynor TR, Smart A, Briggs JP, Schnermann J. Inhibition of macula densa–stimulated renin secretion by pharmacological blockade of cyclooxygenase-2. *Am J Physiol*. 1999;277:F706–F710.
9. Harding P, Sigmon DH, Alfie ME, Huang PL, Fishman MC, Beierwaltes WH, Carretero OA. Cyclooxygenase-2 mediates increased renal renin content induced by low-sodium diet. *Hypertension*. 1997;29:297–302.
10. Wang JL, Cheng HF, Harris RC. Cyclooxygenase-2 inhibition decreases renin content and lowers blood pressure in a model of renovascular hypertension. *Hypertension*. 1999;34:96–101.
11. Yang T, Endo Y, Huang YG, Smart A, Briggs JP, Schnermann J. Renin expression in COX-2 knockout mice on normal or low-salt diets. *Am J Physiol*. 2000;279:F819–F825.
12. Harris RC, McKanna JA, Akai Y, Jacobson HR, Dubois RN, Breyer MD. Cyclooxygenase-2 is associated with the macula densa of rat kidney and increases with salt restriction. *J Clin Invest*. 1994;94:2504–2510.
13. Weichert W, Paliege A, Provoost AP, Bachmann S. Upregulation of juxtaglomerular NOS1 and COX-2 precedes glomerulosclerosis in frown-hooded hypertensive rats. *Am J Physiol*. 2001;280:F706–F714.
14. Cheng HF, Wang JL, Zhang MZ, McKanna JA, Harris RC. Nitric oxide regulates renal cortical cyclooxygenase-2 expression. *Am J Physiol*. 2000; 279:F122–F129.
15. Wolf K, Castrop H, Hartner A, Goppelt-Strube M, Hilgers KF, Kurtz A. Inhibition of the renin-angiotensin system upregulates cyclooxygenase-2 expression in the macula densa. *Hypertension*. 1999;34:503–507.
16. Yang T, Singh I, Pham H, Sun D, Smart A, Schnermann JB, Briggs JP. Regulation of cyclooxygenase expression in the kidney by dietary salt intake. *Am J Physiol*. 1998;274:F481–F489.
17. Mann B, Hartner A, Jensen BL, Hilgers KF, Hocherl K, Kramer BK, Kurtz A. Acute upregulation of COX-2 by renal artery stenosis. *Am J Physiol*. 2001;280:F119–F125.
18. Cheng HF, Wang JL, Zhang MZ, McKanna JA, Harris RC. Role of p38 in the regulation of renal cortical cyclooxygenase-2 expression by extracellular chloride. *J Clin Invest*. 2000;106:681–688.
19. Bosse HM, Böhm R, Resch S, Bachmann S. Parallel regulation of constitutive NO synthase and renin at JGA of rat kidney under various stimuli. *Am J Physiol*. 1995;269:F793–805.
20. Schricker K, Hansmann M, Kurtz A. Nitric oxide and prostaglandins are involved in the macula densa control of the renin system. *Am J Physiol*. 1995;269:F825–F830.
21. Singh I, Granss M, Wang WH, Yang T, Killen P, Smart A, Schnermann J, Briggs JP. Coordinate regulation of renal expression of nitric oxide synthase, renin, and angiotensinogen mRNA by dietary salt. *Am J Physiol*. 1996;270:F1027–F1037.
22. Salvemini D, Currie MG, Mollace V. Nitric oxide–mediated cyclooxygenase activation: a key event in the antiplatelet effects of nitrovasodilators. *J Clin Invest*. 1996;97:2562–2568.
23. Bachmann S, Metzger R, Bunnemann B. Tamm-Horsfall protein-mRNA synthesis is localized to the thick ascending limb of Henle's loop in rat kidney. *Histochemistry*. 1990;94:517–523.
24. Sachs L. *Angewandte Statistik*, 7th ed. Heidelberg, Germany: Springer, 1992:361–362.
25. Bachmann S, Bostanjoglo M, Schmitt R, Ellison DH. Sodium transport-related proteins in the mammalian distal nephron: distribution, ontogeny and functional aspects. *Anat Embryol*. 1999;200:447–468.
26. Mann B, Hartner A, Jensen BL, Kammerl M, Kramer BK, Kurtz A. Furosemide stimulates macula densa cyclooxygenase-2 expression in rats. *Kidney Int*. 2001;59:62–68.
27. Theilig F, Bostanjoglo M, Pavenstädt H, Grupp C, Holland G, Slosarek I, Gressner AM, Russwurm M, Koesling D, Bachmann S. Cellular distribution and function of soluble guanylyl cyclase in kidney and liver, rat. *J Am Soc Nephrol*. 2001;12:2209–2220.
28. Ridley SH, Dean JL, Sarsfield SJ, Brook M, Clark AR, Saklatvala J. A p38 MAP kinase inhibitor regulates stability of interleukin-1–induced cyclooxygenase-2 mRNA. *FEBS Lett*. 1998;439:75–80.

Am J Physiol Renal Physiol 285: F19–F32, 2003;
10.1152/ajprenal.00443.2002.

Key enzymes for renal prostaglandin synthesis: site-specific expression in rodent kidney (rat, mouse)

Valentina Câmpean,[1] Franziska Theilig,[1] Alex Paliege,[1] Matthew Breyer,[2] and Sebastian Bachmann[1]

[1]*Anatomisches Institut, Charité, Humboldt Universität, D-10098 Berlin, Germany; and* [2]*Division of Nephrology, Vanderbilt University, Nashville, Tennessee 37232-2372*

Submitted 30 December 2002; accepted in final form 25 February 2003

Câmpean, Valentina, Franziska Theilig, Alex Paliege, Matthew Breyer, and Sebastian Bachmann. Key enzymes for renal prostaglandin synthesis: site-specific expression in rodent kidney (rat, mouse). *Am J Physiol Renal Physiol* 285: F19–F32, 2003; 10.1152/ajprenal.00443.2002.—Prostanoids derived from endogenous cyclooxygenase (COX)-mediated arachidonic acid metabolism play important roles in the maintenance of renal blood flow and salt and water homeostasis. The relative importance of COX-1 and COX-2 isoforms is under active investigation. We have performed a comprehensive histochemical analysis by comparing rat and mouse kidneys for cellular and subcellular localization of COX-1 and -2 and microsomal-type PGE synthase (PGES), the rate-limiting biosynthetic enzyme in PGE_2 synthesis. A choice of different sera was compared, and the results were confirmed by antigen-retrieval techniques, in situ hybridization, RT-PCR, and the use of COX knockout mice. In the glomerulus, significant COX-1 expression was detected in a subset of mesangial cells. Along the renal tubule, the known COX-2 expression in cTAL and macula densa was paralleled by PGES staining. In the terminal distal convoluted tubule, connecting tubule, and cortical and medullary collecting ducts, a significant COX-1 signal was colocalized with PGES; COX-2 was not found in these sites. Intercalated cells were generally negative. Cortical fibroblasts were COX-1 and PGES positive in mice, whereas in rats only PGES could be reliably detected. Lipid-laden interstitial cells of the inner medulla were COX-1, -2, and PGES positive. Vascular smooth muscle cells were not stained. The present data support prominent functions of renal prostanoids, predominantly PGE_2, by defining expression sites of the key enzymes for their biosynthesis in the rat and mouse. Results define the renal cell types involved in prostaglandin autacoid functions within spatially restricted sites such as the juxtaglomerular apparatus, mesangium, distal convolutions and collecting duct, and in compartments of the renal interstitium.

mesangium; thick ascending limb; distal convolutions; collecting duct; interstitium

THE MAMMALIAN KIDNEY IS A major site for the synthesis and action of products derived from cyclooxygenase [COX; prostaglandin synthase (PGES); G_2/H_2]. The enzymatic conversion of arachidonate to PGH_2 is followed by further metabolism into several bioactive prostaglandins such as PGE_2, the major renal prostaglandin, and others like PGI_2, $PGF_{2\alpha}$, PGD_2, or thromboxane A2 (TxA_2; for a review, see Ref. 43). PGE_2 is preferentially catalyzed by the rate-limiting terminal prostanoid synthase [PGE_2 synthase (i.e., PGES)] (15, 24).

As elsewhere in the organism, prostaglandins play multifold roles in the physiology and disease of the kidney. They interfere importantly with the modulation of local hemodynamics, renin release, and tubular salt and water reabsorption (for a review, see Refs. 19 and 40). Renal medullary prostaglandins are involved in the pathogenesis of hypertension, maintenance of renal blood flow, and promotion of urinary salt excretion (37). They further play an important role in electrolyte disorder syndromes such as the antenatal Bartter syndrome (35) and in inflammatory renal disease (61). Renal prostaglandins act as paracrine autacoids, causing local, specific effects according to the renal zonation and distribution of cell types (37, 48, 49); this is also reflected by the spatial distribution of the various receptor subtypes (for a review, see Ref. 6).

There are two COX isoforms that have been identified recently by molecular approaches. Both exhibit similar biochemical activity in converting arachidonate to PGH_2 (9) and are similar in molecular mass (70 and 71 kDa), but they differ largely in amino acid sequence and also with respect to the availability of the downstream-acting prostanoid synthases and the prostanoids ultimately formed (43). They also show differential distribution and regulation. COX-1, the constitutive form, is widely expressed in the organism and is considered to have "housekeeping" functions providing the majority of prostaglandin production (9). The inducible isoform, COX-2, may be increased during inflammation, but among few other tissues it is also expressed constitutively in topographically restricted sites of the kidney (17). The distinct role of the latter has also been elucidated by the use of mutant mice; the kidneys of COX-2-deficient mice fail to develop normally (33), whereas those lacking the gene for COX-1 production do not show conspicuous symptoms under normal conditions (1). Isoform-specific inhibitors have recently attracted a great deal of interest because the selective targeting of pathophysiological sources of

Address for reprint requests and other correspondence: S. Bachmann, AG Anatomie der Charité, Campus Mitte, Philippstr. 12, 10098 Berlin, Germany (E-mail: sbachm@charite.de).

The costs of publication of this article were defrayed in part by the payment of page charges. The article must therefore be hereby marked "*advertisement*" in accordance with 18 U.S.C. Section 1734 solely to indicate this fact.

prostaglandins is considered a promising means of avoiding any adverse renal effects during pharmacological treatment (for a review, see Ref. 18).

Localization of the renal sources of prostaglandin synthesis and release is thus a major issue that has been studied in a number of mammalian species under constitutive and regulated conditions (15, 19, 20, 23, 29, 31, 41, 42, 45, 46, 49, 51). However, important aspects of tissue localization have remained unresolved or controversial, owing to conventional problems in the interpretation of histochemical staining procedures. In particular, COX expression in glomerular cells (10, 30, 31), collecting duct cell types (11, 42, 47), and in the cortical vs. medullary interstitium (31, 37, 50) has been reported inconsistently, and a segmental assignment of cortical COX-1 immunoreactivity has been lacking. The availability of new antibodies and intensified histochemical detection protocols have prompted us to comparatively evaluate in detail COX-1, COX-2, and microsomal PGES distribution using different morphological techniques. Particular emphasis has been put on the identification of epithelial expression sites in the nephron and collecting duct system. With regard to the increasing interest in mutant mice, this study has been comparatively performed in normal rats and mice. Mutant mice have been used as controls for signal specificity. In the present study, we thus aimed to present a comprehensive histochemical analysis to support functional interpretation of site-specific prostaglandin synthesis.

METHODS

Animal preparation. Adult male Sprague-Dawley rats (200-g body wt) were obtained from the local animal facility. Adult male COX-1 and COX-2 null mutant knockout mice (COX-$1^{-/-}$ and COX-$2^{-/-}$) and wild-type control mice (COX-$1^{+/+}$) were from a mouse colony at Vanderbilt University and at the National Institutes of Health (NIH; kindly provided by J. B. Schnermann). Information on the genetic background of these mice can be found elsewhere (37). All experiments were conducted in accordance with the *Guide for the Care and Use of Laboratory Animals* (NIH Publication 85–23, Revised 1996) and the German Law for the Protection of Animals. The kidneys were perfused retrograde through the abdominal aorta using PBS adjusted to 330 mosmol/kgH_2O with sucrose, pH 7.4, for 20 s as described before (38). Next, a solution of 3% paraformaldehyde in PBS was infused for 5 min, followed by PBS adjusted to 330 mosmol/kgH_2O for 1 min. For cryostat sectioning, tissues were protected from freezing artifacts by subsequent overnight immersion in PBS adjusted to 800 mosmol/kgH_2O by sucrose (pH 7.3), shock-frozen in liquid nitrogen-cooled isopentane, and stored at −70°C. For preembedding immunohistochemical analysis, tissue blocks were postfixed for 12 h in 3% paraformaldehyde in PBS containing 0.05% glutaraldehyde, rinsed, and subsequently stored in PBS. For the paraffin technique, tissue was postfixed in 3% paraformaldehyde for another 12 h and then dehydrated and standard paraffin embedded.

Light microscopic immunohistochemistry. Five-micrometer-thick cryostat and paraffin sections were used. Paraffin sections were dewaxed and rehydrated, heated in a microwave oven in 2.9 g/l citrate buffer (pH 6.0) for 20 min, or incubated in a pressure cooker for 90 s in preheated target retrieval solution from a catalyzed signal amplification kit (DAKO, Hamburg, Germany), producing a streptavidin-biotin-peroxidase signal reaction. After being blocked with 5% skim milk in PBS (pH 7.4), sections were incubated with primary antibody for 2 h at room temperature and then overnight at 4°C. In double-labeling experiments, suitable secondary antibodies coupled to different fluorochromes were applied (Dianova, Hamburg, Germany).

Enzymes involved in prostaglandin synthesis were identified using the following antibodies: rabbit polyclonal antibody against amino acids 274–288 of COX-1 (dilution 1:7,000; batch 160109; Cayman Chemical, Ann Arbor, MI); rabbit polyclonal antibody against an NH_2-terminal peptide of COX-1 (amino acids 63–124; dilution 1:500; batch 1754; Santa Cruz Biotechnology, Heidelberg, Germany); rabbit polyclonal antibody against amino acids 584–598 of COX-2 (dilution 1:500; batch 160126; Cayman Chemical); goat polyclonal antibody against a COOH-terminal COX-2 peptide (dilution 1:500; batch 1747; Santa Cruz Biotechnology); and rabbit polyclonal antibody against an NH_2-terminal peptide of microsomal type PGES (amino acids 59–75; dilution 1:5,000; batch 160630; Cayman Chemical). Nephron portions were identified by double labeling with segment-specific antisera on the same sections or on consecutive sections depending on the origin of the antibody. Rabbit antibody to Tamm-Horsfall protein (gift from J. Hoyer, Philadelphia, PA); rabbit antibody to the Na-Cl cotransporter [NCC; gift from David H. Ellison, Portland, OR (38)]; mouse monoclonal antibody against calbindin D_{28K} (Sigma, Taufkirchen, Germany); and guinea pig antiserum against the basolateral Na/Ca exchanger [kindly provided by R. Reilly, New Haven, CT (38)] were used. To confirm the specificity of the antibodies, control experiments were performed by replacing primary antibodies with 5% skim milk in PBS or by preabsorption with the respective peptides used for immunization as far as they were commercially available.

Slides were evaluated with a digital Spot camera from Diagnostic Instruments, processed with Meta Vue software from Universal Imaging supported by Visitron System (Puchheim, Germany), and viewed with a Leica DMRB light microscope equipped with interference contrast optics and an HBO fluorescence lamp.

Ultrastructural analysis. For preembedding immunoperoxidase labeling, 40-μm-thick kidney slices generated with a Vibratome (Leica, Weiterstadt, Germany) were incubated overnight in microtiter plates with the appropriate COX antibodies at relatively high concentrations (dilutions 1:10–1:200), postfixed with 1% osmium tetroxide, stained en bloc with uranyl acetate, and flat embedded in Epon 812. Ultrathin sections were analyzed after additional contrasting in uranyl acetate and lead citrate. Sections were examined with a Leo 906 electron microscope (Zeiss, Oberkochen, Germany). Semithin sections were evaluated as well.

Isolation of glomeruli and RT-PCR analysis. Glomeruli were isolated as described previously (32). Total RNA from isolated glomeruli was extracted using the guanidinium thiocyanate method. Five micrograms of total RNA from each sample were reverse transcribed. The following sets of oligonucleotide primers were used to amplify cDNA: 5′-TATCCGTTGTGGATCTGAC-3′ and 5′-TGGTCCAGGGGTTTCTTAC-3′ (GAPDH; 300 bp); 5′-CCTTCCGTGTGCCAGATTAC-3′ and 5′-GGCTGGCCTAGAACTCACTG-3′ (COX-1; 475 bp); 5′-ACACTCTATCACTGGCATCC-3′ and 5′-GAAGGGACACCCTTTCACAT-3′ (COX-2; 585 bp); and 5′-TGTACGCGGTGGCTGTCATC-3′ and 5′-GCCAGAACATAGGCCCCGG-3′ (PGES; 300 bp). Amplification was performed using *Taq* polymerase for

24–35 cycles with an automated thermal cycler (PerkinElmer, Weiterstadt, Germany). Each cycle consisted of the following steps: denaturation at 98°C, annealing at 63°C, and extension at 72°C. The amplified DNA fragments had the expected lengths as validated by agarose gel electrophoresis and ethidium bromide staining.

Western blot analysis. Freshly isolated kidneys from rats and mice were dissected and cut into small pieces. The samples were homogenized in ice-cold buffer containing 1% Triton X-100, 0.2% SDS, and 1 tablet of protease inhibitor cocktail (Roche, Grenzach-Wyhlen, Germany) in 25 ml PBS buffer, followed by a 10-min treatment in an ultrasonic bath. The homogenates were centrifuged (14,000 *g* at 4°C), and the supernatants were stored at −80°C until assayed. Samples (100 μg/lane) were run on 10% gradient polyacrylamide minigels and blotted onto nitrocellulose membranes. Blots were blocked overnight with 5% nonfat skim milk and then incubated for 1 h at room temperature with antibody against COX-1, COX-2, or PGES. After extensive washing with 5% Tween in PBS, blots were incubated with horseradish peroxidase-coupled IgG. A signal was developed according to the manufacturer's protocol (Sigma).

In situ hybridization. Digoxigenin(DIG)-UTP-labeled riboprobes and an alkaline phosphatase-dependent signal were generated as described (2). COX-1 riboprobe was made from an 800-bp partial cDNA fragment of rat COX-1, COX-2 riboprobe from a 1,300-bp partial cDNA fragment of rat COX-2, and NCC riboprobe from a 700-bp partial cDNA fragment of rat NCC. COX-2 and NCC fragments were subcloned into the *Eco*RV site of pBluescript vector (Stratagene, La Jolla, CA) and the COX-1 fragment into the pCR II-TOPO vector (In-Vitro Gen, Giessen, Germany). To generate sense and antisense riboprobes, the vectors were linearized by *XhoI*/*Bam*HI for COX-1, *KpnI*/*Xho*I for COX-2, and *XhoI*/*Sac*I for NCC (Roche, Mannheim, Germany), respectively. RNA probes were synthesized and in vitro transcribed in the presence of DIG-UTP and T3, T7, or SP6 polymerases (Roche). For in situ hybridization, 7-μm-thick paraffin sections were treated according to an established protocol (2, 38). Riboprobes were applied at concentrations between 10 and 15 ng/ml, and hybridization was performed at 40–50°C. For control, sense probes were applied in parallel with antisense probes. Sheep anti-DIG-alkaline phosphatase conjugate (DAKO) was diluted 1:50 in blocking medium. A signal was generated using 4-nitro blue tetrazolium chloride, 5-bromo-4-chloro-3-indolylphosphate, and levamisole dissolved in 0.1 M Tris·HCl, 0.1 M NaCl, and 0.05 M $MgCl_2$, pH 9.5. Slides were rinsed with PBS and placed under a coverslip with PBS-glycerol and viewed using brightfield microscopy as described above. Radiolabeled in situ hybridization was performed according to established protocols. Before hybridization, tissue sections were deparaffinized, refixed in paraformaldehyde, treated with proteinase K (20 μg/ml), washed with PBS, refixed in 4% paraformaldehyde, and treated with triethanolamine plus acetic anhydride (0.25% vol/vol). The respective ^{35}S-labeled antisense and sense riboprobes were hybridized to the section at 55°C for 18 h. After hybridization and stringency washes, sections were treated with RNase A (10 μg/ml) at 37°C for 30 min. Slides were dehydrated, air-dried, dipped in photoemulsion (Ilford K5; Knutsford, Cheshire, UK), and exposed for 4–5 days at 4°C. Photomicrographs of the radiolabeled in situ hybridization were viewed with darkfield optics using a Zeiss photomicroscope equipped with a digital camera (Spot-Cam; Diagnostic Instruments, Sterling Heights, MI).

RESULTS

Antibodies against COX isoforms. A choice of commercially produced antisera against COX-1, COX-2, and PGES is presently available; however, the present experience has shown that detailed examination of cross-reactivity was in fact necessary to assess the specificity of the immunological probes. Some of the antibodies tested showed significant cross-reactivity among isoforms, contrary to product specifications. Different antibodies to the same epitope did not necessarily yield the same immunohistochemical staining patterns, whereas others stained structures unlikely to express COX isoforms. Isoform specificity, as outlined by the producer, was not always given because sera labeled anti-COX-1 were raised against peptides with similarities to COX-2. Therefore, only comparative analysis of several different approaches such as conventional immunofluorescence staining protocols, ultrastructural immunoperoxidase labeling, and in situ hybridization was successful. In light microscopy, the use of fluorescent antibody labeling resulted in very clear-cut staining with no major background problems; however, brightfield microscopy with peroxidase staining using an antigen-retrieval kit was clearly more sensitive, so that weak signals such as epithelial COX-1 that were not well detected by immunofluorescence could be detected satisfactorily with this technique. The use of controls including COX-1 and COX-2 knockout mice was essential for confirmation of these results. The best signals were obtained using rabbit polyclonal antibody to murine COX-1 (batch 160109; Cayman Chemical); goat polyclonal anti COX-2 antibody (batch 1747; Santa Cruz Biotechnology); and rabbit polyclonal antibody to microsomal PGES (batch 160630; Cayman Chemical).

Identification of kidney structures. For a precise assignment of prostaglandin synthesis to identified portions of the renal tubule, we used morphological criteria as well as the segmental coexpression of defined markers (3, 6). Glomerular and juxtaglomerular cells were identified by fine structural criteria. The proximal tubule was recognized by the presence of brush border; thin limbs and vasa recta by their location within the vascular bundles; medullary and cortical thick ascending limb (mTAL and cTAL, respectively) by the presence, and macula densa by the absence, of Tamm-Horsfall protein; distal convoluted tubule (DCT) by the presence of the NCC; and parts of the DCT and the connecting tubule (CNT) by the Na/Ca exchanger and calbindin. Collecting ducts were identified by their microanatomic location, epithelial height, and presence of intercalated cells; and interstitial cells were identified based on their shape, location, and immunoreactive pattern.

Cortex. The glomerulus and juxtaglomerular apparatus revealed significant COX-1 immunoreactivity in the extraglomerular mesangium in both species. In addition, a subset of mesangial cells of the glomerular tuft was markedly COX-1 positive (Fig. 1). Ultrastructural distribution of COX-1 in rat mesangial cells

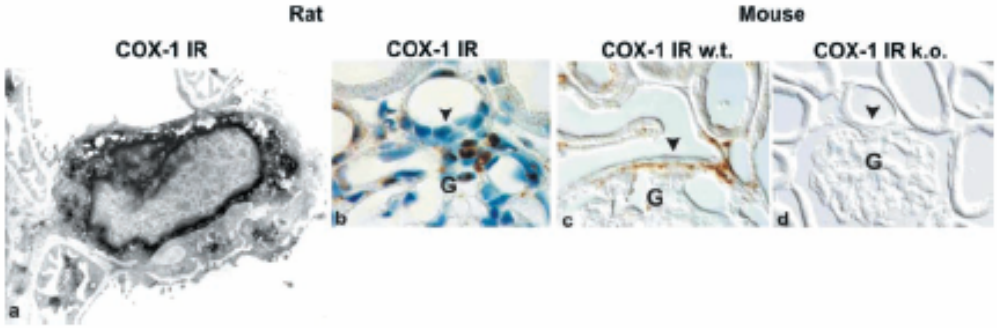

Fig. 1. Distribution of cyclooxygenase (COX)-1 immunoreactivity (IR) in glomerulus and juxtaglomerular apparatus. *a*: Ultrastructural immunoperoxidase staining reveals COX-1 IR in a single mesangial cell; note the perinuclear concentration of signal. *b–d*: In rats and wild-type mice (w.t.), extraglomerular mesangial cells stain significantly for COX-1, whereas in COX-1 knockout mice (k.o.) there is no signal. Arrowheads, macula densa; G, glomerulus. Ultrathin section (*a*) and paraffin sections, hematoxylin stain, and interference contrast (*b–d*, respectively) are shown. Approximate magnifications: ×5,500 (*a*), ×800 (*b* and *c*), and ×400 (*d*).

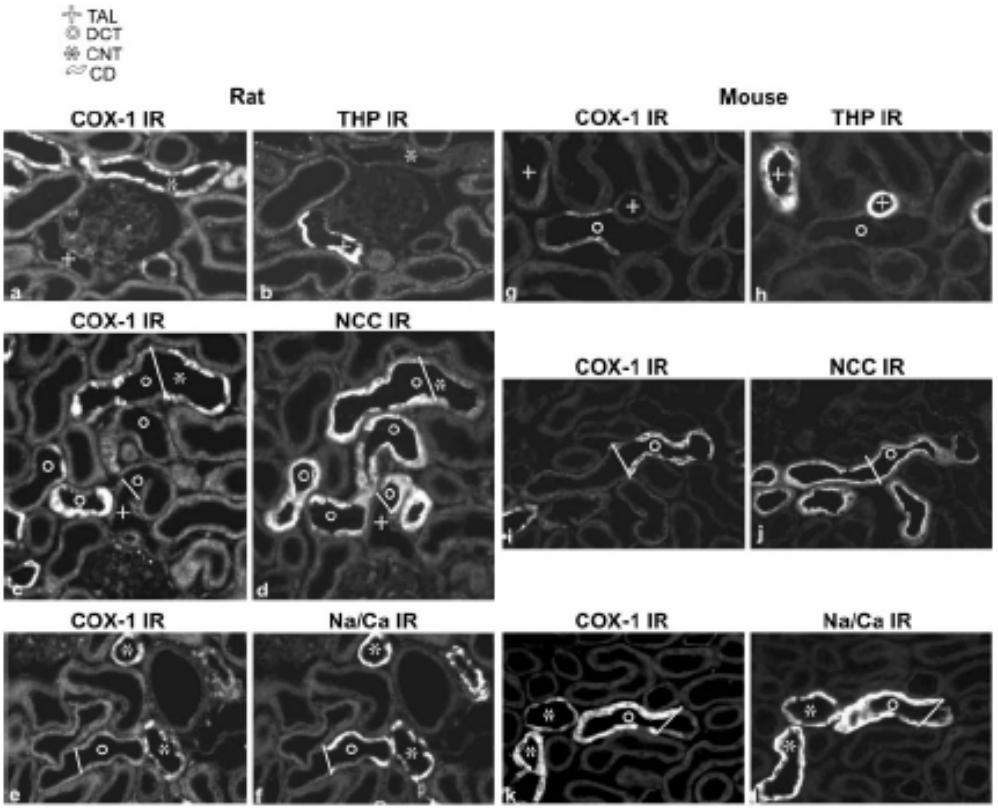

Fig. 2. Distribution of COX-1 IR in cryostat sections of rat and mouse renal cortex as revealed by double-labeling or consecutive-sectioning techniques using segmental markers of the nephron combined with different fluorochromes: Tamm Horsfall protein (THP) for thick ascending limb (TAL; +), thiazide-sensitive Na-Cl cotransporter (NCC) for the distal convoluted tubule (DCT; °); and Na/Ca exchanger (Na/Ca) for the distal convoluted tubule (DCT) and the connecting tubule (CNT; *). Insertions of white bars indicate the junctions between segments and subsegments of the distal convolutions according to previous mapping (3, 6). *a*, *b*, *g*, and *h*: COX-1 is absent from THP-positive TAL. *c*, *d*, *i*, and *j*: COX-1 is absent from early DCT but present in late DCT and CNT. *e*, *f*, *k*, and l: COX-1 is present in terminal DCT and CNT. CD, collecting duct. Approximate magnification: ×400.

showed a mild cytoplasmic and a stronger nuclear envelope staining (Fig. 1*a*). Along the nephron, COX-1 immunoreactivity was absent from thin limbs of the loop of Henle, mTAL, cTAL, macula densa, postmacular segment, and initial DCT (*subsegment 1* or DCT1; Fig. 2, *a* and *b*); the onset of a COX-1-immunoreactive signal was detected in terminal DCT, CNT, and cortical collecting duct (CCD) principal cells, as revealed by immunofluorescence staining (Fig. 2, *c–l*) and by an antigen-retrieval technique using CSA-immunoperoxidase staining (Fig. 3). Both techniques showed largely the same results in rats and mice. Intercalated cells were negative. In segments from COX-1 knockout mice, no signal was detected (Fig. 3, *g* and *h*). Fine structural distribution of epithelial COX-1 immunoreactivity similar to that in mesangial cells showed a moderate cytosolic staining and an enhanced signal at the perinuclear envelope, as revealed by preembedding immunoperoxidase staining (Fig. 3, *c* and *d*). In mice, a major proportion of the cortical interstitium showed COX-1-immunoreactive interstitial fibroblasts in the cortical labyrinth (Fig. 4*a*). In situ hybridization as well revealed the presence of COX-1 transcript in the distal convolutions of rat kidney (Fig. 5, *a* and *b*); in mice, COX-1 mRNA distribution was analogous but weaker than in rats, with only a few scattered cells showing significant staining (Fig. 5, *c* and *d*). Arteriolar endothelia only occasionally showed mildly positive COX-1-immunoreactive staining in both species.

Compared with COX-1 immunolocalization, COX-2 expression in rat renal cortex was not found in the distal convolutions, but, rather, it was restricted to scattered single cTAL cells or smaller groups of cells, thus confirming earlier work (17, 45) (Fig. 6, *a* and *b*). A COX-2-immunoreactive signal was concentrated in the macula densa region of cTAL, although macula densa cells proper were rarely stained (Fig. 6, *a* and *f*). In situ hybridization showed similar distribution of positive cTAL cells (Fig. 6*c*). Ultrastructurally, COX-2 immunostaining of macula densa cells proper revealed prominent staining of the nuclear envelope and little cytosolic labeling, whereas in adjacent or upstream

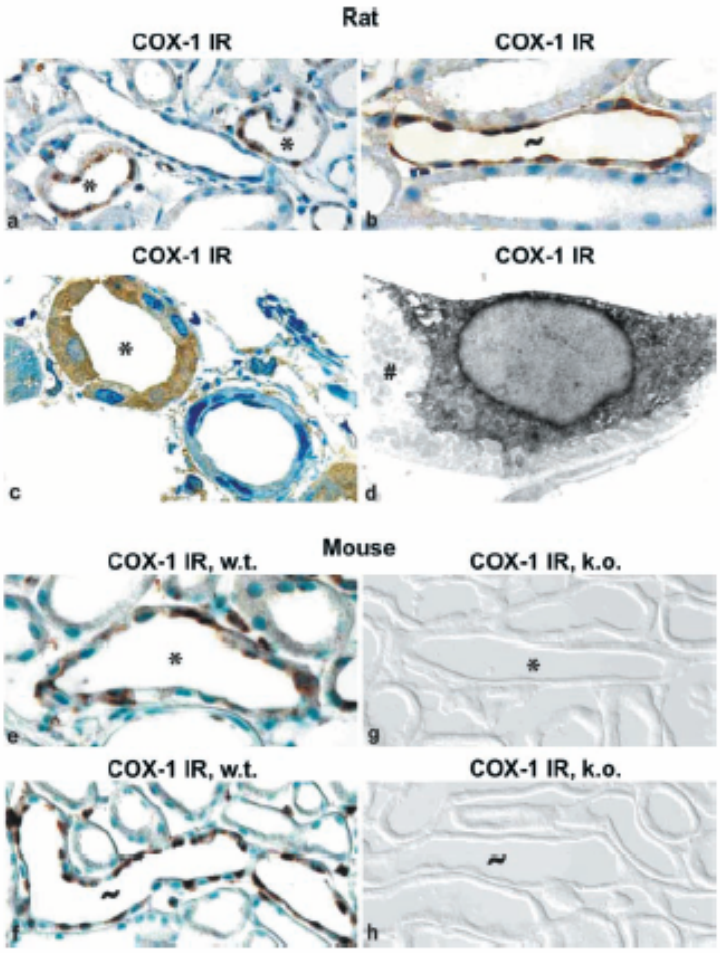

Fig. 3. Distribution of COX-1 in CNT (*) and CD (~) in rat, w.t. mouse, and COX-1 k.o. mouse renal cortex using immunoperoxidase staining. *a*, *c*, and *e*: single CNT profiles are seen in the vicinity of cortical arterioles. *d*: ultrastructural labeling of a CNT cell with enhanced perinuclear signal; note an adjacent, negative intercalated cell (#). *g* and *h*: In the k.o. mouse, absence of staining is seen. Paraffin sections, hematoxylin stain, and interference contrast (*a*, *b*, and *e–h*); semithin section (*c*); and ultrathin section (*d*) are shown. Approximate magnifications: ×400 (*a*); ×800 (*b*, *e–h*); ×1,000 (*c*); and ×5,500 (*d*).

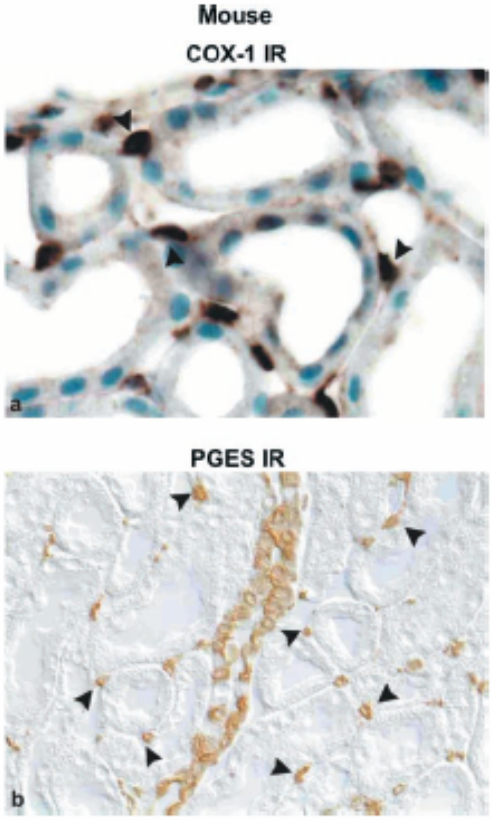

Fig. 4. Distribution of COX-1 and PGE synthase (PGES) in mouse cortical interstitial cells (arrowheads). Paraffin sections with hematoxylin counterstain (*a*) and interference contrast (*b*) are shown. Approximate magnification: ×1,000.

locations of cTAL, positive cells showed predominantly cytosolic labeling that extended into the interdigitating cell processes (Fig. 6, *d* and *e*). In mice, COX-2 staining was different from that in rats, with a signal mostly confined to the macula densa (Fig. 6*h*). Apart from TAL, all other structures of the nephron, glomerulus, and interstitium were negative. Generally, vascular COX-2 immunostaining was not observed. The COX-2 knockout mouse did not show renal COX-2 immunoreactivity either (data not shown).

We next investigated the distribution of PGES in rats and mice to establish whether this downstream-acting enzyme would be associated with one or both of the COX isoforms. PGES staining in glomeruli was restricted to occasional single cells that were not identified. In agreement with COX-2 localization, PGES immunoreactivity was detected in rat terminal cTAL portions, macula densa, and the short postmacular segment in rats (Fig. 6*g*), and in mice, a signal was restricted to the macula densa, in agreement with COX-2 localization (Fig. 6*i*). The DCT1 was entirely negative in rats, whereas PGES staining in the terminal DCT, CNT, and CCD was intensive; in mice, an analogous distribution was encountered (Fig. 7, *a–h*). Double staining for PGES and COX-1 or COX-2 confirmed these results (Figs. 6, *f* and *g*, and 8, *a–h*). In mice, a major proportion of the cortical interstitium showed PGES-immunoreactive interstitial fibroblasts in the cortical labyrinth, which is in agreement with COX-1 localization (Fig. 4*b*); in rats, this pattern was far less conspicuous.

Medulla. Significant epithelial COX-1 immunostaining was detected in the principal cells of collecting ducts from outer and inner medulla in rats and mice (Fig. 9, *a* and *d*). Medullary collecting duct (MCD) staining extended all the way from the outer to inner medulla and papilla and was also found along the papillary surface, but not in the pelvic epithelium; this pattern was also found for PGES immunoreactivity (Fig. 9, *c* and *f*), except for the pelvic epithelium, which was strongly PGES positive. COX-1 in situ hybridization produced only a faint signal in MCD portions compared with CNT or CCD, indicating lower mRNA levels at these sites (data not shown). COX-1 immunostaining was also observed in the majority of the outer medullary interstitial cells in mice, whereas in rats interstitial cells of this portion were rarely stained. In the papillary portion of the inner medulla, however, both species showed strong perinuclear COX-1 staining of the lipid-laden interstitial cells, except for a small terminal portion of the papillary tip interstitium.

By contrast, medullary COX-2 staining produced no signal in the collecting ducts in either species (Fig. 9, *b* and *e*). The lipid-laden inner medullary interstitial cells of the inner medulla and papilla, however, showed significant COX-2 immunoreactivity, although interindividual variability was high. In the papillary tip in

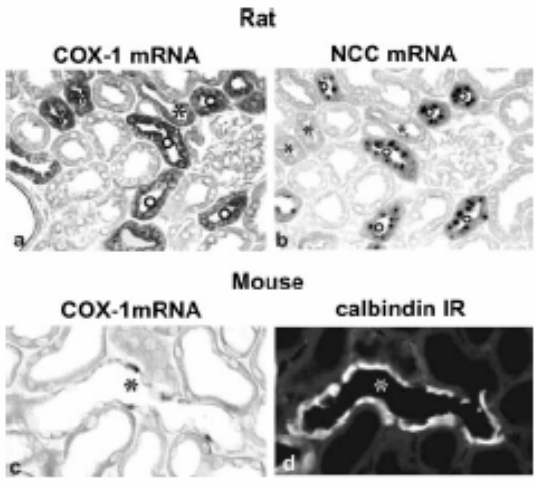

Fig. 5. In situ hybridization of paraffin sections showing COX-1 mRNA in rat and mouse kidney. Segmental markers of the nephron (NCC mRNA for DCT;°) and IR calbindin for DCT and CNT (*) are shown in consecutive sections. COX-1 mRNA partially colocalizes with NCC mRNA in rat kidney (*a* and *b*) and with calbindin in mouse kidney (*c* and *d*). Approximate magnifications: ×400 (*a* and *b*) and ×800 (*c* and *d*).

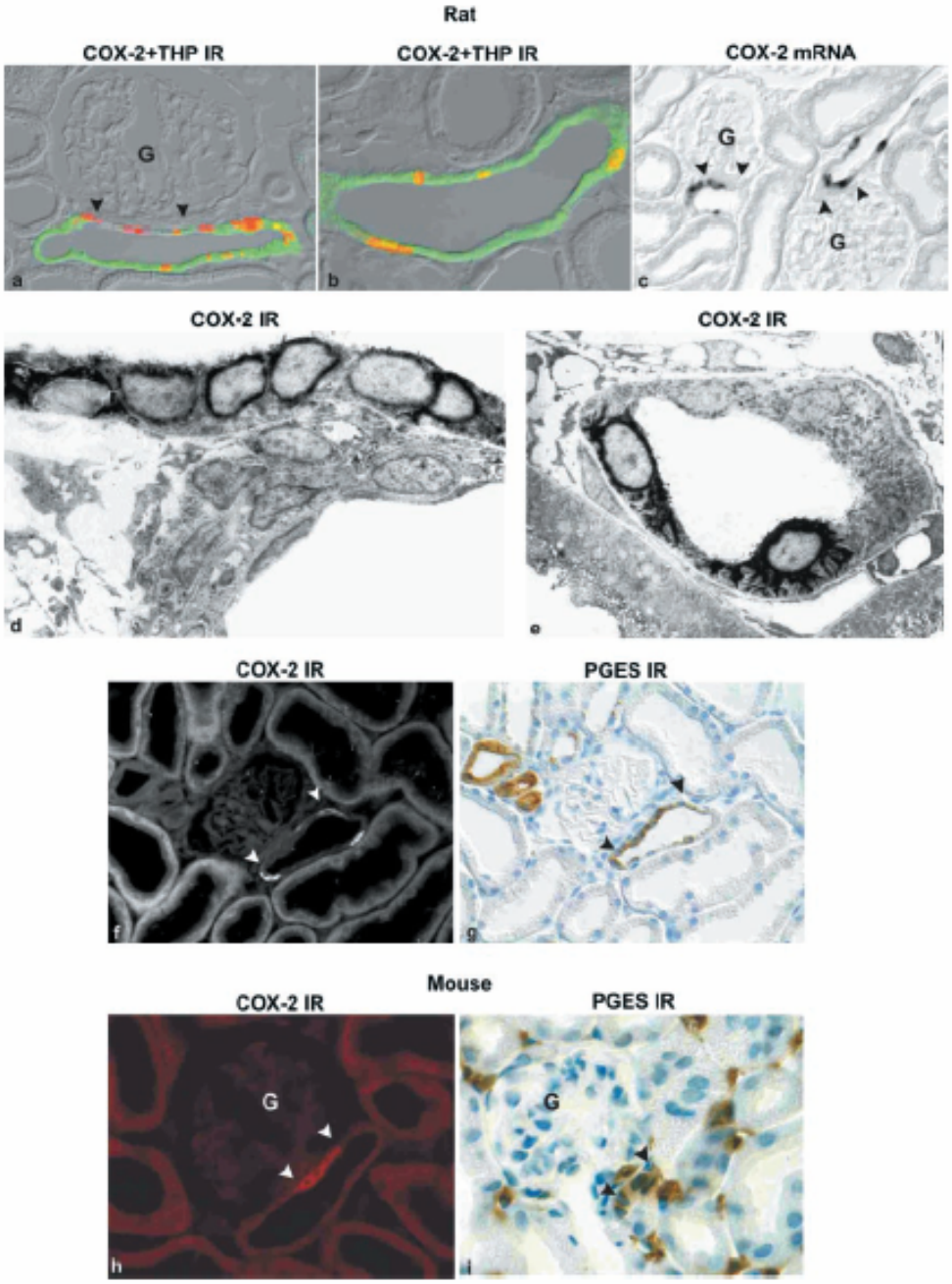

Fig. 6. Distribution of COX-2 in rat and mouse renal cortex. *a* and *b*: Juxtaglomerular (*a*) and further-upstream portions (*b*) of cortical TAL (cTAL) and macula densa (between arrowheads) showing COX-2 immunofluorescence [red or yellow; double-stained with anti-THP antibody (green) to mark TAL]. *c*: In situ hybridization reveals staining in analogous location. *d* and *e*: Ultrastructural immunoperoxidase labeling shows prominent nuclear envelope staining in macula densa cells (*d*) and predominant cytosolic staining extending in cTAL cell processes (*e*). *f* and *g*: PGES immunoperoxidase staining is restricted to macula densa and adjacent cTAL cells (*g*), whereas concomitant COX-2 staining in macula densa may be weak as shown (*f*). *h* and *i*: COX-2 in mouse macula densa colocalizes with PGES. G, glomerulus. Approximate magnifications: ×400 (*a*, *f*, and *g*); ×600 (*b*, *h*, and *i*); ×300 (*c*); ×3,600 (*d*); and ×2,200 (*e*).

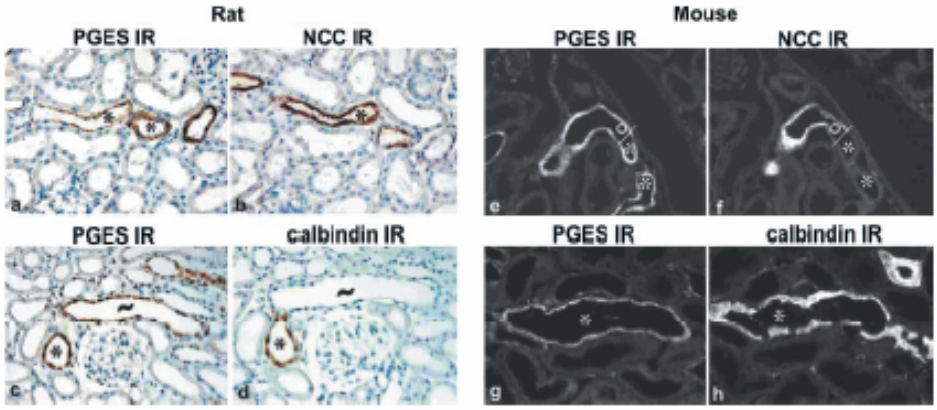

Fig. 7. Distribution of microsomal PGES in rat and mouse renal cortex. Consecutive sections are stained for PGES and for NCC as a marker of DCT (°) and calbindin as a marker of DCT and CNT (*). –, Collecting duct. Immunoperoxidase staining in rat, immunofluorescence staining in mouse. Approximate magnification: ×200.

rats, interstitial cells were mostly negative. In mice, COX-2 staining along the papillary interstitium was scarce. However, a remarkable increase in staining was incidentally observed when mice had been exposed to surgical stress (laparotomy and exposition of kidney during several hours).

PGES-immunoreactive cells in the rat and mouse medulla were distributed analogously to COX-1-expressing cells. Significant epithelial PGES staining was detected in the principal cells of MCD from outer and inner medulla (Fig. 9, *c* and *f*). The distribution of COX isoforms and PGES is summarized (Fig. 10 and Table 1).

Complementary localization of COX isoforms in knockout mice. Localizing COX-1 or COX-2 expression in the respective complementary knockouts showed no principal differences in the typical position or signal intensity of the respective mRNA or immunoreactive staining (Fig. 11).

RT-PCR analysis. The expression of COX-1, COX-2, and PGES mRNA was detected in extracts from rat glomeruli. GAPDH was used as a positive control (Fig. 12*A*).

Western blot analyses. Western blotting was performed to confirm antibody specificity. COX-1 immunoreactivity showed a single, distinct band at 70 kDa, COX-2 at 72 kDa, and PGES at 17 kDa (Fig. 12, *B–D*).

DISCUSSION

In this study, we have presented a comprehensive analysis of the expression sites of enzymes involved in renal prostaglandin synthesis using histochemical techniques for cell-type identification. Among several commercially available antisera labeled anti-COX-1 or anti-COX-2 raised against peptides, we have made a careful choice after having applied rigorous criteria for specificity, and we have corroborated our results by in situ hybridization and the use of knockout mice.

Glomerulus. In the renal corpuscle, COX-1 was the dominant isoform in rats to be expressed in a subset of glomerular mesangial cells. This agrees with previous results by Soler et al. (44) reporting the release of untransformed PGH_2 as the major product from cultured mesangial cells. Because we could not detect the downstream-acting PGES in mesangial cells, it appears plausible that this precursor prostanoid is released also in vivo from the glomerular tuft. With respect to nephritic conditions, stimulated COX-1 levels together with increased EP2 receptor expression have been suggested to be potentially beneficial (21). In the human kidney, immunoreactive COX-1 has been localized to podocytes during development, and to endothelial cells of the glomerular hilus (31); these cell types, however, were not positive in our studies. In contrast to COX-1, immunoreactive COX-2 was not detected reliably in the glomerulus, although COX-2 mRNA was clearly detectable using RT-PCR. The absence of COX-2 protein in glomerular extracts from control tissue was also reported in another study by Western blot analysis (10), and even under inflammatory conditions no immunoreactive COX-2 was detected in podocytes (30). The rodent glomerulus therefore appears to be a minor site of prostanoid synthesis originating from the action of mesangial COX-1, but in turn it may well be a sensitive target for local prostaglandins because podocytes express various prostanoid receptors (4).

Loop of Henle. Along the nephron, the first evidence for the parameters tested was found in the loop of Henle of rat kidney with COX-2- and PGES-expressing portions of cTAL and macula densa. By contrast, COX-1 was absent from these cells, confirming earlier work (17, 42). COX-2 expression in rats differed from that in mice because a COX-2 signal in rats was typically found in scattered individual cells or cell groups along the cTAL and in a small proportion of macula densa, as established elsewhere (23, 45, 46, 51; for a review, see also Refs. 17, 19, and 40), whereas in mice, COX-2-positive cells were less numerous and concentrated in macula densa and a few directly adjacent

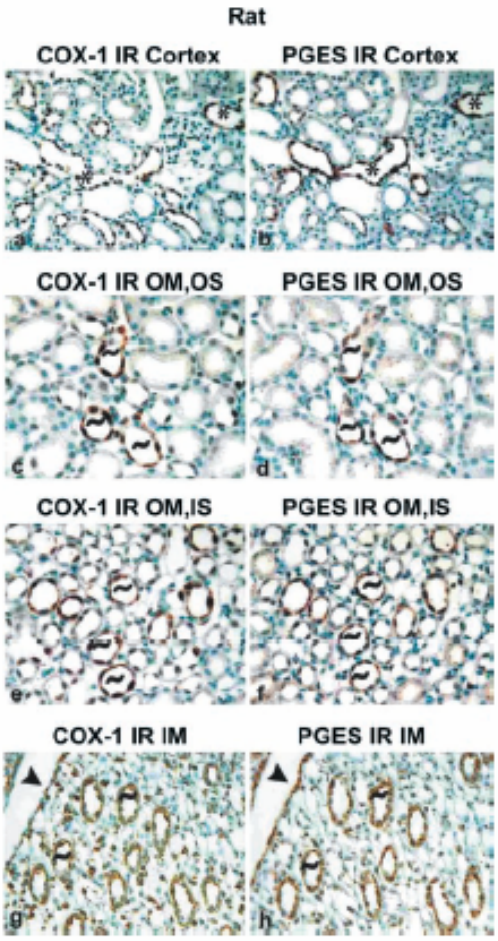

Fig. 8. Comparative distribution of COX-1 and PGES in rat kidney cortex and medulla immunoperoxidase stained on consecutive sections. There is complete overlap of signals in CNT (*) and in medullary collecting duct profiles of different levels (−). Note COX-1 and PGES signals also in the papillary surface epithelium (arrowheads in *g* and *h*). Approximate magnification: ×400.

TAL cells. The total number of COX-2-positive TAL cells in normal rats has been shown elsewhere to amount to <2% of total TAL cells (46). The numbers of COX-2-positive cells in both species, however, simply reflect a balanced physiological state because they can be increased solidly under experimental changes, indicating the inducible nature of COX-2 in TAL, the same as elsewhere. In contrast to previous in vitro studies, we could not detect COX-2 in rat mTAL (12). Other mammalian species such as dogs, rabbits, sheep, monkeys, and humans showed basically similar tubular immunoreactive staining, although in humans, macula densa/cTAL staining is only visible with disease or advanced age (29, 31, 34).

Numerous studies on experimentally induced changes of COX-2 activity have used biochemical assays on tissue homogenates for quantitative evaluation. However, regarding the paucity of cellular expression and the heterogenous distribution of COX-2-positive cells, the present study underlines that histochemical quantification establishing the number and size of COX-2 loci, or the number of positive individual cells related to volume of tissue, should result in a more reliable evaluation. Micromorphological distinctions between macula densa and cTAL COX-2 expression may thus be respected (17, 45, 51).

The action of COX-2 in cTAL is relevant to essential functions of the epithelium itself and of the tubulovascular signaling mechanism that reacts to the local release of PGE_2, the major prostaglandin from TAL (40). On one hand, COX-2-derived prostanoids seem to be permissive for the effect of loop diuretics (27) and exert an inhibitory effect on Na-K-Cl cotransport in mTAL cells (26). It has accordingly been established that PGE_2 directly inhibits solute reabsorption in in vitro perfused mTAL, although data on cTAL are less clear cut, and the identification of an E-type prostaglandin receptor in cTAL is still controversial (5, 25). On the other hand, there is firm evidence that low chloride activates COX-2 in TAL and macula densa (for a review, see Ref. 40); in cultured macula densa cells, a correlation between activated COX-2 and increased prostaglandin release has been established (48). The latter seems to be a critical component in macula densa control of renin synthesis and of its release. This was particularly evident from hyperreninemic states resulting from furosemide treatment, renal arterial stenosis, or loss-of-function mutations of Na-K-Cl transport components in TAL, which were paralleled by a recruitment of COX-2-positive cells (40). An interaction with the renin-angiotensin system is also well recognized, because an ANG II-dependent negative-feedback effect on tubular sites of COX-2 synthesis has been reported, and mice that are nullizygote for ANG II receptor subtypes expressed high levels of COX-2 in macula densa (8). Our finding of intensive, constitutive COX-1 expression in the extraglomerular mesangial cells in this context is intriguing, although its particular relevance in the regulatory physiology of the juxtaglomerular apparatus remains to be established. Local release of prostaglandins from both sources may thus affect glomerular microcirculation and control of glomerular filtration rate, although controversy as to the particular receptors involved must still be resolved.

It has been established that the expression of COX-2 during development is much stronger than in the adult rodent kidney. This has also been evaluated quantitatively (51). Regarding our observation that in mouse cTAL, the COX-2 signal is proportionately less extended than in rat cTAL, it is noteworthy that COX-2 gene disruption in mice nevertheless causes major damage to nephron development (33); this underlines the prominent role of perinatal prostaglandin synthesis at the juxtaglomerular site at least in the rodent kidney, because no other COX-2-immunoreactive cell type was detected in cortex.

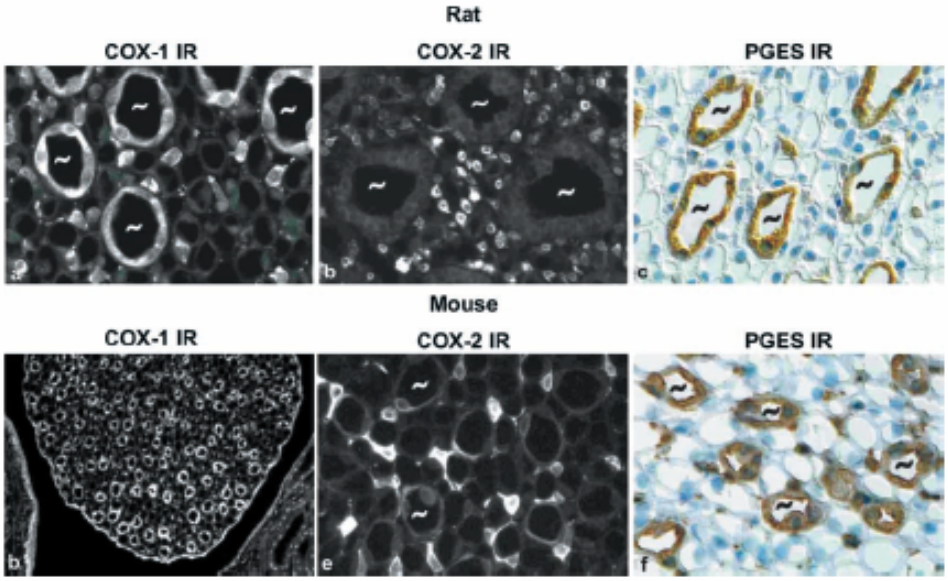

Fig. 9. Comparative distribution of COX-1, COX-2, and PGES in rat and mouse renal inner medulla. MCD (–) and interstitial cells may be distinguished in all sections. Note the absence of COX-2 from MCD profiles (*b* and *e*). Paraffin sections partly counterstained with hematoxylin are shown. Approximate magnifications: ×1,000 (*a* and *e*), ×600 (*b*, *c*, and *f*), and ×400 (*d*).

Fine structural analysis showed the typical perinuclear location of immunoreactive COX-2, which was also found for COX-1 in mesangial cells, thus confirming that both COX isoforms predominantly integrate into the outer leaflet of the nuclear membrane; however, additional cytoplasmic label was observed as well in cTAL cells, including their fine cellular processes, suggesting that COX-2 may also exert its effects in

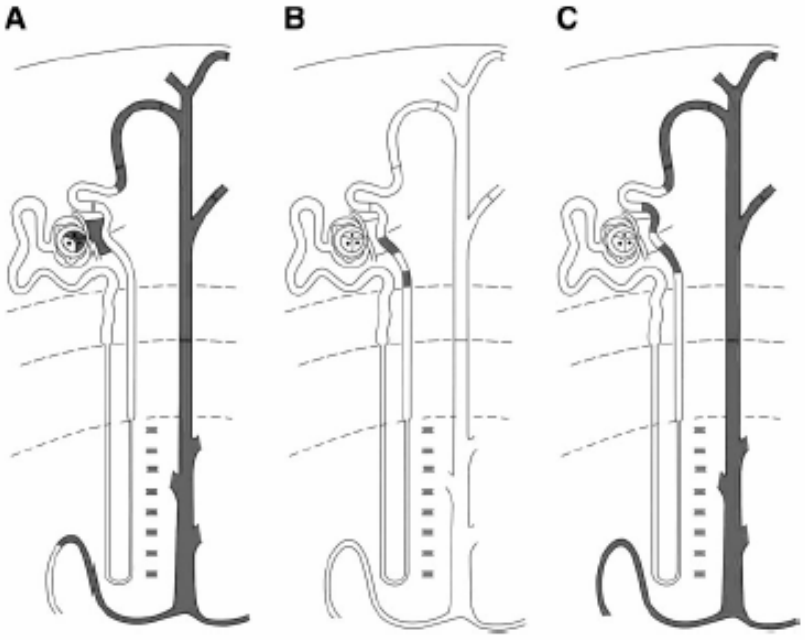

Fig. 10. Schematic topographical representation of COX-1 (*A*)-, COX-2 (*B*)-, and PGES (*C*)-immunoreactive sites (shaded areas) in rat kidney. With the exception of the COX-2 signal in the TAL/macula densa region, this distribution is also found in mouse kidney.

Table 1. *Distribution of COX isoforms and PGES in rat and mouse kidneys*

	COX-1		COX-2		PGES	
	Rat	Mouse	Rat	Mouse	Rat	Mouse
Cortex						
IGM	+	+	−	−	−	−
EGM	++	++	−	−	−	−
TAL	−	−	+++	−	+	+
MD	−	−	++	+++	+	+
MDR	−	−	+++	+	−	−
DCT	++	++	−	−	+++	+++
CNT	++	++	−	−	+++	+++
CD-PC	++	++	−	−	+++	+++
IC	+/−	+++	−	−	+	+++
OM, OS						
CD-PC	++	+++	−	−	++	++
IC	−	++	−	−	−	−
OM, IS						
CD-PC	+++	++	−	−	++	++
IC	−	+	−	−	−	−
IM						
CD	++	++	−	−	+++	+++
IC	++	++	+++	−	+	++
PE	++	++	−	−	++	++
PVE	−	−	−	−	+++	+++

COX, cyclooxygenase; PGE, prostaglandin E synthase; IGM, intraglomerular mesangium; EGM, extraglomerular mesangium; TAL, thick ascending limb; MD, macula densa; MDR, macula densa region; DCT, distal convoluted tubule; CNT, connecting tubule; CD-PC, collecting duct-principal cell; IC, intercalated cells; PE, papillary epithelium; PVE, pelvic epithelium; OM, outer medulla; IM, inner medulla; OS, outer stripe; IS, inner stripe. Intensity levels of COX-1, COX-2, and PGES are as follows: +, low; ++, medium; +++, high; −, absence of signal.

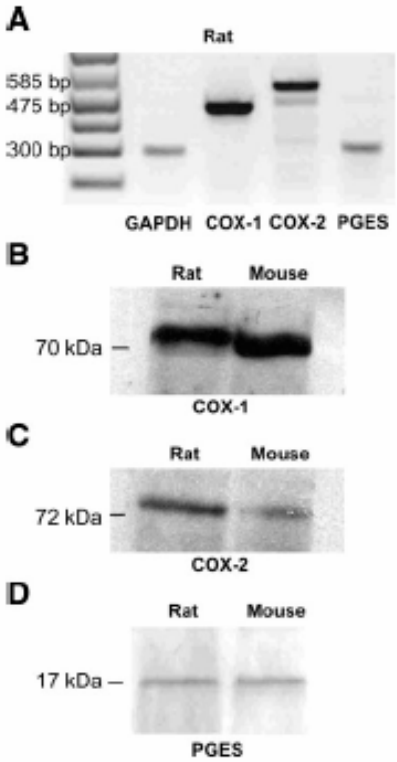

Fig. 12. *A*: representative RT-PCR analysis of COX-1, COX-2, and PGES mRNA in extracts from isolated rat glomeruli with GAPDH as a reference standard. *B–D*: representative Western blots for COX-1, COX-2, and PGES, respectively, from protein extracts of whole rat and mouse kidneys.

membrane compartments distant from the nucleus. This finding proves in more detail what others have stated earlier in the neonatal (51) and adult (23) rat kidney using distinct methods. The intracellular signaling events related to the action of COX-2 in cTAL have partly been identified. Rapid phosphorylation of p38 and ERK1/2 kinases and stimulation of MAP kinase pathways are involved (7, 48). Expression of microsomal-type PGES in cTAL and macula densa suggests that the formation and release of PGE_2 at these sites are functionally coupled to the action of this enzyme.

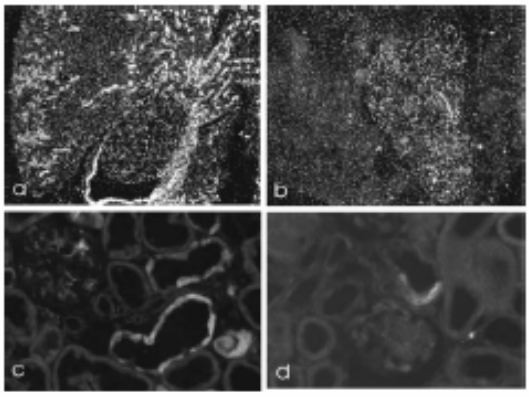

Fig. 11. Representative images of a comparative localization of COX-1 expression in a COX-2 knockout mouse (*a* and *c*) and of COX-2 expression in a COX-1 knockout mouse (*b* and *d*). *a* and *b*: in situ hybridization with radiolabeled probes showing darkfield overview of kidneys with typical COX-1 mRNA expression in CNT, CCD, and MCD and medullary interstitial cells. *c* and *d*: immunofluorescence staining showing typical distribution of COX-1 in connecting tubules and COX-2 in macula densa cells. Approximate magnifications: ×50 (*a* and *b*) and ×400 (*c* and *d*).

Distal convolutions and collecting duct. Expression of COX-1 in the collecting duct has been described previously (42, 47), but evidence for detailed protein localization in the distal convolutions was missing. We have shown that the portion immediately after the postmacula segment of the TAL, i.e., the initial DCT, was devoid of COX, whereas in the terminal DCT portion, significant COX-1 staining was obvious in both species, and expression continued into the CNT, CCD, and MCD portions, and was accompanied throughout by significant PGES immunoreactivity in both species. By contrast, intercalated cells in our hands were never stained for any of the products investigated in either species, which is at variance with observations by Ferguson et al. (11) reporting COX-1 and COX-2 signals

only in intercalated cells of the CCD. Probe-specificify problems may be the reason for this discrepancy.

Endogenously formed or exogenously applied PGE_2 is well known to reverse the effect of antidiuretic hormone (ADH) in the collecting duct. When added to vasopressin-prestimulated collecting ducts, it potently inhibits water absorption (22), and it may also reduce sodium reabsorption in the collecting duct via a calcium-coupled mechanism (14). By contrast, basolateral effects of PGE_2 may also include a stimulation of water reabsorption in this segment (22). There is further evidence that in inner MCD Na-K-ATPase activity was diminished by PGE_2. Receptors in the collecting duct that mediate these local effects are essentially EP1 and, with spacial restrictions, EP3, as shown pharmacologically and by expression analysis (5, 25). It is not clear why the late DCT and the CNT show the strongest signal of all renal epithelia for COX-1 and PGES. Local effects may be mediated via the EP4 receptor (25) and may interfere with local hormonal systems such as the kallikrein-bradykinin system (36) or with the function of aldosterone, because these segments are sensitive to mineralocorticoids and express the amiloride-sensitive epithelial sodium channel (for a review, see Ref. 3). As in the collecting duct, COX-1 action in CNT may interfere with the effects of ADH. The pronounced coexpression of COX-1 and PGES in the pelvic epithelium underlines the similarity to the MCD, although the functional significance of this observation is not clear. Previous work has demonstrated the distribution of a mouse PGES form in distal tubule using in situ hybridization and immunostaining; labeling was concentrated in Tamm-Horsfall-negative distal tubules, which is compatible with the present findings (15).

Interstitial cells. The renal interstitium has long been recognized as the major source for prostaglandin biosynthesis, with the medulla as the principal location. However, in mice we also found strong immunoreactivity for COX-1 in cortical interstitium. Rats failed to show a clear signal at this site, although interstitial PGES was found in both species, suggesting PGE_2 release by these cells. Medullary interstitial cells were shown to abundantly and constitutively express both COX isoforms in rat, whereas COX-2 in mice was infrequent. Our findings are in agreement with previous work in rats and humans (31, 37, 51) and extend findings to mice. Prostaglandin synthesis in the medulla adjusts local microcirculation (reviewed in Ref. 5). Relevant effectors in this context may be the EP2 or EP4 receptors located in the vasa recta to mediate the response to high-salt intake and protect against systemic hypertension (28). The overlap of COX-1 and -2 expression in rats is puzzling and makes a distinction between in vivo contributions of the isoforms difficult; this is further hampered by the segregated COX-1 expression in the MCD; these questions have partly been addressed recently with respect to hormonal influences and intracellular localization specificities in rats (50). The coexpression of PGES with COX in the interstitial cells further supports in vitro data that the major prostanoid resulting from local COX activity may indeed be PGE_2 (16). The particularly well-identified role of the action of COX-2 comprises its response to physiological renal stress such as water deprivation, and it has further been shown that COX-2 allows the interstitial cells to survive hypertonic stress after dehydration (49).

Other structures. In contrast to other reports, vascular labeling with antibodies to COX isoforms was not reliably detected, except for an occasional endothelial COX-1 signal. In general, regarding COX-2 expression, the reader should be aware that we have reported only the constitutive localization of COX-2, whereas under inflammatory conditions or induction by altered steroid levels, many more cells and cell types may express COX-2 in the kidney as elsewhere in the body (46; for a review, see also Ref. 13).

Complementary localization of COX isoforms in knockout mice. The lack of obvious changes in the localization of COX-1 and COX-2 expression in the respective, complementary knockouts suggests that deficiency of one isoform has a major compensatory impact on the expression of the other.

In sum, our data underscore prominent functions of renal prostaglandin synthesis by defining the expression sites of the key enzymes involved in their biosynthesis. For this purpose, data raised in rats were compared with those in mice to broaden the knowledge for experimental settings that make use of knockout mice. Results define the renal cell types involved in presumed prostaglandin release within spatially restricted sites such as the juxtaglomerular apparatus, mesangium, distal convolutions and collecting duct, and in compartments of the renal interstitium.

We thank Hermann Pavenstädt (Dept. of Nephrology and Internal Medicine, University of Freiburg, Freiburg, Germany) for providing us with rat glomerular mRNA extracts. Technical help in immunohistochemistry by Kerstin Riskowsky and Gudrun Holland is gratefully acknowledged.

This work was supported by funds from the Deutsche Forschungsgemeinschaft (Ba 700/14–1 and 14–2).

REFERENCES

1. **Athirakul K, Kim HS, Audoly LP, Smithies O, and Coffman TM.** Deficiency of COX-1 causes natriuresis and enhanced sensitivity to ACE inhibition. *Kidney Int* 60: 2324–2329, 2001.
2. **Bachmann S, Bosse HM, and Mundel P.** Topography of nitric oxide synthesis by localizing constitutive NO synthases in mammalian kidney. *Am J Physiol Renal Fluid Electrolyte Physiol* 268: F885–F898, 1995.
3. **Bachmann S, Bostanjoglo M, Schmitt R, and Ellison DH.** Sodium transport-related proteins in the mammalian distal nephron—distribution, ontogeny and functional aspects. *Anat Embryol* 200: 447–468, 1999.
4. **Bek M, Nüsing R, Kowark P, Henger A, Mundel P, and Pavenstädt H.** Characterization of prostanoid receptors in podocytes. *J Am Soc Nephrol* 10: 2084–2093, 1999.
5. **Breyer MD and Breyer RM.** Prostaglandin E receptors and the kidney. *Am J Physiol Renal Physiol* 279: F12–F23, 2000.
6. **Câmpean V, Kricke J, Ellison D, Luft FC, and Bachmann S.** Localization of thiazide-sensitive Na^+-Cl^- cotransport and associated gene products in mouse DCT. *Am J Physiol Renal Physiol* 281: F1028–F1035, 2001.

7. Cheng HF, Wang JL, Zhang MZ, McKanna JA, and Harris RC. Role of p38 in the regulation of renal cortical cyclooxygenase-2 expression by extracellular chloride. *J Clin Invest* 106: 681–688, 2000.
8. Cheng HF, Wang JL, Zhang MZ, Miyazaki Y, Ichikawa I, McKanna JA, and Harris RC. Angiotensin II attenuates renal cortical cyclooxygenase-2 expression. *J Clin Invest* 103: 953–961, 1999.
9. DeWitt DL and Smith WL. Primary structure of prostaglandin G/H synthase from sheep vesicular gland determined from the complementary DNA sequence. *Proc Natl Acad Sci USA* 85: 1412–1416, 1988.
10. Dunlop ME and Muggli EE. Hyaluronan increases glomerular cyclooxygenase-2 protein expression in a p38 MAP-kinase-dependent process. *Kidney Int* 61: 1729–1738, 2002.
11. Ferguson S, Hébert RL, and Laneuville O. NS-398 upregulates constitutive cyclooxygenase-2 expression in the M-1 cortical collecting duct cell line. *J Am Soc Nephrol* 10: 2261–2271, 1999.
12. Ferreri NR, An SJ, and McGiff JC. Cyclooxygenase-2 expression and function in the medullary thick ascending limb. *Am J Physiol Renal Physiol* 277: F360–F368, 1999.
13. Fitzpatrick FA and Soberman RJ. Regulated formation of eicosanoids. *J Clin Invest* 107: 1347–1351, 2001.
14. Guan Y, Zhang Y, Breyer RM, Fowler B, Davis L, Hébert RL, and Breyer MD. Prostaglandin E_2 inhibits renal collecting duct Na^+ absorption by activating the EP1 receptor. *J Clin Invest* 102: 194–201, 1998.
15. Guan Y, Zhang Y, Schneider A, Riendeau D, Mancini JA, Davis L, Kömhoff M, Breyer RM, and Breyer MD. Urogenital distribution of a mouse membrane-associated prostaglandin E_2 synthase. *Am J Physiol Renal Physiol* 281: F1173–F1177, 2001.
16. Hao CM, Kömhoff M, Guan Y, Redha R, and Breyer MD. Selective targeting of cyclooxygenase-2 reveals its role in renal medullary interstitial cell survival. *Am J Physiol Renal Physiol* 277: F352–F359, 1999.
17. Harris RC. Cyclooxygenase-2 in the kidney. *J Am Soc Nephrol* 11: 2387–2394, 2000.
18. Harris RC Jr. Cyclooxygenase-2 inhibition and renal physiology. *Am J Cardiol* 89: 10–17, 2002.
19. Harris RC and Breyer MD. Physiological regulation of cyclooxygenase-2 in the kidney. *Am J Physiol Renal Physiol* 281: F1–F11, 2001.
20. Harris RC, McKanna JA, Akai Y, Jacobson HR, Dubois RN, and Breyer MD. Cyclooxygenase-2 is associated with the macula densa of rat kidney and increases with salt restriction. *J Clin Invest* 94: 2504–2510, 1994.
21. Hartner A, Pahl A, Brune K, and Goppelt-Struebe M. Upregulation of cyclooxygenase-1 and the PGE_2 receptor EP_2 in rat and human mesangioproliferative glomerulonephritis. *Inflamm Res* 49: 345–354, 2000.
22. Hébert RL, Jacobson HR, Fredin D, and Breyer MD. Evidence that separate PGE_2 receptors modulate water and sodium transport in rabbit cortical collecting duct. *Am J Physiol Renal Fluid Electrolyte Physiol* 265: F643–F650, 1993.
23. Ichitani Y, Holmberg K, Maunsbach AB, Haeggstrom JZ, Samuelsson B, DeWitt D, and Hokfelt T. Cyclooxygenase-1 and cyclooxygenase-2 expression in rat kidney and adrenal gland after stimulation with systemic lipopolysaccharide: in situ hybridization and immunocytochemical studies. *Cell Tissue Res* 303: 235–252, 2001.
24. Jakobsson PJ, Thorén S, Morgenstern R, and Samuelsson B. Identification of human prostaglandin E synthase: a microsomal, glutathione-dependent, inducible enzyme, constituting a potential novel drug target. *Proc Natl Acad Sci USA* 96: 7220–7225, 1999.
25. Jensen BL, Stubbe J, Hansen PB, Andreasen D, and Skøtt O. Localization of prostaglandin E_2 EP2 and EP4 receptors in the rat kidney. *Am J Physiol Renal Physiol* 280: F1001–F1009, 2001.
26. Kaji DM, Chase HS Jr, Eng JP, and Diaz J. Prostaglandin E_2 inhibits Na-K-2Cl cotransport in medullary thick ascending limb cells. *Am J Physiol Cell Physiol* 271: C354–C361, 1996.
27. Kammerl MC, Nüsing RM, Richthammer W, Krämer BK, and Kurtz A. Inhibition of COX-2 counteracts the effects of diuretics in rats. *Kidney Int* 60: 1684–1691, 2001.
28. Kennedy C, Zhang Y, Brandon S, Guan S, Coffee K, Funk C, Magnuson M, Oates J, Breyer M, and Breyer R. Hypertension and reduced fertility in mice lacking the prostaglandin EP2 receptor. *Nat Med* 5: 217–220, 1999.
29. Khan KN, Venturini CM, Bunch RT, Brassard JA, Koki AT, Morris DL, Trump BF, Maziasz TJ, and Alden CL. Interspecies differences in renal localization of cyclooxygenase isoforms: implications in nonsteroidal antiinflammatory drug-related nephrotoxicity. *Toxicol Pathol* 26: 612–620, 1998.
30. Kitahara M, Eitner F, Ostendorf T, Kunter U, Janssen U, Westenfeld R, Matsui K, Kerjaschki D, and Floege J. Selective cyclooxygenase-2 inhibition impairs glomerular capillary healing in experimental glomerulonephritis. *J Am Soc Nephrol* 13: 1261–1270, 2002.
31. Kömhoff M, Grone HJ, Klein T, Seyberth HW, and Nüsing RM. Localization of cyclooxygenase-1 and -2 in adult and fetal human kidney: implication for renal function. *Am J Physiol Renal Physiol* 272: F460–F468, 1997.
32. Kreisberg JI, Hoover RL, and Karnovsky MJ. Isolation and characterization of rat glomerular epithelial cells in vitro. *Kidney Int* 14: 21–30, 1978.
33. Morham SG, Langenbach R, Loftin CD, Tiano HF, Vouloumanos N, Jennette JC, Mahler JF, Kluckman KD, Ledford A, and Lee CA. Prostaglandin synthase 2 gene disruption causes severe renal pathology in the mouse. *Cell* 83: 473–482, 1995.
34. Nantel F, Meadows E, Denis D, Connolly B, Metters KM, and Giaid A. Immunolocalization of cyclooxygenase-2 in the macula densa of human elderly. *FEBS Lett* 457: 475–477, 1999.
35. Reinalter SC, Jeck N, Brochhausen C, Watzer B, Nüsing RM, Seyberth HW, and Kömhoff M. Role of cyclooxygenase-2 in hyperprostaglandin E syndrome/antenatal Bartter syndrome. *Kidney Int* 62: 253–260, 2002.
36. Rodríguez F, Llinás MT, Moreno C, and Salazar FJ. Role of cyclooxygenase-2-derived metabolites and NO in renal response to bradykinin. *Hypertension* 37: 129–134, 2001.
37. Qi Z, Hao CM, Langenbach RI, Breyer RM, Redha R, Morrow JD, and Breyer MD. Opposite effects of cyclooxygenase-1 and -2 activity on the pressor response to angiotensin II. *J Clin Invest* 110: 61–69, 2002.
38. Schmitt R, Ellison DH, Farman N, Rossier BC, Reilly RF, Reeves WB, Oberbäumer I, Tapp R, and Bachmann S. Developmental expression of sodium entry pathways in rat distal nephron. *Am J Physiol Renal Physiol* 276: F367–F381, 1999.
39. Schneider A and Stahl R. Cyclooxygenase-2 (COX-2) and the kidney: current status and potential perspectives. *Nephrol Dial Transplant* 13: 10–12, 1998.
40. Schnermann J. Cyclooxygenase-2 and macula densa control of renin secretion. *Nephrol Dial Transplant* 16: 1735–1738, 2001.
41. Schumacher K, Castrop H, Strehl R, de Vries U, and Minuth WW. Cyclooxygenases in the collecting duct of neonatal rabbit kidney. *Cell Physiol Biochem* 12: 63–74, 2002.
42. Smith WL and Bell TG. Immunohistochemical localization of the prostaglandin-forming cyclooxygenase in renal cortex. *Am J Physiol Renal Fluid Electrolyte Physiol* 235: F451–F457, 1978.
43. Smith WL, DeWitt DL, and Garavito RM. Cyclooxygenases: structural, cellular, and molecular biology. *Annu Rev Biochem* 69: 145–182, 2000.
44. Soler M, Camacho M, Sola R, and Vila L. Mesangial cells release untransformed prostaglandin H_2 as a major prostanoid. *Kidney Int* 59: 1283–1289, 2001.
45. Theilig F, Câmpean V, Paliege A, Breyer M, Briggs JP, Schnermann J, and Bachmann S. Epithelial COX-2 expression is not regulated by nitric oxide in rodent renal cortex. *Hypertension* 39: 848–853, 2002.

46. Vio CP, Cespedes C, Gallardo P, and Masferrer JL. Renal identification of cyclooxygenase-2 in a subset of thick ascending limb cells. *Hypertension* 30: 687–692, 1997.
47. Vitzthum H, Abt I, Einhellig S, and Kurtz A. Gene expression of prostanoid forming enzymes along the rat nephron. *Kidney Int* 62: 1570–1581, 2002.
48. Yang T, Park JM, Arend L, Huang Y, Topaloglu R, Pasumarthy A, Praetorius H, Spring K, Briggs JP, and Schnermann J. Low chloride stimulation of prostaglandin E2 release and cyclooxygenase-2 expression in a mouse macula densa cell line. *J Biol Chem* 275: 37922–37929, 2000.
49. Yang T, Schnermann JB, and Briggs JP. Regulation of cyclooxygenase-2 expression in renal medulla by tonicity in vivo and in vitro. *Am J Physiol Renal Physiol* 277: F1–F9, 1999.
50. Zhang MZ, Hao CM, Breyer MD, Harris RC, and McKanna JA. Mineralocorticoid regulation of cyclooxygenase-2 expression in rat renal medulla. *Am J Physiol Renal Physiol* 283: F509–F516, 2002.
51. Zhang MZ, Wang JL, Cheng HF, Harris RC, and McKanna JA. Cyclooxygenase-2 in rat nephron development. *Am J Physiol Renal Physiol* 273: F994–F1002, 1997.

Danksagung

Recht herzlich bedanke ich mich bei meinen Eltern, Regina und Wulf, Großeltern, Albert und Ursula, und bei meinen Geschwistern Stefanie und Michael nicht nur für die finanzielle, sondern auch für die moralische Unterstützung. Sie haben mir während meiner Promotionszeit immer zur Seite gestanden. Ebenso gilt mein Dank Silvia Marx für die Durchsicht meiner Doktorarbeit.

Für alle technischen Hilfen im Labor und wissenschaftlichen Unterstützungen möchte ich mich bei Kerstin und Petra sowie bei Magdalena, Ilka, Frau Oberbäumer, Jörn und Fatima und ganz besonders auch bei meinem Mitdoktoranden Alex bedanken.

Schließlich gilt mein besonderer Dank Herrn Prof. S. Bachmann für seine wohlwollende Unterstützung, wissenschaftliche Beratung sowie für die Möglichkeit an aus- und inländischen Kongressen und Aufenthalten teilzunehmen und mich selbst wie auch meine Vorliebe für die Wissenschaft zu fördern.

Eidesstattliche Erklärung

Hiermit erkläre ich, Franziska Theilig, an Eides Statt, dass diese Dissertation von mir selbst und ohne die unzulässige Hilfe Dritter verfasst wurde, dass die Dissertation auch in Teilen keine Kopie anderer Arbeiten darstellt und die benutzten Hilfsmittel sowie die Literatur vollständig an entsprechender Stelle in der Arbeit angegeben sind.

(Franziska Theilig)

Erklärung über Anteil an Publikationen

I. Theilig F, Bostanjoglo M, Pavenstädt H, Grupp C, Holland G, Slosarek I, Gressner AM, Russwurm M, Koesling D, Bachmann S: Cellular distribution and function of soluble guanylyl cyclase in rat kidney and liver. J Am Soc Nephrol 12: 2209-2220, 2001

Bei dieser Publikation führte ich die immunhistochemischen Markierungen, die In situ Hybridisierung, die Western blot- und die RT-PCR Analyse und anschließende Dokumenation sowie die Auswertung der elektronenmikroskopischen Aufnahmen durch. Auch habe ich die Interaktionen mit unseren Kooperationspartnern arrangiert.

II. Theilig F, Câmpean V, Paliege A, Breyer M, Briggs JP, Schnermann J, Bachmann S: Epithelial COX-2 expression is not regulated by NO: Colocalization studies in rat and mouse renal cortex. Hypertension 39: 848-853, 2002

Hier habe ich die Tierexperimente, die Schwanz-plethysmographische Blutdruckmessung, die immunhistochemischen und In situ-Färbungen, die anschließende Auswertung und Dokumentation an Goldblatt-Ratten, an Furosemid-behandelten Ratten und NOS1 -/- Mäusen durchgeführt.

III. Câmpean V, Theilig F, Paliege A, Breyer M, Bachmann S: Key enzymes for renal prostaglandin synthesis: site-specific expression in rodent kidney (rat, mouse). Am J Physiol 285: F19-F32, 2003.

Mein Anteil an dieser Arbeit bestand aus der immunhistochemischen Markierung, molekulare Sondengenerierung und In situ-Hybridisierung und Befundaufnahme an der Maus. Weiter habe ich die RT-PCR -Analyse von Glomerulumextrakten, bestätigende Antikörper-Überprüfung an den Knock-out Modellen sowie Überprüfung durch Western blot Analyse ausgeführt.

Generell habe ich bei den Publikationen, die in der Folge meiner praktischen Tätigkeit während meiner Promotionszeit entstanden sind, bei der Erstellung der Manuskripte wesentlichen Anteil gehabt.

(Franziska Theilig) (Prof. Dr. S. Bachmann)

Publikationsliste Franziska Theilig

Kongressbeiträge

Bachmann S, Theilig F, Pavenstädt H, Weichert W: NOS and COX signalling in kidney: Regulation and pathophysiological aspects. Kidney Blood Press Res 23: 214, 2000

Bachmann S, Theilig F, Paliege A, Schülke M, Weichert W, Provoost A: Expression and localization of COX-2 in rodent kidney under normal and experimental conditions. Kidney Blood Press Res 23: 407, 2000

Bachmann S, Theilig F, Pavenstädt H, Holland G, Slosarek I, Koesling D: Nitric oxide signalling in kidney and liver: distribution and function of soluble guanylyl cyclase (sGC) β1 subunit. FASEB J 14 (4), A139, 2000

Theilig F, Holland H, Pavenstädt H, Gressner AM, Koesling D, Bachmann S: Histochemical localization and function of soluble guanylyl cyclase in kidney and liver. 42. Symposium der Gesellschaft für Histochemie, Les Diablerets, 20-23.9.2000

Bachmann S, Theilig F: Differential expression of cyclooxygenase isoforms and nitric oxide synthase 1 in 2K, 1C Goldblatt model, rat. Experimental Biology 2001 (31.3.-4.4.2001), Orlando, FASEB J 15(4), A137, 155.3, 2001

Theilig F, Wiedmann B, Seyberth HW,.Bachmann S: Functional regulation of Cyclooxygenase-1, Prostaglandin E_2 Synthase and Prostaglandin I_2 Synthase under Goldblatt-hypertension. ASN

Theilig F, Câmpean V, Paliege A, Bachmann S: Intracellular co-expression of NOS1 and COX-2 is not relevant for the numerical increase of COX-2 positive cells under various chronic stiumuli. J Am Soc Nephrol 12, 41A, A0216, 2001

Theilig F, Weichert W, Bachmann S: Parakrine Signalwirkung von NOS und COX in der Niere: Regulation und Rollen bei glomerulärer Hyperfunktion. Verhandlungen der Anatomischen Gesellschaft 96: 206-207, 2001

Theilig F, Câmpean V, .Bachmann S: Cellular NOS1 and COX-2 coexpression is unrelated to increases in COX-2 under various chronic stimuli. Kidney Blood Press Res 24, 228, 2001

Câmpean V, Theilig F, Wiedmann B, Bachmann S: Cellular distribution of COX-1 vs.COX-2 in kidney supports heterogeneity in isoform function. Kidney Blood Press 24, 359, 2001

Câmpean V, Theilig F,Wiedmann B, Riskowsky K, Holland G, Bachmann S: Comparative histochemical analysis of COX-1 vs. COX-2 localization in rat kidney. J Am Soc Nephrol 12: A0142, 2001

Theilig F, Câmpean V,.Paliege A,Bachmann S: Intracellular co-expression of NOS1 and COX-2 is not relevant for the numerical increase of COX-2 positive cells under various chronic stimuli. J Am Soc Nephrol 12: A0216, 2001

Câmpean V, Theilig F, Riskowsky K, Holland G, Wiedmann B, Bachmann S: Comparative histgochemical analysis of COX-1 vs. COX-2 localization in rat kidney. Verhandlungen der Anatomischen Gesellschaft 97: 31-32, 2002

Theilig F, Nafz B, Bachmann S: Differential regulation of COX-1 and COX-2 under angiotensin and bradykinin blockade. FASEB J 16(5), A1171, 875.6, 2002

Theilig F, Bouby N, Nafz B, Nüsing R, Ronco P, Bachmann S: Renal cortical enzymes for prostaglandin synthesis in the Goldblatt model – Effects of angiotensin and bradykinin. World Congress of Nephrology, Berlin, 8-13.6.2003

Wack J, Schlichting U, Theilig F, Jerichow T, Kriz W, Le Hir M, Willnow T, Bachmann S: Kidney-specific inactivation of the megalin gene impairs essential proximal tubule functions in health and disease – insights from histochemistry. FASEB Summer Conference on Renal Hemodynamics, Callaway Gardens, 26.6.-1.7.2004

Castrop H, Huang Y, Mizel D, Hansen P, Theilig F, Bachmann S, Deng C, Briggs J, Schnermann J: Störung des tubuloglomerulären Feedbacks in Ecto-5'-nucleotidase/CD73 defizienten Mäusen. Kongreß der Gesellschaft für Nephrologie, Basel, 18.-21.9.2004

Theilig F, Jerichow T, Willnow T, Le Hir M, Kriz W, Bachmann S: Rolle der Megalin-vermittelten Endozytose bei tubulointerstitieller Schädigung der Niere. 21. Arbeitstagung der Anatomischen Gesellschaft, Würzburg 29.9.-1.10.2004

Theilig F, Jerichow T, Willnow T, Le Hir M, Kriz W, Bachmann S: Glomerulonephritis in megalin deficient mice – a model to study the effect of protein hyperfiltration on nephron loss. ASN Congress, St. Louis, 27.10.-1.11.2004

Originalartikel

Bachmann S, Theilig F: Appareil juxtaglomérulaire, monxyde d'azote et signalisation à la macula densa. Actualités néphrologiques Jean Hamburger Hôpital Necker 2000, 245-254, 2000

Theilig F, Bostanjoglo M, Pavenstädt H, Grupp C, Holland G, Slosarek I, Gressner AM, Russwurm M, Koesling D, Bachmann S: Cellular distribution and function of soluble guanylyl cyclase in rat kidney and liver. J Am Soc Nephrol 12: 2209-2220, 2001

Theilig F, Câmpean V, Paliege A, Breyer M, Briggs JP, Schnermann J, Bachmann S: Epithelial COX-2 expression is not regulated by NO: Colocalization studies in rat and mouse renal cortex. Hypertension 39: 848-853, 2002

Câmpean V, Theilig F, Paliege A, Breyer M, Bachmann S: Key enzymes for renal prostaglandin synthesis: site-specific expression in rodent kidney (rat, mouse). Am J Physiol 285: F19-F32, 2003.

Henn V, Edemir B, Stefan E, Wiesner B, Lorenz D, Theilig F, Schmitt R, Vossebein L, Tamma G, Beyermann M, Krause E, Herberg FW, Valenti G, Bachmann S, Rosenthal W, Klussmann E: Identification of a novel A-kinase anchoring protein 18 isoform and evidence for its role in the vasopressin-induced aquaporin-2 shuttle in renal principal cells. J.Biol.Chem. 279:26654-26665, 2004

Castrop H, Huang Y, Hashimoto S, Mizel D, Hansen P, Theilig F, Bachmann S, Deng C, Briggs J, Schnermann J: Impairment of tubuloglomerular feedback regulation of GFR in ecto-5'-nucleotidase/CD73-deficient mice. J.Clin.Invest 114:634-642, 2004

* Kulaksiz H, Theilig F, Bachmann S, Gehrke SG, Rost D, Janetzko A, Cetin Y, Stremmel W: The iron-regulatory peptide hormone hepcidin: expression and cellular localization in the mammalian kidney. J.Endocrinol. 184:361-370, 2005

* Doppel-Erstautorenschaft